Impacts of Hydraulic Modeling Methods on Bridge Scour Analysis

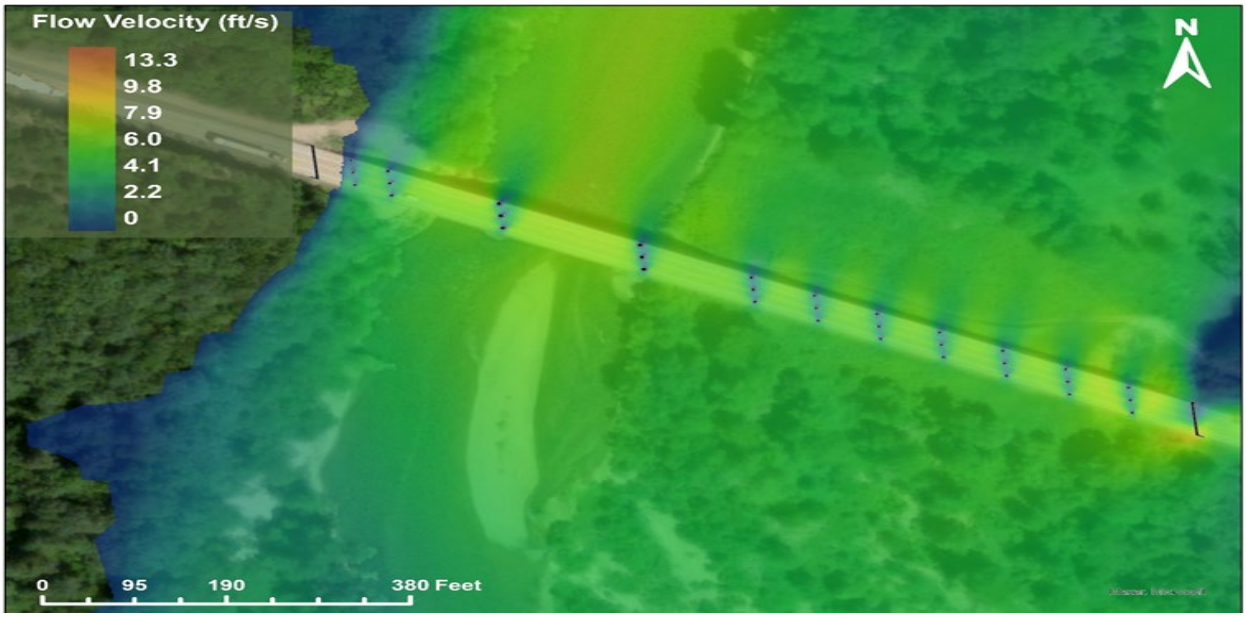

August 2023
Final Report

Project number TR202017
MoDOT Research Report number cmr 23-013

PREPARED BY:

Amanda L. Cox, Ph.D., P.E.

Ronaldo Luna, Ph.D., P.E.

Peter Kickham

Harrison Wooters

Water Access Technology, Environment, and Resources (WATER) Institute

PREPARED FOR:

Missouri Department of Transportation

Construction and Materials Division, Research Section

TECHNICAL REPORT DOCUMENTATION PAGE

1. Report No.	2. Government Accession No.	3. Recipient's Catalog No.
cmr 23-013		

4. Title and Subtitle	5. Report Date
Impacts of Hydraulic Modeling Methods on Bridge Scour Analysis	July 2023 Published: August 2023
	6. Performing Organization Code

7. Author(s)	8. Performing Organization Report No.
Amanda L. Cox, Ph.D., P.E. https://orcid.org/0000-0003-0719-2669 Ronaldo Luna, Ph.D., P.E. https://orcid.org/0009-0009-8325-5781 Peter Kickham https://orcid.org/0009-0000-5706-4636 Harrison Wooters https://orcid.org/0009-0005-0940-2625	

9. Performing Organization Name and Address	10. Work Unit No.
Water Access Technology, Environment, and Resources (WATER) Institute Saint Louis University 3450 Lindell Blvd. St. Louis, MO 63103	**11. Contract or Grant No.** MoDOT project # TR202017

12. Sponsoring Agency Name and Address	13. Type of Report and Period Covered
Missouri Department of Transportation (SPR-B) Construction and Materials Division P.O. Box 270 Jefferson City, MO 65102	Final Report (April 2020-June 2023)
	14. Sponsoring Agency Code

15. Supplementary Notes

Conducted in cooperation with the U.S. Department of Transportation, Federal Highway Administration. MoDOT research reports are available in the Innovation Library at https://www.modot.org/research-publications.

16. Abstract

This study has three primary purposes: 1) to investigate the impacts of hydraulic modeling methods on bridge scour analysis, 2) to develop recommendations for sediment/soil sampling methods, and 3) to conduct bridge scour risk assessments. Field data were collected at five study sites to obtain the required terrain and soil/sediment input data for hydraulic modeling and scour analyses. The recommended methods developed for soil/sediment sampling in the overbank areas are soil augers or test pits, and for overwater locations, a FISP or clamshell sampler is recommended. Contraction, abutment, and pier scour depths were computed using the HEC-18 guidelines with hydraulic conditions determined from a 1-D model (HEC-RAS) and a 2-D model (SRH-2D). Determining the required input parameters for scour calculations from HEC-RAS results was found to be difficult with many potential sources of human error. In contrast, the Hydraulic Toolbox program for scour calculations can auto-populate the required input parameters directly from SRH-2D output data. For all bridge sites evaluated, estimates for at least one of the main scour categories (i.e., channel contraction scour, pier scour, or abutment scour) were more than 50% different between the HEC-RAS 1-D and SRH-2D results. The key findings from comparing model results were: 1) the angle of attack was the dominant pier scour input parameter and 2) flow conveyance over inundated roadway embankments was significantly greater for SRH-2D relative to the HEC-RAS model. The 2-D modeling methods are recommended for future use given the significant differences observed between the 1-D and 2-D scour results, increased availability of terrain data, current computing resources, and ease of use. Finally, due to differences in the HEC-RAS and SRH-2D estimated scour depths, reanalyzing high-risk and/or visually vulnerable bridges is recommended.

17. Key Words	18. Distribution Statement
Bridge scour; Hydraulic modeling; Soil/sediment field sampling	No restrictions. This document is available through the National Technical Information Service, Springfield, VA 22161.

19. Security Classif. (of this report)	20. Security Classif. (of this page)	21. No. of Pages	22. Price
Unclassified.	Unclassified.	102	$199,996

IMPACTS OF HYDRAULIC MODELING METHODS ON BRIDGE SCOUR ANALYSIS

FINAL REPORT

July 2023

Amanda Cox[1,2], Ronaldo Luna[1,2], Peter Kickham[1] and Harrison Wooters[1]

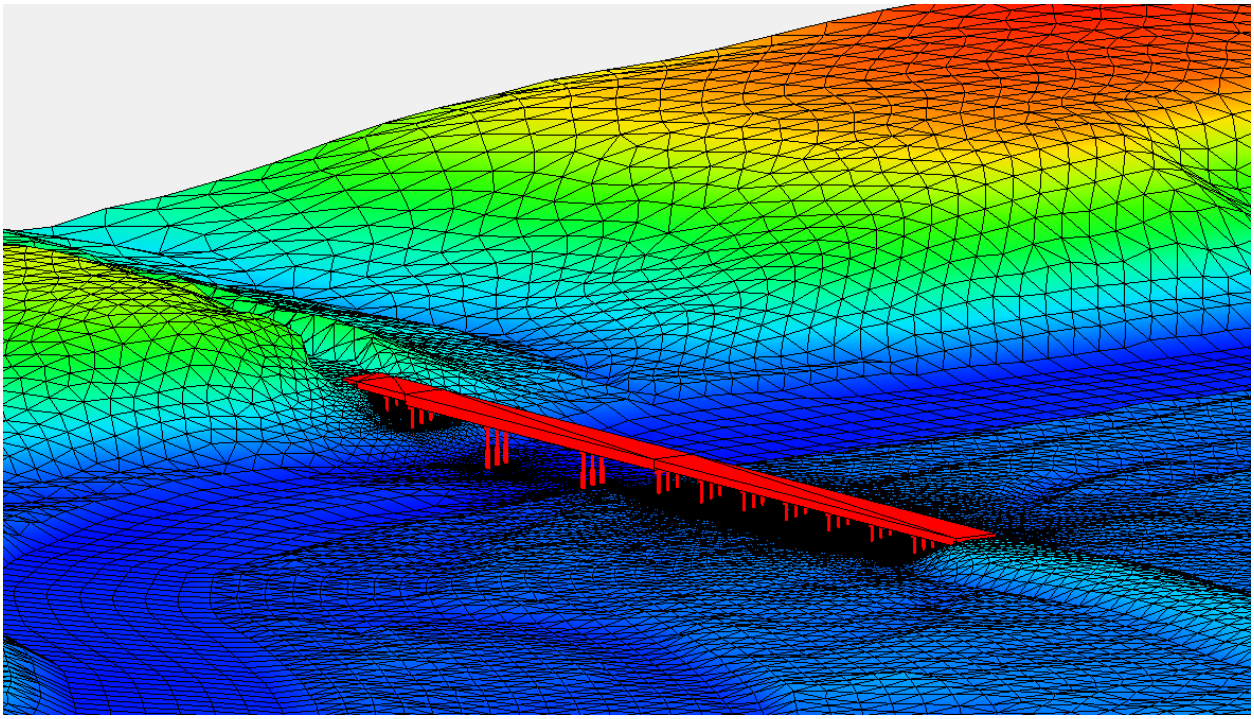

WATER INSTITUTE
SAINT LOUIS UNIVERSITY

Award Identification Number: TR202017

Submitted by:

WATER Institute
Saint Louis University
3450 Lindell Blvd.
St. Louis, MO 63103

Submitted to:

Missouri Department of Transportation
Research, Development & Technology
1671 Missouri Blvd
Jefferson City, MO 65102

[1]Saint Louis University, WATER Institute
[2]Saint Louis University, Civil Engineering

Copyright Permissions

Authors herein are responsible for the authenticity of their materials and for obtaining written permissions from publishers or individuals who own the copyright to any previously published or copyrighted material used herein.

Disclaimer

The opinions, findings, and conclusions expressed in this document are those of the investigators. They are not necessarily those of the Missouri Department of Transportation, U.S. Department of Transportation, or Federal Highway Administration. This information does not constitute a standard or specification.

Acknowledgments

The authors would like to acknowledge the Missouri Department of Transportation for funding this study. We would also like to thank Kelly Brady, Matt Williams, and Eric Looper from the USGS for their assistance with bedload sampling and Scott Hogan from the FHWA for his support with the hydraulic modeling and scour analysis. Finally, the authors would also like to acknowledge the following SLU undergraduate students for their contributions to field data collection and 1-D hydraulic modeling: Warren Radford, Chloe Groner, Jose Mattingly Hernandez, Emilio Mattingly Hernandez, and Laura Gray.

TABLE OF CONTENTS

LIST OF FIGURES

LIST OF TABLES

EXECUTIVE SUMMARY

This study examines the analysis methods to estimate bridge scour in Missouri bridges. In the 1990s the Missouri Department of Transportation (MoDOT) engaged in a project to assess the bridge scour for about 200 bridges in their highway network. This study consisted of 1-D hydraulic modeling and scour analysis of the riverine systems crossed by the respective bridges. These previous studies used the WSPRO software and incorporated only four cross sections for each model. Since then, the analysis methods and data available have changed significantly meriting a re-evaluation of how to conduct bridge scour analysis. The research objectives of this study included the following:

- Provide recommendations for sediment/soil sampling methods;
- Compare scour estimates computed using 1-D and 2-D hydraulic modeling approaches; and
- Conduct a risk assessment, due to scour, for the bridges studied by the project.

The first phase of the project involved the selection of bridge sites for detailed study. Initially, ten sites were selected for a preliminary site reconnaissance and further screening. In collaboration with the MoDOT Technical Advisory Council for this project and personnel from the Research Section, the final selection of five bridge sites was made to undergo detailed analysis. The selected sites varied in bridge size and typology, from 40 feet to over 1,000 feet in bridge length.

Following the selection process, the research team focused on collecting field data and assembling data from existing data sources for the five bridge sites. The geologic, mapping, and topographic (lidar) information available was collected from the different sources and compiled for each bridge site. The field data collected consisted of soil/sediment samples, bathymetry data (ADCP), GPS data, ground-based lidar, and structural information.

The collected field data were processed and prepared for use in the hydraulic modeling and scour analysis methods. The soil/sediment samples were analyzed in the geotechnical laboratories to determine the soil parameters needed for soil classification and scour analysis. The topographic and bathymetric information from the field and other sources were assembled into one terrain model of the riverbed and floodplain for each site. Several techniques were involved in stitching (or joining) the different datasets for below water (bathymetry) and overbank terrain (topography).

Once the datasets were assembled, hydraulic modeling was conducted using 1-D and 2-D methods. Two storm events were evaluated for every simulation conducted for this study, 100- and 500-yr storms. The 1-D hydraulic models included WSPRO (from the previous MoDOT studies) and HEC-RAS, and SRH-2D was used as the 2-D model. The hydraulic parameters computed by the models were used as input for the scour calculations, which were facilitated by the FHWA's Hydraulic Toolbox software program. All HEC-RAS and SRH-2D scour calculations were conducted in accordance with the HEC-18 fifth edition guidelines, while the previous WSPRO studies used methods from the fourth edition of HEC-18. The resulting contraction, abutment, pier scour, and total scour estimates were evaluated and plotted along the cross-section of the bridge including structural elements, such as girders, bents, pile caps, piles, and abutments.

The recommended methods for soil/sediment sampling in the overbank areas were soil augers or test pits and over water with a FISP or clamshell sampler. The overall locations are on the upstream side of the bridge about 20 ft in front of every bridge bent, including the abutment bents. The depth of sampling of the near-surface erodible materials is sufficient to a depth of 3 feet. This provides adequate variability of soil conditions that match the input for the scour calculations.

One of the important final tasks was to assess the risk caused by the predicted scour upon the bridge structure. Given that each bridge has a unique foundation, these assessments were done individually for the soil, bedrock, and foundation conditions.

A comprehensive comparison of computed scour results from the different hydraulic modeling methods (1-D WSPRO, 1-D HEC-RAS, and 2-D SRH-D) was conducted. Key findings from comparing model results were: 1) the angle of attack was the dominant pier scour input parameter (automatically computed with 2-D modeling but difficult to estimate with 1-D modeling) and 2) flow conveyance over inundated roadway embankments was significantly greater for SRH-2D relative to the HEC-RAS model, resulting in the HEC-RAS models computing higher discharges and velocities through the bridge opening. Further, the contrast between user interfaces of the different models proved to be challenging when using HEC-RAS for 1-D hydraulic modeling. Selecting cross-section locations near bridges was difficult for many of the sites due to the river meandering and roadway orientation. Preparing model input parameters for each cross-section of the 1-D model (e.g., roughness values and ineffective flow areas) was also significantly more tedious in comparison to the 2-D input methods. The ability of the Hydraulic Toolbox software program to automatically determine input parameters for scour calculations directly from the SRH-2D output data format made nearly all inputs significantly easier, faster, and more accurate than determining input parameters from 1-D model outputs. To use Hydraulic Toolbox with input parameters from HEC-RAS, each input was either manually copied from the 1-D model results or manually computed using flow hydraulic parameters available from the 1-D model results. In these manual computations of input scour parameters, many potential sources of human error would threaten the validity of the results if the complicated specified procedures were not followed.

It was concluded that given the new availability of terrain data, current computing resources, and ease of use, the 2-D modeling methods are recommended for future use at MoDOT. It is recognized that advanced training in handling complex data sets of terrain and data collection at bridge sites may be pertinent for in-house staff or some consultants. Further, due to the differences in the HEC-RAS and SRH-2D estimated scour depths, reanalyzing high-risk and/or visually vulnerable bridges is recommended.

1 INTRODUCTION

Ground transportation and dynamic river networks have complex intersections that require bridges to enable safe passage across water conveyance channels. Throughout Missouri, approximately 10,000 bridges exist in the state transportation system in addition to another 15,000 bridges on local roads. Erosion of bridge foundations, also known as bridge scour, is the leading cause of bridge failure in the United States (Arneson et al., 2012). Total scour at a bridge is the result of three different types of scour processes: 1) long-term bed degradation caused by regional channel instability, 2) contraction scour caused by flow contraction through a narrowed bridge opening, and 3) local scour caused by flow acceleration and increased hydrodynamic forces around bridge piers and abutments. Bridges threatened by scour, termed "scour critical", can be identified using the National Bridge Inspection Standards (NBIS). The scour vulnerability of a structure is rated using a scale that progresses from "no threat of scour" to "failed bridge due to scour". A scour critical bridge is one deemed unstable due to observed scour or scour potential determined from a scour evaluation study. Bridge scour evaluations, a part of the NBIS, aid in predicting the depth and size of scour that will occur at bridge sites during extreme flood events.

Bridge scouring is a complex, three-dimensional process that historically has been evaluated using one-dimensional (1-D) hydraulic analysis techniques coupled with empirical relationships from laboratory data and a single sediment sample collected from the streambed (Arneson et al., 2012). Over the past decade, the FWHA has been promoting the use of two-dimensional (2-D) hydraulic modeling (e.g., Sedimentation and River Hydraulics Two-Dimensional (SRH-2D) program) for hydraulic analysis instead of 1-D models as computational efficiencies have increased and the data necessary to support 2-D models, such as lidar data, have become more prevalent (FHWA, 2019). The quality and amount of input data, such as topography and channel bathymetry, were previously limited by available technology and data collection inefficiencies. Compared to modern techniques, former data collection methods were time-consuming and expensive, and generally provided low-resolution data. Topographic/bathymetric data are now available at greater convenience with enhanced resolution capabilities, making the use of more accurate hydraulic models less expensive and more accessible. Currently, a limited number of studies have compared different modeling methods and input data resolutions for estimating bridge hydraulic conditions and associated scour (Garcia-Santiago, 2021; Yu, 2008; Deal, 2017).

The primary objectives of this project were to:

- Provide recommendations for sediment/soil sampling collection methods including sampling locations and depths.
- Compare scour estimates computed from:
    - 1-D low-resolution hydraulic models (WSPRO) with a single sediment sample,
    - 1-D high-resolution hydraulic models (HEC-RAS) with sediment samples collected at several locations within the approach cross section, and
    - 2-D hydraulic models (SRH-2D) with sediment samples collected at several locations within the approach cross section; and
- Conduct a risk assessment, due to scour, for the bridges studied by the project.

To meet the project objective, the following tasks were completed:

- a literature review of past and present scour modeling methods and similar studies;
- a selection of five bridges sites in Missouri that represent a broad spectrum of field conditions;
- data collection for the five sites, including compilation of existing data (e.g., lidar, bridge plans, and borehole data) and field data collection (e.g., sediment samples, bathymetry, and GPS coordinates);

- numerical hydraulic modeling using 1-D and 2-D computer software programs;
- scour estimation based on hydraulic modeling results; and
- a comparison of methods and results.

This report details the tasks completed to address the above objectives and is organized to present the following information: background information (Chapter 2), selection of study site locations (Chapter 3), field data collection and processing methods (Chapter 4), methods used for hydraulic and scour analysis (Chapter 5), results of hydraulic and scour analysis (Chapter 6), discussion of results (Chapter 7), and conclusions and recommendations for future research (Chapter 8). The bulk of the detailed results are shown in the appendices as high-resolution color graphics, but highlighted results and examples are presented within the body of the report.

2 BACKGROUND AND LITERATURE REVIEW

Various methods have been developed to analyze bridge scour, each with its strengths and limitations. The most commonly employed approach is one-dimensional (1-D) or two-dimensional (2-D) numerical modeling of hydraulic conditions (e.g., approach flow depth and approach velocity) coupled with empirical equations to estimate the scour depth. In addition to this method, other methods for estimating scour include physical modeling and numerical hydraulic modeling that includes sediment transport processes that can simulate the erosion of the bed material over time. Construction and operation of physical models are generally time-consuming and cost prohibitive for bridge scour analysis but are used for high-risk sites that have complex pier scour conditions such as unique pier shapes or multiple adjacent piers that may generate complex flow conditions. Process-based numerical modeling of scour has significant potential but requires bed material erosion input properties which can be difficult to estimate such as critical velocity and/or shear stress for erosion and erosion rate. This section details the different types of numerical modeling used for bridge scour analysis and provides information on the empirical analysis methods used to estimate scour.

2.1 Numerical Hydraulic Modeling Methods

For bridge scour analysis, numerical hydraulic models are used to estimate hydraulic conditions near the bridge site which are then used as inputs into empirical equations to estimate scour depths. Numerical hydraulic models currently used to calculate pier and abutment scour at bridges over rivers fall into one of three categories: 1-D, 2-D, or 3-D, as shown in Figure 2-1. Each model type incorporates an increasing level of data and demand for computational capacity, with 3-D being the most comprehensive at capturing flow conditions. Though 3-D models are the most detailed, they are not always necessary or feasible, which is why 1-D and 2-D models are more commonly used. The limited use and documentation of 3-D models to predict scour has also prevented industry adoption of the practice.

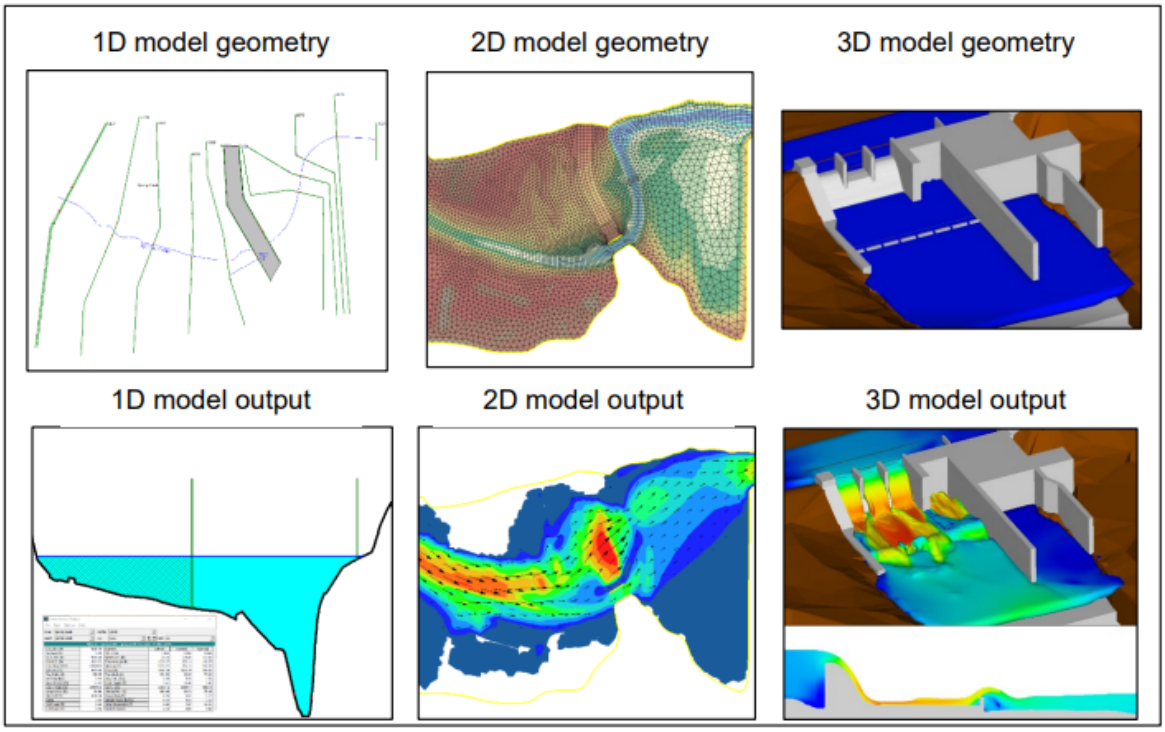

Figure 2-1: Example 1-D, 2-D, and 3-D model geometry and output (FHWA, 2019).

Before the implementation of computer software in hydraulic modeling, the standard-step numerical method calculated water surface profiles and flow conditions using the principles of conservation of mass and conservation of energy (Chow, 1959). The US Army Corps of Engineers (USACE) Hydraulic Engineering Center (HEC) developed software in the late 1960s which utilized Chow's standard-step method to compute water surface profiles. This popular program known as "HEC-2 Water Surface Profiles" (USACE, 1991) evolved and became available in 1984. HEC-2 initiated a transition in the US from mathematical equations to numerical models for performing bridge hydraulic analyses (FHWA, 2019).

The original modeling software programs, including HEC-2, were only capable of computing cross-section averaged flow velocity in one-dimension, the streamwise direction. Water-Surface PROfile (WSPRO), another 1-D model developed by the FHWA and USGS, was built with an emphasis on bridge waterways (FHWA, 1998). HEC's River Analysis System (HEC-RAS) replaced HEC-2 in 1995 with an advanced graphical user interface while incorporating aspects of the WSPRO bridge modeling methodology. Though the assumption of strictly streamwise flow may be accurate for channels of uniform flow and geometry, most natural river systems – especially those containing complex bridge openings, behave differently than the model assumes. Therefore, model outputs provide little insight into the actual 3-D flow interacting with bridge piers, abutments, and roadways.

2.1.1 HEC-RAS Analysis Methods

HEC-RAS uses the standard step hydraulic analytical method to compute water surface profiles and associated flow depths and flow velocities at defined cross-section locations along a river reach (Brunner, 2016). For steady-state subcritical flow, the standard step method input requires a downstream water surface elevation and a flow rate. With a known downstream hydraulic condition, the water surface elevation at the next upstream cross section is computed using conservation of energy principles coupled with the Manning's equation to estimate energy loss between the two cross sections. The following is the conservation of energy equation form used in HEC-RAS:

$$z_2 + y_2 + \frac{\propto_2 V_2^2}{2g} = z_1 + y_1 + \frac{\propto_1 V_1^2}{2g} + h_e \qquad \text{Eq. (2.1)}$$

where z is the elevation of the main channel inverts (ft); y is the depth of water (ft); V is the average velocity (ft/s); $\propto$ is the velocity weighting coefficient; g is the gravitational constant; and h_e is the energy head loss (ft). Subscripts 1 and 2 denote the downstream and upstream cross-section locations, respectively. The energy loss term, h_e, is composed of the friction losses and expansion or contraction losses:

$$h_e = L\bar{S_f} + C\left(\frac{\propto_2 V_2^2}{2g} - \frac{\propto_1 V_1^2}{2g}\right) \qquad \text{Eq. (2.2)}$$

where L is the discharge weighted reach length (ft); $\bar{S_f}$ is the average friction slope between two cross sections (computed using the average conveyance method); C is the expansion or contraction loss coefficient; and all other terms have been previously defined. The average friction slope is computed using the average conveyance method as shown in Eq. 2.3:

$$\bar{S_f} = \left(\frac{Q_1 + Q_2}{K_1 + K_2}\right)^2 \qquad \text{Eq. (2.3)}$$

where Q is the flow rate and K is the conveyance as defined by:

$$K = \frac{1.486}{n} A R^{\frac{2}{3}} \quad \text{Eq. (2.4)}$$

where n is the Manning's roughness coefficient; A is the flow area (ft^2); and R is the hydraulic radius (ft).

Using the standard step method, calculations progress upstream from cross section to cross section. The resulting output data includes the water-surface profile along the reach and flow depths and flow velocities at each cross section for the channel, left overbank (LOB), and right overbank areas (ROB).

2.1.2 SRH-2D Analysis Methods

SRH-2D uses the 2-D steady-state St. Venant equations (also known as the shallow water equations) which are based on conservation of momentum and conservation of mass principles coupled with depth-averaged velocities (Lai, 2008). The 2-D steady-state St. Venant equations are given as the following:

$$\frac{\partial h}{\partial t} + \frac{\partial hU}{\partial x} + \frac{\partial hV}{\partial y} = 0 \quad \text{Eq. (2.5)}$$

$$\frac{\partial hU}{\partial t} + \frac{\partial hUU}{\partial x} + \frac{\partial hVU}{\partial y} = \frac{\partial hT_{xx}}{\partial x} + \frac{\partial hT_{xy}}{\partial y} - gh\frac{\partial z}{\partial x} - \frac{\tau_{bx}}{\rho} + D_{xx} + D_{xy} \quad \text{Eq. (2.6)}$$

$$\frac{\partial hV}{\partial t} + \frac{\partial hUV}{\partial x} + \frac{\partial hVV}{\partial y} = \frac{\partial hT_{xy}}{\partial x} + \frac{\partial hT_{yy}}{\partial y} - gh\frac{\partial z}{\partial y} - \frac{\tau_{by}}{\rho} + D_{yx} + D_{yy} \quad \text{Eq. (2.7)}$$

where h is flow depth (ft); t is time (s), x and y are horizontal Cartesian coordinates; U and V are depth-averaged velocity components in x and y directions, respectively, T_{xx}, T_{xy}, and T_{yy} are depth-averaged stresses due to turbulence stress (lb/ft^2); and D_{xx}, D_{xy}, D_{yx} and D_{yy} are dispersion terms due to depth averaging (ft^2/s^2), ρ is water density (slugs/ft^3), and τ_{bx} and τ_{by} are the bed shear stresses (lb/ft^2). Bed friction components are computed using the following form of the Manning's equation:

$$\begin{pmatrix}\tau_{bx}\\ \tau_{by}\end{pmatrix} = \rho\left(\frac{gn^2}{h^{1/3}}\right)\begin{pmatrix}U\\ V\end{pmatrix}\sqrt{U^2+V^2} \quad \text{Eq. (2.8)}$$

where n is the Manning's roughness coefficient and other terms have been previously defined. Lai (2008) provides additional information on how turbulent stress and dispersion terms are computed.

The governing equations (Eq. 2.5 – Eq. 2.7) are discretized using the finite-volume approach. The solution domain is an unstructured mesh (quadrilateral or triangular elements) for which all dependent variables are stored at the center of the polygon. To compute a solution, Eq. 2.5, 2.6, 2.7, and 2.8 are integrated over the elements using the Gauss theorem. Additional information on this process is available in the SRH-2D theory and user's manual (Lai, 2008). Key SRH-2D output values include water-surface elevation, flow depth, and flow velocity at the center of each element.

2.2 Bridge Scour Calculation Methods

Three different mechanisms can cause bridge scour: long-term degradation, contraction scour, and local scour around piers and abutments. These different types of scour are combined to determine an estimated cross-section bed elevation after a storm event known as a scour prism. The following sections review the available methods most commonly used to calculate bridge scour, which are the methods used in this study.

2.2.1 Contraction Scour

Contraction scour occurs when the flow area is decreased (i.e., contracted) at a bridge section relative to the approach flow conditions. This phenomenon causes increased unit discharge rates and associated flow velocities that result in increased transport capacity and bed material erosion. Contraction scour is classified and evaluated as either a live-bed, clear-water, or pressure flow condition. Generally, live-bed contraction scour occurs when the flow velocity in the upstream approach section is greater than the critical flow velocity for D_{50} transport, and clear-water contraction scour occurs when the flow velocity in the upstream approach section is less than the critical flow velocity for D_{50} transport. Eq. 2.9 is the equation provided by HEC-18 to compute the critical velocity of the median particle size, V_c:

$$V_c = 11.17 y^{1/6} D_{50}^{1/3} \qquad \text{Eq. (2.9)}$$

where y is the average flow depth upstream of the bridge (ft); and D_{50} is the median grain particle size. Armoring of the bed by large sediment particles may limit live-bed contraction scour depths. Accordingly, HEC-18 recommends computing both live-bed and clear-water contraction scour depths and using the smaller of the two values. Pressure flow occurs when the bottom of the bridge deck is submerged and the flow area under the bridge is acting as an orifice. For the pressure flow conditions, contraction scour should be computed using the pressure-flow analysis, live-bed analysis, and clear-water analysis method and the largest of the computed scour depths is used for design.

2.2.1.1 Live-Bed Contraction Scour

For live-bed contraction scour, HEC-18 uses the following formula to compute the flow depth in the contracted section following scour, y_2 (i.e., original flow depth in contract section plus contraction scour depth):

$$\frac{y_2}{y_1} = \left(\frac{Q_2}{Q_1}\right)^{6/7} \left(\frac{W_2}{W_1}\right)^{k_1} \qquad \text{Eq. (2.10)}$$

where y_1 is the average flow depth in the upstream main channel (ft); y_2 is the average flow depth in the contracted section (ft); y_0 is existing flow depth in the contracted section prior to scour (ft); Q_1 is the flow in the upstream channel transporting sediment (cfs); Q_2 is the flow in the contracted channel (cfs); W_1 is the bottom width of the upstream main channel that is transporting bed material (ft); W_2 is the bottom width of the main channel in the contracted section minus the pier widths (ft); and k_1 is an exponent determined by the mode of bed material transport. Although Eq. 2.10 is not a complicated formula, several nuances should be considered when determining the input values for each variable. HEC-18 goes into significant detail about how the input values are determined for various conditions.

2.2.1.2 Clear-Water Contraction Scour

For clear-water contraction scour, HEC-18 uses the following formula to compute the flow depth in the contracted section following scour, y_2:

$$y_2 = \left[\frac{0.0077 Q^2}{D_m^{2/3} W^2}\right]^{3/7} \qquad \text{Eq. (2.11)}$$

where Q is the discharge through the bridge or on the set-back overbank area at the bridge associated with the width, W (ft); D_m is the diameter of the smallest non-transportable particle in the bed material

(estimated as $1.25D_{50}$) in the contracted section (ft); and W is the bottom width of the contracted section minus pier widths (ft).

2.2.1.3 Pressure Flow Contraction Scour

To compute scour depth for pressure flow conditions, initially a y_2 value is computed using either Eq. 2.10 for live-bed conditions or Eq. 2.11 for clear-water conditions. The separation zone thickness is then computed using the following formula:

$$\frac{t}{h_b} = 0.5\left(\frac{h_b h_t}{h_u^2}\right)^{0.2}\left(1-\frac{h_w}{h_t}\right)^{-0.1} \qquad \text{Eq. (2.12)}$$

where h_b is the vertical size of the bridge opening prior to scour (ft); h_t is the distance from the water surface to the lower face of the bridge girders (ft); h_w is the weir flow height ($h_w = h_t - T$ for $h_t > T$ or $h_w = 0$ for $h_t < T$); T is the height of the obstruction including girders, deck, and parapet. The pressure flow contraction scour depth is then computed as follows:

$$y_s = y_2 + t + h_b \qquad \text{Eq. (2.13)}$$

Figure 2-2 is a schematic illustrating the variables used in the pressure flow contraction scour analysis. As with the other contraction scour analysis methods, HEC-18 provides several additional considerations that can influence the values that should be used in the calculations.

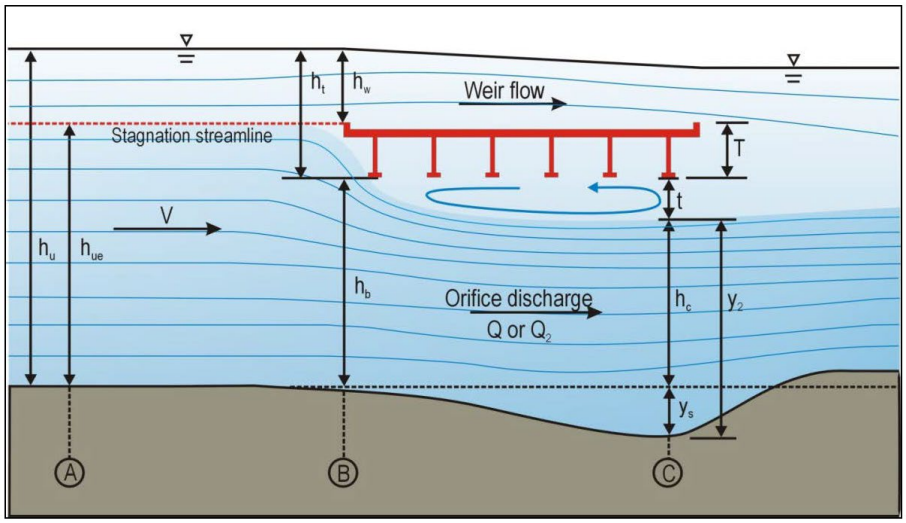

Figure 2-2. Schematic illustrating variables used in the pressure flow contraction scour analysis (from Arneson, 2012)

2.2.2 Abutment Scour

The National Cooperative Highway Research Program (NCHRP) (2010) method detailed in HEC-18 was used for abutment scour computations. This method defines three types of abutment scour conditions: (a) scour occurring when the abutment is in or close to the main channel (type A), (b) scour occurring when the abutment is set back from the main channel (type B), and (c) scour occurring when the embankment breaches and the abutment foundation acts as a pier (type C). Scour conditions (a) and (b) were used for this study. Figure 2-3 shows an illustration of the conditions (a) and (b) from HEC-18.

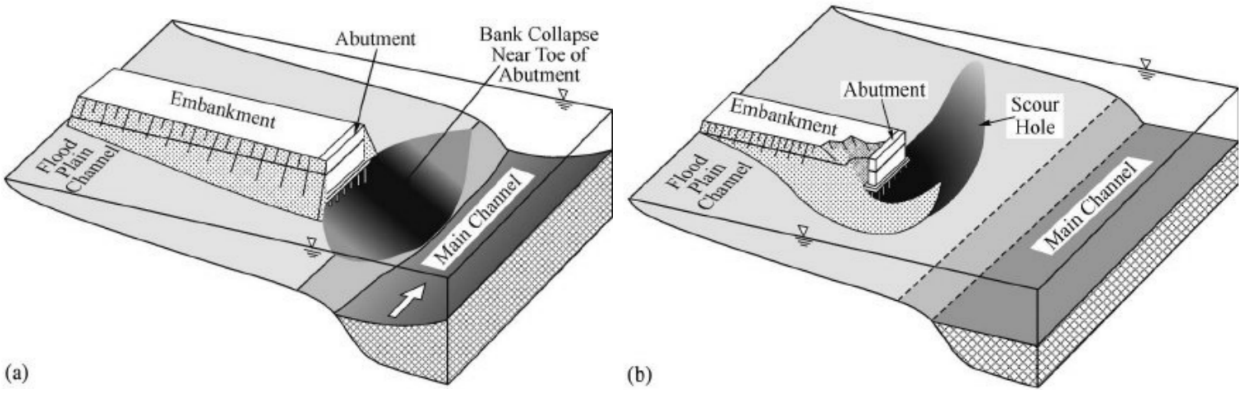

Figure 2-3. Schematics illustrating abutment scour conditions for (a) type A abutment configuration and (b) type B abutment configuration (adapted from Arneson et al., 2012)

The NCHRP (2010) abutment scour approach applies an amplification factor to a simplified contraction scour estimate (not the actual computed contraction scour). Eq. 2.14 provides the equation to compute the maximum flow depth resulting from abutment scour in ft, y_{max} :

$$y_{max} = \alpha_A y_c \text{ or } y_{max} = \alpha_B y_c \quad \text{Eq. (2.14)}$$

where α_A is the amplification factor for scour conditions (a); α_B is the amplification factor for scour condition (b); and y_c is the flow depth including the simplified live-bed or clear-water contraction scour estimate (ft). Eq 2.15 is then used to compute the abutment scour depth in ft, y_s :

$$y_s = y_{max} - y_0 \quad \text{Eq. (2.15)}$$

where y_0 is the flow depth prior to scour (ft). For scenarios with a projected embankment length greater than 75% of the floodplain width (i.e., condition (a)), Eq. 2.16 is used to compute the flow depth including the simplified contraction scour estimate, y_c :

$$y_c = y_1 \left(\frac{q_2}{q_1}\right)^{6/7} \quad \text{Eq. (2.16)}$$

where y_1 is the upstream flow depth (ft); q_2 is the unit discharge in the constricted opening accounting for non-uniform flow distribution (ft²/s); and q_1 is the upstream unit discharge (ft²/s). For scenarios with a projected embankment length less than 75% of the floodplain width (i.e., condition (b)), Eq. 2.17 is used to compute y_c :

$$y_c = \left(\frac{q_2}{11.17 D_{50}^{1/3}}\right)^{6/7} \quad \text{Eq. (2.17)}$$

where q_2 is the unit discharge in the constricted opening accounting for non-uniform flow distribution (ft²/s) and all other variables have been previously defined.

The amplification factors, α_A and α_B are determined from charts as a function of the abutment shape (spill-through or wingwall) and the q_2/q_1 ratio. The amplification factors range from approximately 1.1 to 2.6 depending on the conditions. Since the NCHRP (2010) method uses a simplified approach to compute the contraction scour prior to amplification, the contraction scour computed by the methods detailed in Section 2.2.1 may result in a scour depth larger than the computed abutment scour depth. In this case, the larger contraction scour depth is the controlling scour depth value.

2.2.3 Pier Scour

Pier scour is caused by flow acceleration near the channel obstruction. Figure 2-4 illustrates the scour process using flow lines. Flow lines approaching the pier are deflected down and around the pier stem causing 3-D vortices that progress downstream. The largest scour depth occurs immediately upstream of the pier caused by the downward flow acceleration at that location. The vortices extend the scour hole downstream of the pier stem. Pier scour depths are dependent upon approach flow conditions, pier geometry, and bed material. HEC-18 provides pier scour calculation methods for several conditions including a simple pier structure with granular bed material, a complex pier structure with granular bed material, a simple pier structure with coarse-bed material, and a simple pier structure with cohesive bed material. To provide the largest number of data points for comparison of modeling methods and to maintain consistency with the original WSPROs studies, the cohesive pier scour method was not employed in this study. The following sections detail the analysis methods for the simple pier, complex pier, and coarse bed pier conditions. As recommended by the fifth edition of HEC-18 (Arneson et al., 2012), the thalweg hydraulic conditions were used for calculations at each pier as the thalweg may migrate laterally during large flow events. This contrasts with the HEC-18 fourth edition method that uses local hydraulic conditions to compute scour, which was used in the WSPRO studies (Richardson and Davis, 2001).

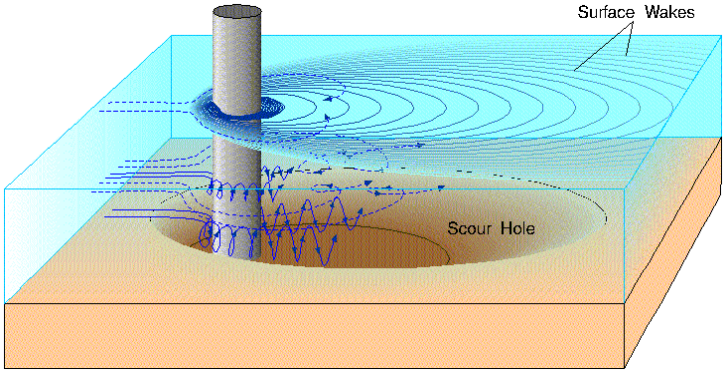

Figure 2-4: Illustration of flow dynamics causing scour at a bridge pier (from Amini, 2016).

2.2.3.1 Simple Pier Scour Analysis Method

The HEC-18 pier scour equation was used to compute scour depths for simple pier structures with non-coarse bed material or complex piers that did not have the pile cap exposed by the computed contraction scour depth. The HEC-18 formula to compute pier scour depth, y_s, in ft is shown in Eq. 2.18:

$$\frac{y_s}{y_1} = 2.0 K_1 K_2 K_3 \left(\frac{a}{y_1}\right)^{0.65} Fr_1^{0.43} \qquad \text{Eq. (2.18)}$$

where y_1 is the flow depth directly upstream of the pier (ft); K_1 is the correction factor for pier nose shape; K_2 is the correction factor for flow angle of attack; K_3 is the correction factor for bed condition; a is the pier width (ft); L is the pier length (ft); Fr_1 is the Froude number as defined by $V_1/\sqrt{gy_1}$; V_1 is the mean flow velocity directly upstream of the pier (ft/s). The pier nose shape correction factor, K_1, ranges from 0.9 for a sharp nose to 1.1 for a square nose. The flow angle of attack correction factor is computed using Eq. 2.19:

$$K_2 = \left(\cos\theta + \frac{L}{a}\sin\theta\right)^{0.65} \qquad \text{Eq. (2.19)}$$

where θ is the flow angle of attack and all other terms have been previously defined. The correction for bed conditions, K_2, is determined by the channel bedforms and ranges from 1.1 for plane bed conditions to 1.3 for large dunes.

2.2.3.2 Complex Pier Scour Analysis Method

The complex pier scour analysis method was used for complex pier structures that had the pile cap exposed by the computed contraction scour. The complex pier scour analysis method determines the total pier scour depth by computing and adding scour depths associated with each pier component (i.e., pier stem, pile cap, and piles). The method is used when the pile cap is exposed by the computed contraction scour. The method is called "superposition of scour components" and computes and sums scour depths associated with bridge components that are exposed to flow. The following formula is used to compute the total scour depth from superposition of the pier components, y_s, in ft:

$$y_s = y_{s\,pier} + y_{s\,pc} + y_{s\,pg} \qquad \text{Eq. (2.20)}$$

where $y_{s\,pier}$ is the scour component for the pier stem in the flow (ft); $y_{s\,pc}$ is the scour component for the pier cap or footing in the flow (ft); and $y_{s\,pg}$ is the scour component for the piles exposed to the flow (ft). Scour depths for each of the components are computed using the simple pier scour equation (Eq. 2.18) with an equivalent sized pier that accounts for the irregular pier components, modified flow depths and velocities, and height adjustments for the pier stem and pile group. The method is fully described in Arneson et al. (2012) but not included herein due to the complexity of the analysis and the report space limitations.

2.2.3.3 Coarse-Bed Pier Scour Analysis Method

The coarse-bed pier scour calculation method was used to compute scour depths for simple pier structures with clear-water conditions and bed material with a D_{50} greater than or equal to 20 mm and a sediment gradation coefficient ($\sigma = D_{84}/D_{50}$). Eq. 2.21 provides the formula to compute coarse-bed pier scour depth, y_s, in ft:

$$y_s = 1.1 K_1 K_2 a^{0.62} y_1^{0.38} \tanh\left(\frac{H^2}{1.97\sigma^{1.5}}\right) \qquad \text{Eq. (2.21)}$$

where K_1, K_2, a, y_1, and V_1 are defined in Eq. 2.18; H is the densimetric particle Froude number ($V_1/\sqrt{g(S_g - 1)D_{50}}$); S_g is the sediment specific gravity; and all other terms have been previously defined.

2.3 Comparisons of 1-D and 2-D Hydraulic Modeling for Bridge Scour

Prior studies have compared scour estimations between 1-D and 2-D numerical hydraulic models. A study of a singular bridge site in Puerto Rico (Garcia-Santiago, 2021) compared scour outputs using the same 1-D and 2-D modeling software – HEC-RAS and SRH-2D. On this occasion, only the output hydraulic conditions of SRH-2D were input to the FHWA's Hydraulic Toolbox to estimate scour. Scour depths between the two models varied by more than 50% in some instances, and so did the hydraulic conditions used to estimate scour, such as velocity in the approach section and flow depth directly upstream. The study determined the outputs of SRH-2D to be more accurate since the program automatically calculates variables that must be estimated and manually entered into HEC-RAS, including skew angle of abutments, angle of attack of the piers, ineffective areas, and contraction/expansion coefficients, among others.

Prior to SRH-2D, Flo2dh, part of the FHWAs Finite Element Surface-water Modeling System (FESWMS), was a 2-D model built specifically to predict hydraulic conditions and bridge scour. Flo2dh did not see widespread utilization due to difficulty in use. There were few instances of actual model

applications which were subjected to field verification (Yu, 2008). HEC-RAS, a 1-D model, proved much simpler to set up and therefore preferred.

Another comparison between HEC-RAS and SRH-2D took into consideration results from various bridge sites, finding the simulation duration of SRH-2D may be prohibitively time-consuming (Deal, 2017). SRH-2D predicted deeper scour than HEC-RAS across the different study sites, possibly due to significant differences in flow divisions through multiple bridge openings (Deal, 2017).

3 STUDY BRIDGE SITES

3.1 Bridges Selected for Preliminary Field Site Visits

In consultation with the MoDOT Technical Advisory Committee and Project Manager, ten potential bridge sites were initially identified for the study. Sites were selected to provide a broad representation of the different site conditions throughout Missouri. The key elements of interest were bridge size, bridge skew relative to the river flow path, and bed material composition. The availability of bathymetric data was also a consideration for site selection. A map of the ten recommended bridge sites for preliminary field site visits is shown in Figure 3-1 and Table 3-1 lists the bridge names and other relevant details for each of the ten sites. The following summarizes some of the key details for the selected sites:

- Bathymetric Data Available: four sites have USGS bathymetric data (A-1411, A-3760, L-0550, and A-4497).
- Bed Material: based on surficial geologic information, four sites likely have cohesive riverbed material (A-3618, H-0024, J-0287, and L-0564), and the remaining six sites likely have cohesionless riverbed sediments.
- Bridge Skew: three sites are likely skewed based on visual inspection of aerial imagery (H-0024, L-0022, and L-0564).
- Bridge Size Classification: two sites are major bridges with lengths greater than 1000 ft (A-4497 and L-0550), the remaining eight sites are typical bridges with lengths between 20 and 999 ft.

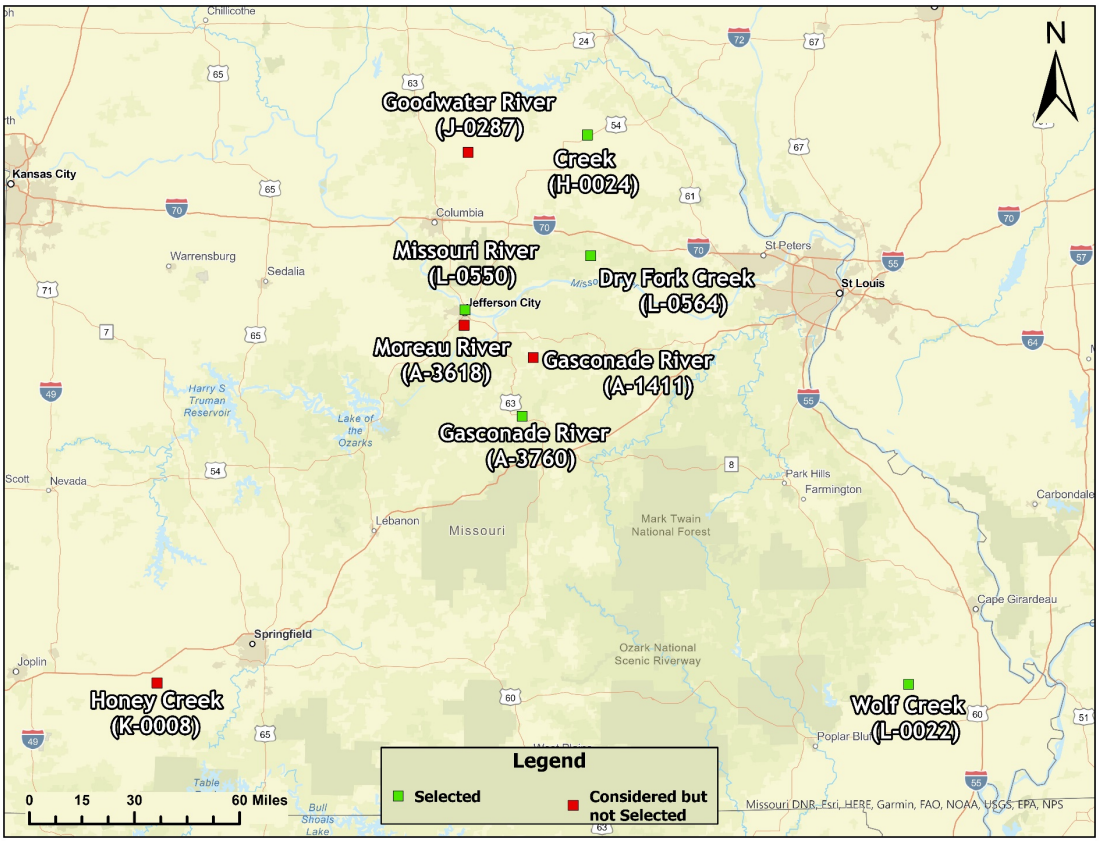

Figure 3-1: Map of bridge sites recommended for preliminary field site visits.

Table 3-1. Reconnaissance of the ten initial bridge sites identified.

Bridge ID	Route	River Crossing	County	Scour Category	USGS Data	Bathy-metry Data	Bridge Length (ft)	Likely Cohesive	Ozarks Location	Size Class.	Skew (deg)
A-1411	MO 89 S	Gasconade River	Osage	C	Y	Y	792	N	Y	Typical Bridge	0
A-3618	RT B S	Moreau River	Cole	C	Y	N	474	Y	Y	Typical Bridge	0
A-3760	US 63 S	Gasconade River	Maries	A	N	Y	994	N	Y	Typical Bridge	0
A-4497	US 54 E	Missouri River	Cole	B	Y	Y	3124	N	Y	Major Bridge	0
H-0024	RT P S	Creek	Audrain	D	N	N	45	Y	N	Typical Bridge	0
J-0287	MO 151 S	Goodwater Creek	Audrain	C	N	N	87	Y	N	Typical Bridge	0
K-0008	MO 39 S	Honey Creek	Lawrence	A	N	N	297	N	N	Typical Bridge	0
L-0022	MO 25 S	Wolf Creek	Stoddard	A	N	N	77	N	Y	Typical Bridge	40
L-0550	US 54 W	Missouri River	Callaway	C	Y	Y	3093	N	Y	Major Bridge	0
L-0564	RT K E	Dry Fork Creek	Montgo-mery	C	N	N	236	Y	N	Typical Bridge	35

3.2 Reconnaissance to Preliminary Bridge Sites

Field reconnaissance visits to each bridge site were conducted to visually evaluate accessibility, upstream and downstream hydraulics conditions, bridge geometries, and bed and bank sediment material. The research team in collaboration with MoDOT personnel at each district conducted initial reconnaissance at each site. Through the Research Section team, the respective districts were contacted to secure support for the site visits for the ten sites initially selected following the above criteria and availability of data. These bridge site reconnaissance visits served to document the field conditions at each site. General information was collected for the purpose of further reducing the list to the selected five bridge sites. During each site visit, notes were taken regarding the geological features, site access, water levels, canopy, and general conditions of the bridge compared to the plans.

3.3 Final Selection of Bridge Sites

Based on the field site visits, five bridge sites were recommended in consultation with the MoDOT Technical Advisory Committee and Project Manager. The selection process resulted in the five bridge sites representing several bridge types from major, typical, to small bridges. They are in different physiographic regions: SE Lowlands, Ozarks, and Glaciated Plains. One bridge was originally selected in the Western Plains, but it did not rank high enough to make the top five bridges. Figure 3-1 shows the locations of the sites selected with a red marker. Further, Table 3-2 lists the bridge names and other relevant details for each of the sites selected, including: route, river crossing, county location, scour category, and bridge length. For each site, the following information was determined: bridge size classification, whether the site has available USGS bathymetric data, whether the site is collocated with a USGS gage station, whether the site likely has cohesive bed material, and whether the bridge is likely skewed relative to the river. The following summarizes some of the key details for the selected sites:

- Bathymetric Data Availability: two sites have USGS bathymetric data (A-3760 and L-0550).
- Bed Material: based on field site observations, available engineering drawings, and surficial geologic information, two sites have cohesive riverbed material (H-0024 and L-0564), and the remaining three sites have cohesionless riverbed sediments.
- Bridge Skew: three sites are skewed based on field site observations and visual inspection of aerial imagery (H-0024, L-0022, and L-0564).
- Bridge Size Classification: one site is a major bridge (bridge length greater than 1000 ft) (L-0550), and the remaining four sites are typical bridges (bridge length between 20 and 999 ft).

A photograph of each of the five bridge sites is included in Figure 3-2 to accompany the summary in Table 3-2. The selected sites have diverse bridge sizes and typology and are a good representative sample of the bridges in the State of Missouri.

Table 3-2. List of the five (5) bridge sites selected for the study.

Bridge Name	Route	River Crossing	County	Scour Category	Bridge Length	Likely Skewed
H-0024	RT P S	Creek	Audrain	D	45 ft	0
L-0022	MO 25 S	Wolf Creek	Stoddard	A	77 ft	40
L-0564	RT K E	Dry Fork Creek	Montgomery	C	236 ft	35
A-3760	US 63 S	Gasconade River	Maries	A	994 ft	N
L-0550	US 54 E	Missouri River	Cole	B	3124 ft	N

Figure 3-2. Composite of the five bridge sites selected for this study.

4 FIELD DATA COLLECTION AND PROCESSING METHODS

Numerical hydraulic models and the associated empirical scour calculations require an array of inputs to estimate flow conditions and bridge scour depths. The field data collection and processing methods are described in this section including: geologic and geomorphological data, sediment/soil data, bridge plans, topographic/bathymetric data, and hydrologic data. Most bridge sites involved at least two data collection site visits and all the data were recorded and stored in accordance with the data management plans submitted to MoDOT. All reported elevation values for this study used the NAVD 88 vertical datum. Further, the georeferenced data used the NAD 1983 State Plane Missouri East or Central FIPS 2401 (US Feet) projected coordinate system.

4.1 Geologic and Geomorphological Data

Several sources are available to study geology and geomorphology in the State of Missouri and how the different rivers continue defining the riverine system. The primary sources used were from the Missouri Department of Natural Resources (MoDNR) Geologic Survey and MoDOT. Even though in several areas in the state the bedrock is exposed, this study focused mostly on the surficial geologic materials and not structural geology. The state is typically divided into four physiographic areas, as shown in Figure 4-1. This project considered bridge sites at all four regions in the state of Missouri, which are: (1) Glaciated Plains, (2) Western Plains, (3) Ozarks, and (4) Southeastern Lowlands.

Figure 4-1. Physiographic map of Missouri (Missouri State Highway Commission, 1962).

More detailed geologic maps are available through the MoDNR with georeferenced delineations in the form of GIS databases (ArcGIS and Google Earth) and were used in the analysis. However, a generalized view of the State's surficial material is shown in Figure 4-2 available from the MoDNR. Additionally, there are other surficial materials maps developed at a higher resolution scale, which show more detail. These printed maps are mainly available for areas with a higher population or local interest and are not available for the entire State.

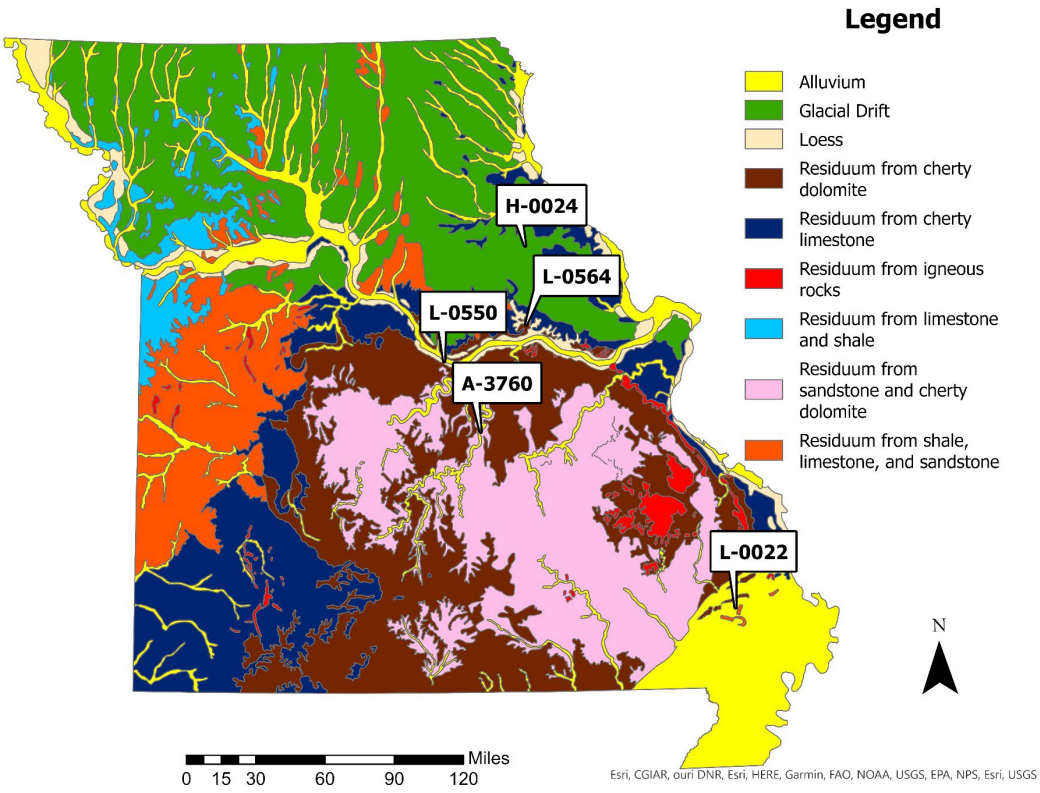

Figure 4-2. Surficial materials map of Missouri (adapted from MoDNR, 2023).

The surficial materials map shows Missouri contains generally the following: alluvium, loess, glacial drift, residuum, bedrock, and surface water:

- **Alluvium** is mainly composed of sediment deposited by river and stream systems located near riverbanks and stream valleys (Kleiss, 2000). The surrounding areas of the lakes in Missouri are also locations of various alluviums. Alluvial textures range from sand, silt, and clay. Specific alluvial textures are described on the MoDNR surficial map legend.
- **Loess** soils result from the glacial transport of silty material. Loess was frozen silt contained in glaciers; during thawing of the glaciers, the sediment was deposited. Wind then transported the soil to its resting position (Minor, 1974). These Aeolian processes have scattered loess throughout the State of Missouri blanketing areas with thick to thin layers of soil. The thickest deposits of loess are concentrated in relatively flat topographies (Missouri State Highway Commission, 1962).
- **Glacial drift** develops from glacial melting of sediment blanketing the region. Glacial drift soils are generally a clay or sandy texture and predominantly reside in Northern Missouri. Glacial drift is frequently blanketed by loess; however, erosion of the fine-grained loess material has caused glacial drift to become the surface soil in many areas (Minor, 1974).
- **Residuum** develops from the long-term weathering of exposed rock. Residuum texture is predominantly clay with varying amounts of the sand, gravel, and stone content. The residuum soil types have different mineral parent material such as chert, limestone,

dolostone, and shale (MoDNR, 2007). The mineral composition dictates how the rock weathers and the soil type that will result from that weathering including soil grain size and structure.

- **Bedrock** is the exposed rock at the ground surface from various geologic time periods. The types of bedrock outcropping are dependent on the period of the formation of the rock, such as the Ordovician Period or the Mississippian Period (MoDNR, 2007). In perspective to the previous soils, bedrock is relatively unweathered and is virtually unaffected by slope erosion like alluvium, residuum, glacial drift, or loess.
- **Surface water** is the numerous networks of streams, reservoirs, and lakes found within the State of Missouri. Surface water does not have soil or geologic properties, however, has implications for the surrounding soil types and topographies.

4.2 Sediment/Soil Sampling and Laboratory Analysis

This section describes the methods used for soil sampling that took place over water (riverbed) and onshore (floodplains and embankments). All soil sampling was directed and conducted by the research team, except for the larger rivers that required a watercraft and assistance from a third party. Generally, the soil sampling locations were on the upstream side of the bridge in front of the bridge piers. These locations varied depending on the access to the locations and obstructions. Additionally, the soil laboratory analysis was completed by the research team at the SLU geotechnical labs.

4.2.1 River Bedload Material (manual and from watercraft)

All the bridge/river sites analyzed had some level of water passing through, but the water levels varied from a couple of feet to tens of feet. In some instances, researchers could cross the river with high boots or waders, when water depths were about 1 to 4 ft depth. For the smaller bridge/river sites (L-0022, H-0024, and L-0564) sampling was conducted with hand tools. An attempt was made to use an SPT split barrel and Shelby Tube samplers, but in most cases, it was unsuccessful and impractical. The hand tool methods that resulted in effective sampling were hand augers, shovels, and scoops, depending on the soil type. The hand auger was effective for soils that contained some fines, at least 15%. The shovel and scoops were effective when the water level was shallow. When the soil samples were cohesive, they were placed in glass jars and when the soils were granular or bedload, they were placed in canvas bags.

In the larger bridge/river sites, the use of a watercraft was needed to conduct soil sampling. The sampling tools were specialized bedload samplers. Depending on the depth of water and flow, the type of sampler would vary. Typically, samplers developed by Federal Interagency Sedimentation Project (FISP) were used overboard a watercraft. The FISP samplers have a torpedo shape that lines up with the water flow and is then lowered by a winch or by hand so when the sampler hits the bottom, it scoops sediment into the sampler with a spring-loaded clamshell mechanism. These tools have a limited sampling depth of no more than six inches, which is considered surface sampling of the bottom sediments. If deeper materials are ever required a mechanical drill or vibrating tool will be required. Figure 4-3 shows the different types of samplers used in this project.

(a) US BM-60 Sampler, 32 lbs 175cc sample size

(b) US BM-60, 100 lbs, 300cc sample size

(c) BM-54 sampler being used from a USGS boat using a crane-mounted winch.

Figure 4-3. Bedload sediment samplers (source: Federal Interagency Sedimentation Project, 2023).

4.2.2 Floodplain and Embankments

Several soil sampling devices were considered for the floodplain and embankment locations. Both the SPT split barrel and thin walled (Shelby tube) samplers were evaluated but given the shallow depth of sampling and lack of access to drill rig equipment, they were not used further. The primary tools used for sampling were hand augers, scoops, and shovels. The sampling depth was limited to the top 2-3 feet below the root line typically present in the floodplains and embankments. The main channel samples were surficial and not more than approximately six inches deep when using the BM-54 sampler or hand shovels. All samples collected were disturbed, or their density or consistency was not preserved. The soil samples were placed in glass jars with a rubber seal, labeled, and transported to the SLU geotechnical laboratories on the same day of sampling. Soil samples were stored in a temperature-controlled environment and were analyzed or tested within one or two weeks of arriving at the labs. Figure 4-4 shows a few examples of how the soil sampling took place in the field.

Figure 4-4. Soil sampling within the floodplains and embankments.

4.2.3 Soils Laboratory Analysis

Once the samples arrived at the SLU soil mechanics laboratory they were organized, logged, and prepared for soil analysis testing. Immediately after opening the sample containers, the water content of all the soil samples was determined by subsampling the original sample. Samples varied from very coarse bedload material to fine-grained alluvial soils. Therefore, the different soil analysis tests were assigned by the Co-PI Dr. Luna. A laboratory assignment sheet was used to assign lab tests to all the relevant samples. So, the fine-grained soils were subjected to hydrometer analysis and Atterberg limits, followed in general accordance with the ASTM D4318 standard. The coarse-grained samples were assigned for #200 sieve wash or full sieve analysis, and the tests were conducted in general accordance with the ASTM D6913 standard (ASTM, 2023).

4.3 MoDOT Bridge Plans

The MoDOT Research Section made available bridge plans that varied in age from the 1920s to the 2000s. This wide range of dates resulted in varied levels of detail in the plans. Some small old bridge plans consisted of only two pages and the more modern large bridge plans were over 100 pages in length. Some

of the bridge plans included rehabilitation and retrofit plans, even countermeasures for bridge scour. The bridge plan records were all in electronic form scanned from the original documents stored at MoDOT. Many of the bridge drawings provided elevations in the NGVD29 vertical datum; these elevations were converted to NAVD88 to establish a consistent datum for all project elevations. Plan views and profile elevation views of the bridge drawings were digitized and georeferenced to provide the geometric data required for hydraulic modeling and scour analysis.

4.4 Topographic/Bathymetric Data Collection and Processing

Topographic and/or bathymetric datasets were acquired for each of the sites to create surface geometry needed by both the 1-D and 2-D hydraulic models. The datasets came from different types of sources, some that were available online and others collected in the field for this project. The following sections describe the methods used for terrain data collection.

4.4.1 GPS Topography

Survey grade measurements were made at key locations within the bridge sites. These locations were at the bridge abutments, wing walls, and water levels to serve as benchmark points for all other survey information used at the site like Acoustic Doppler Current Profiler (ADCP) and lidar. GPS points collected on the bridge were used to georeference bridge plans enabling digitizing bridge components within the hydraulic models.

The collection method used consisted of handheld Trimble GPS units with the antenna mounted on a tripod or rod. The GPS unit was connected via a Wi-Fi/cellular device to the MoDOT Virtual Reference Station (VRS) to enable differential correction. The Global navigation satellite system (GNSS) data are broadcast as a real time network (RTN) via cellular communication. Survey data provided by the receiver, once corrected, have a 2-3 cm accuracy per the Missouri GNSS website (MoDOT, 2023).

4.4.2 Lidar Topography

Lidar data used in this project were obtained from existing online sources. Most counties in the state of Missouri have topographic lidar data available at the Missouri Spatial Data Information Service (MSDIS) website server (https://msdis.missouri.edu/data/lidar/). The data can be downloaded via a web-based GIS interface tool by county or by masking a desired area. All the lidar data are less than five years old and typically have a resolution point spacing of 10 meters (~30 feet). The downloaded data files (*.LAS format) consist of point clouds that were converted to a triangular irregular network (TIN) or a raster.

A Scanstation 2 terrestrial lidar unit was used to collect higher-resolution topographic data for the Wolf Creek (L-0022) site in the region immediately adjacent to and under the bridge (data collected on June 16, 2021). The instrument creates a point cloud of measurements and has a surface precision of approximately 6 mm at a 50 m range. The GPS unit was used to georeference the location of the lidar point cloud data.

4.4.3 ADCP Bathymetry

The SLU research team acquired bathymetric data using a Teledyne RD RiverPro 1200 HZ ADCP at two of the five bridge sites. This method is appropriate for rivers that are relatively shallow and calm. At the Dry Fork Creek (L-0564) site, ADCP data were acquired by wading with an ADCP catamaran (collection date of August 9, 2021). At the Gasconade (A-3760) site, the ADCP catamaran was pulled by a small private boat (collection date of November 19, 2021). The ADCP coverage extended from approximately 15 channel widths upstream of each bridge to approximately 15 channel widths downstream of each bridge. Photographs of data collection at the Gasconade River and Dry Fork Creek are shown in Figure 4-5.

Figure 4-5. Photographs of ADCP data collection
(a) Dry Fork Creek (L-0564) and (b) Gasconade River (A-3760).

4.4.4 USGS Multi-beam Bathymetry

Multi-beam bathymetric data were acquired from USGS online sources for the Gasconade River (A-3760) site (field data collection conducted in June 2017) (Huizinga, 2019) and the Missouri River (L-0550) site (field data collection conducted in May 2017) (Huizinga, 2020). Multi-beam data have the highest resolution available for bathymetric data. Figure 4-6 shows the multi-beam data for the Missouri River (L-0550) site.

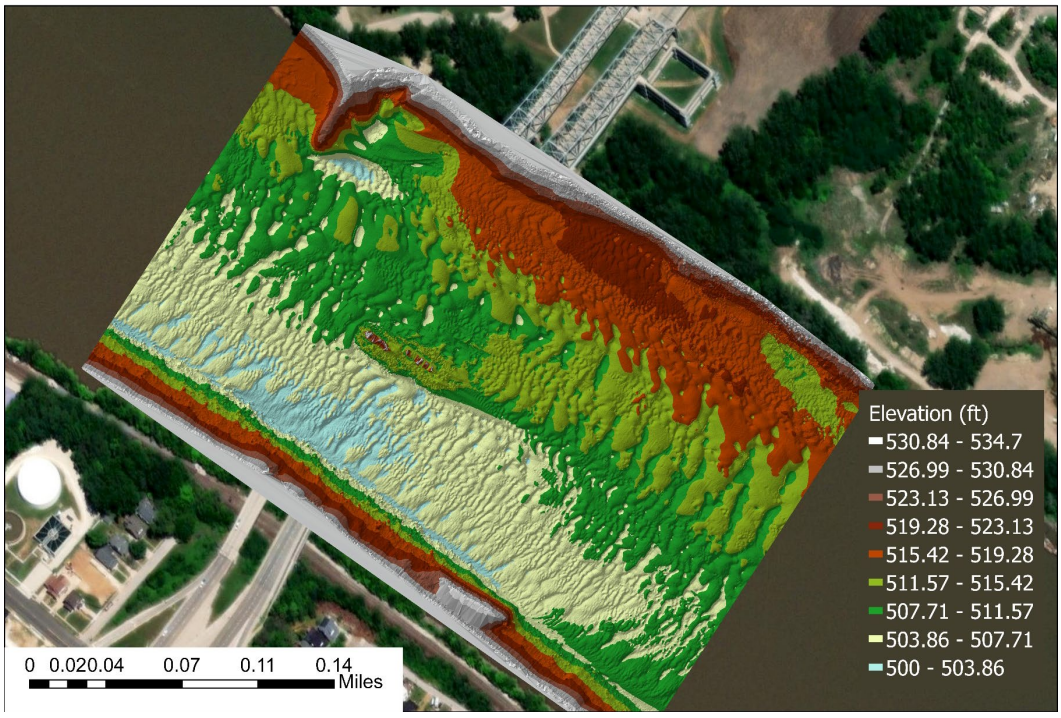

Figure 4-6. USGS multi-beam data for Missouri River (L-0550) site.

4.4.5 USACE Cross Section Bathymetry

For the Missouri River (L-0550) site, single-beam bathymetric data in the form of cross sections were acquired from the U.S. Army Corps of Engineers (USACE). The cross sections, shown in Figure 4-7, were collected in 2019.

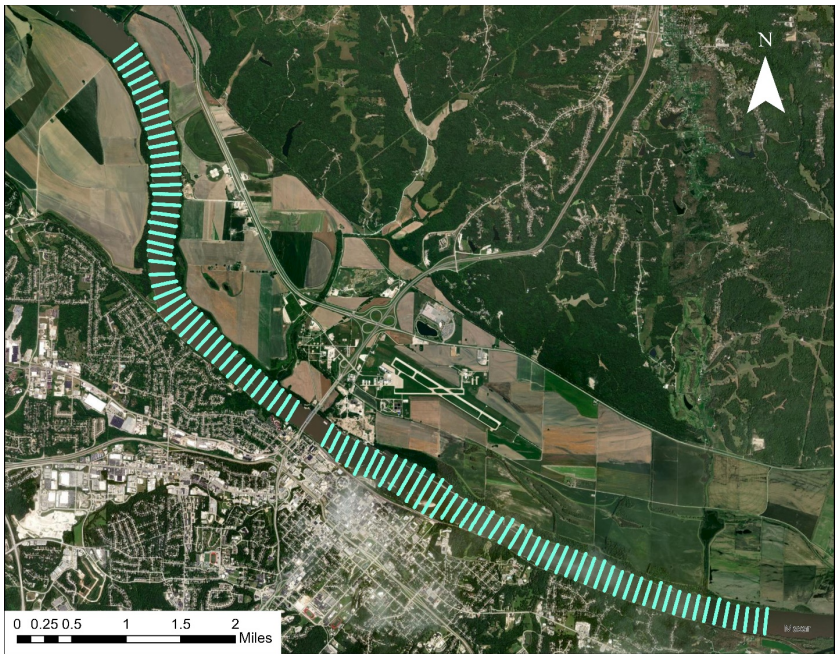

Figure 4-7. Locations of USACE 2019 single-beam cross sections at the Missouri River (L-0550) site.

4.4.6 Generating Composite Topographic/Bathymetric Surfaces

Topographic and bathymetric datasets for each site were combined to create a single composite surface raster using ArcGIS Pro (all elevations in NAVD88 vertical datum). Information on the terrain data sets used for each bridge site is shown in Table 4-1. Lidar data were filtered with ArcGIS Pro to exclude vegetation coverage, which could skew elevation levels by dozens of feet where trees were present. Since lidar technology is unable to penetrate water, bathymetric data from a variety of collection methods, depending on the site, were added to the surface to make up the channel bottom bed area. Geoprocessing tools were utilized within ArcGIS Pro to remove lidar data from the channel area and replace it with bathymetric data. Once all elevation data were stitched into a single raster, it was converted to a TIFF file and exported for use in the modeling software. Figure 4-8 shows an example surface from the Gasconade River site (A-3760) which integrates lidar topographic data with bathymetric data obtained via multi-beam near the bridge section and ADCP for sections upstream and downstream of the bridge. Composite elevation surface plots for all bridge sites are provided in Appendix A. For the bridge TIFF files, the raster cell sizes were 2.0 ft for the Creek (H-0024), Wolf Creek (L-0022), and Dry Fork Creek (L-0564) sites; 6.6 ft for the Gasconade River (A-3760) site; and 30.0 ft for the Missouri River (L-0550) site. These raster cell sizes were selected based on the relative size of the channel to ensure suitable representations of channel terrains.

Table 4-1. Topographic and bathymetric data collection methods.

Bridge Site	Topographic Data Sources	Bathymetric Data Sources
Creek (H-0024)	2017 MSDIS LiDAR DEM, GPS (SLU)	Not applicable ephemeral stream
Wolf Creek (L-0022)	2017 MSDIS LiDAR DEM, 2021 Terrestrial lidar (SLU)	Not applicable ephemeral stream
Dry Fork Creek (L-0564)	2017 MSDIS LiDAR DEM, LiDAR Project	2021 ADCP (SLU)
Gasconade River (A-3760)	2017 MSDIS LiDAR DEM	2021 ADCP (SLU), 2017 Multi-beam (USGS)
Missouri River (L-0550)	2017 MSDIS LiDAR DEM	2017 Multi-beam (USGS), 2019 Single-beam (USACE)

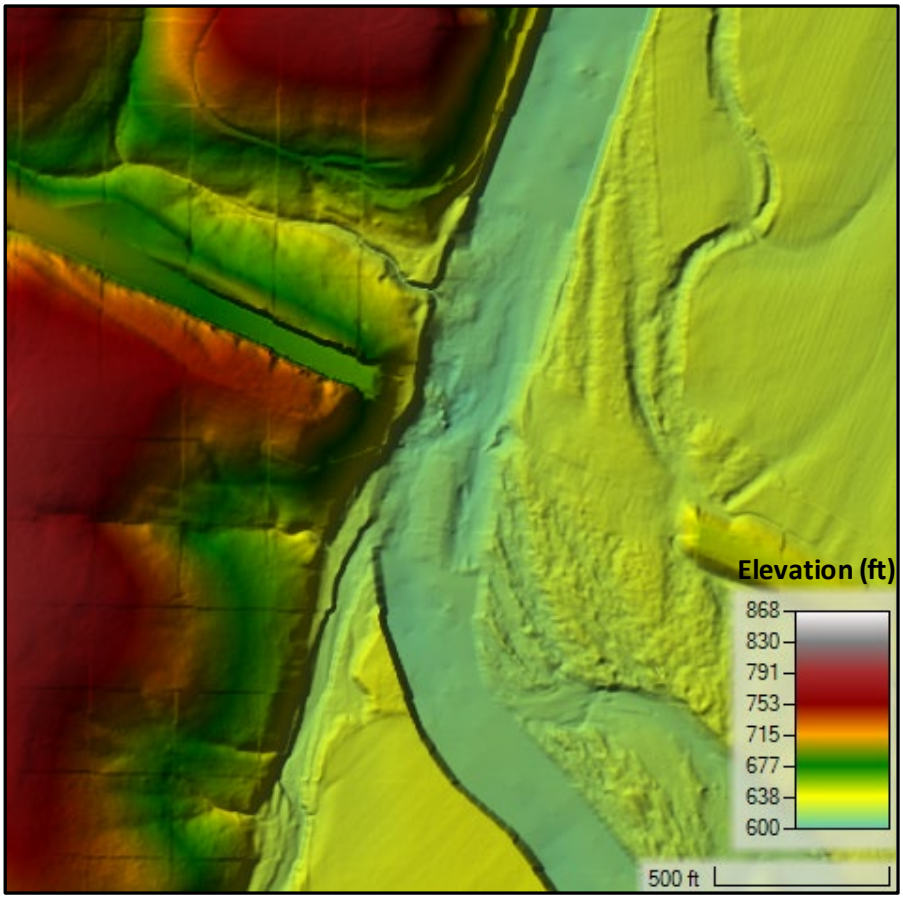

Figure 4-8. Composite topographic/bathymetric surface for the Gasconade River site (A-3760).

4.5 Hydrologic Data

The flow rates used in the hydraulic modeling for three of the bridge sites were obtained utilizing StreamStats. StreamStats is a Web-GIS-based application developed by the United States Geological Survey (USGS) capable of estimating streamflow statistics using delineated watershed or basin areas. For the Creek (H-0024), Dry Fork Creek (L-0564), and Gasconade River (A-3760) bridge sites, StreamStats was used to determine the rural peak-flow statistics for the 100-year and 500-year design storm event (Southard and Veilleux, 2014).

The StreamStats application is limited, in that it cannot delineate a basin that stretches over the boundary of two states. As the Missouri River site has a vast watershed that extends into neighboring states, StreamStats was unable to provide peak flow statistics. Thus, the flow rates used in the hydraulic modeling of the Missouri River site (L-0550) were obtained from the previously published WSPRO study (Huizinga and Rydlund, 2003).

For the Wolf Creek (L-0022) site, upon a comparison of the peak flow statistics given by StreamStats and the flow rates used in the WSPRO study, the StreamStats discharge estimates were found to be nearly seven times lower than the values used in the WSPRO study. Preliminary results from hydraulic modeling were assessed and the WSPRO flow rates were determined to be more appropriate flow magnitudes that inundated the floodplain. Therefore, the hydraulic modeling of the Wolf Creek (L-0022) bridge site also utilized discharge flow rates from the previous WSPRO study (Rydlund and Huizinga, 2001).

5 METHODS USED FOR HYDRAULIC ANALYSIS AND BRIDGE SCOUR ANALYSIS

5.1 One-Dimensional Hydraulic Modeling (HEC-RAS)

5.1.1 HEC-RAS Geometry Inputs

HEC-RAS geometry inputs include a terrain surface (TIFF format), cross-section locations, roughness values, ineffective flow areas, and bridge cross-section details. The TIFF surfaces derived from the methods detailed in Section 4.4 were used as terrain inputs for each site. Cross sections aligned perpendicular to the channel and floodplain paths were digitized on each terrain surface. Figure 5-1 shows an example of the delineated cross section for the Gasconade River A-3760 bridge site. Figures showing cross-section locations for all sites are located in Appendix A.

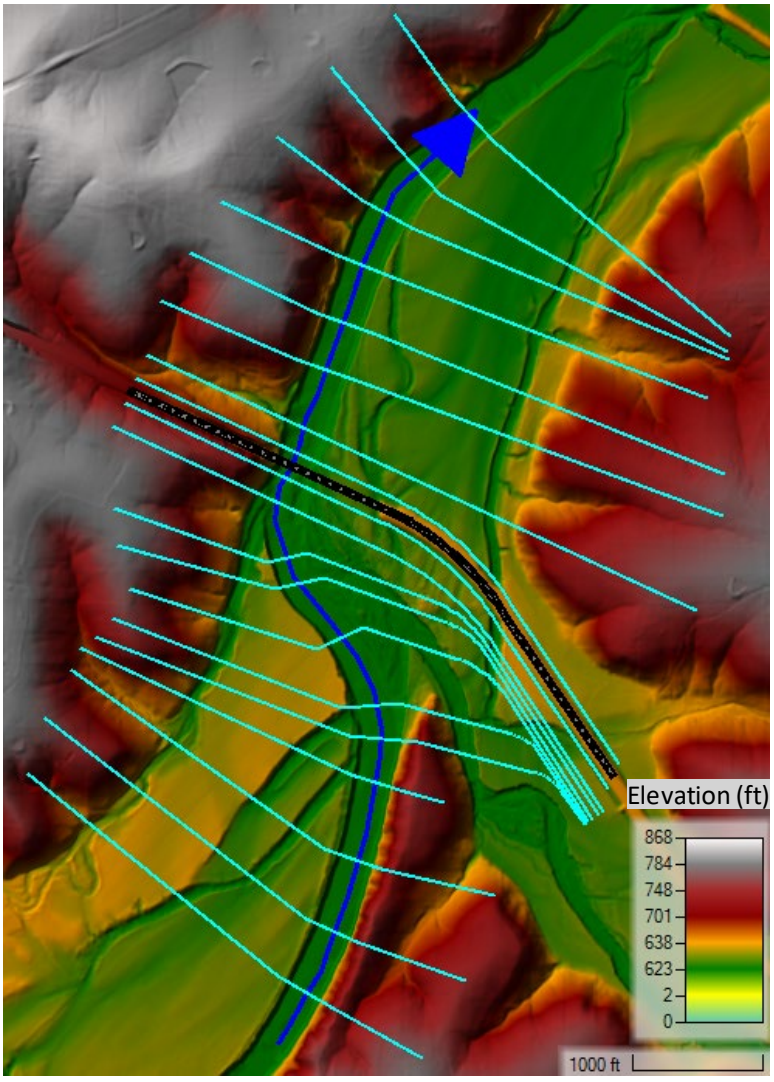

Figure 5-1. Gasconade River (A-3760) – HEC-RAS plan view of cross sections and elevations.

Roughness values used for the HEC-RAS modeling are listed in Table 5-1. These values are consistent with the values used in the previous WSPRO studies (Huizinga and Rydlund, 2002; Rydlund and Huizinga, 2001; Rydlund and Huizinga, 2002a; Rydlund and Huizinga, 2002b; Huizinga and Rydlund, 2003). For the HEC-RAS modeling, roughness values were constants not varied by flow depth. The overall

roughness values had a wide range of values from 0.031 in the downstream channel of the Gasconade River (A-3760) site to 0.130 for timber brush areas at the Dry Fork Creek (L-0564) site.

Table 5-1. Summary of Manning's roughness coefficients for HEC-RAS 1-D modeling.

Surface Condition	Manning's Roughness Coefficient
Creek (H-0024)	
Channel	0.042
Cornfield	0.045
Kept Pasture	0.040
Heavy Timber	0.060
Light Timber	0.050
Wolf Creek (L-0022)	
Kept Pasture	0.048
Moderate Timber	0.078
Channel (Upstream)	0.045
Channel (Bridge Reach)	0.050
Channel (Downstream)	0.045
Thick Brush	0.070
Moderate Brush	0.055
Dry Fork Creek (L-0564)	
Cornfield	0.055
Moderate Brush	0.085
Thick Brush	0.130
Channel (Upstream)	0.042
Channel (Bridge Reach)	0.042
Channel (Downstream)	0.045
Timber and Brush	0.110
Moderate Timber	0.065

Surface Condition	Manning's Roughness Coefficient
Gasconade River (A-3760)	
Cornfield	0.043
Timber and Brush	0.080
Channel (Upstream)	0.035
Channel (Bridge Reach)	0.033
Channel (Downstream)	0.031
Brush Covered Bluff	0.070
Moderate Underbrush	0.060
Missouri River (L-0550)	
Dense Timber	0.100
Pasture	0.040
Moderate Brush	0.090
Channel	0.030
Cornfield	0.050
Crops and US Highway	0.070

Modeling bridges in HEC-RAS requires geometry inputs for the bridge deck, piers, and abutments. The bridge deck is defined with station-elevation data for the high and low chords. Pier geometries are defined by pier centerline station and pier widths at specified elevations. Abutment geometries are defined by station-elevation data. Figure 5-2 shows an example bridge cross-section from the Gasconade River (A-3760) site.

Ineffective flow areas are caused by having a contracted channel area at the bridge cross-section which prevents flow conveyance at nearby upstream and downstream cross-section flow areas. For each site, ineffective flow areas were defined upstream and downstream of the bridge cross-section assuming a 1:1 contraction and expansion rate in the immediate vicinity of the bridge. This approach was selected based on guidance provided by the HEC-RAS hydraulic reference manual (Brunner, 2016). Figure 5-3 illustrates an example of ineffective flow areas for the Dry Fork Creek (L-0564) site.

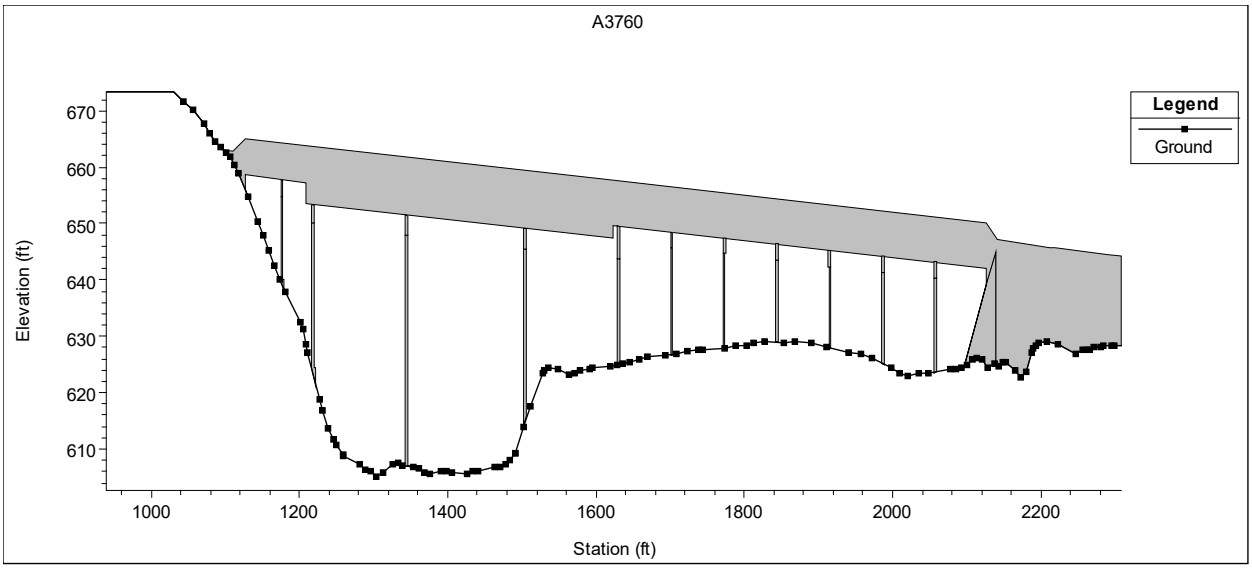

Figure 5-2. Example bridge cross section from the Gasconade River (A-3760) site.

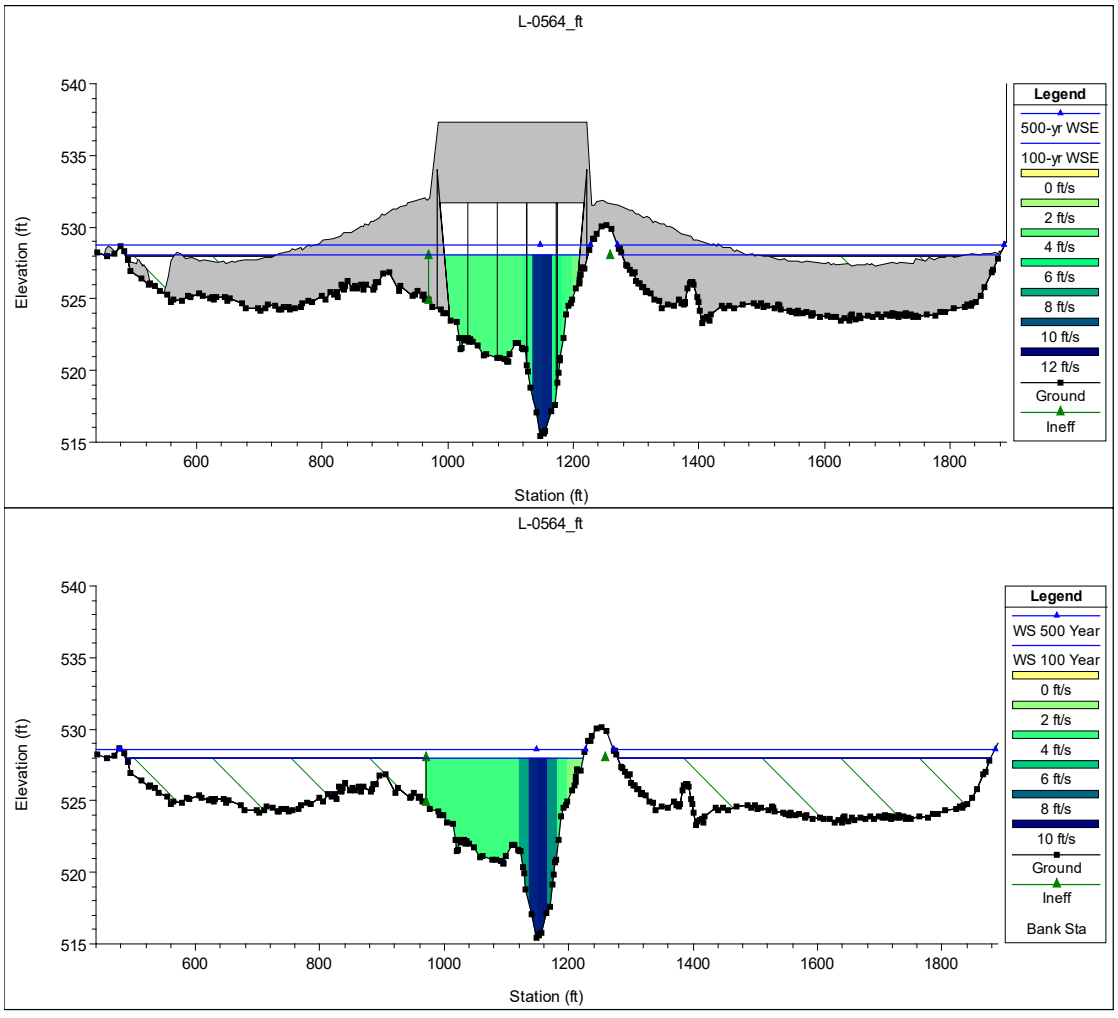

Figure 5-3. Example of ineffective flow areas from the Dry Fork Creek (L-0564) site: top is the cross section at the bridge and bottom is the cross section just downstream from the bridge.

5.1.2 HEC-RAS Steady-State Simulation Inputs

For steady-state simulations, HEC-RAS requires information on flow rates and downstream hydraulic control conditions (i.e., water-surface elevation for subcritical flow). Table 5-2 provides this information for each model and includes details on the number of cross sections, length of river section, and channel bedslope. For all models, the downstream hydraulic control was set to the water-surface elevation for the normal depth. To maintain consistency for model comparisons, the downstream normal depth determined from the SRH-2D program was used for the HEC-RAS models. The SRH-2D program determines normal depth using Manning's equation with channel geometry, flow rate, channel bedslope, and roughness information. The bedslopes used for normal depth input were computed using a trendline on the thalweg elevation profile of each channel.

Table 5-2. Summary of HEC-RAS modeling inputs and settings.

	Creek H-0024	Wolf Creek L-0022	Dry Fork Creek L-0564	Gasconade River A-3760	Missouri River L-0550
100-yr Flow Rate (cfs)	1,615	2,051	8,775	202,500	588,000
500-yr Flow Rate (cfs)	2,180	2,674	11,500	270,000	772,000
Number of Cross Sections	18	22	26	19	21
Length of River Section (ft)	2,406	2,900	4,278	7,336	44,229
Bedslope (ft/ft)	0.002623	0.00283	0.001228	0.000296	0.000212
Setting for Downstream Water-Surface Elevation Control	Normal Depth	Normal Depth	Normal Depth	Normal Depth	Normal Depth

The HEC-RAS simulations conducted for this study used Windows-based personal computers (PCs) or laptops with standard desktop capabilities. Due to the simplicity of the 1-D calculations, the simulations required only a few seconds to complete even for the large bridges crossing significant river basins containing numerous cross-sections.

5.2 Two-Dimensional Hydraulic Modeling (SRH-2D)

5.2.1 SRH-2D Geometry Inputs

SRH-2D geometry inputs include a terrain surface (TIFF format), roughness value coverage, and an unstructured mesh. The TIFF surfaces derived from the methods detailed in Section 4.4 were used as terrain inputs for each site. Manning's roughness coefficient coverages were digitized based on aerial imagery. Figure 5-4 shows the Manning's roughness coverage for the Gasconade River (A-3760) site and Table 5-3 details the Manning's roughness coefficients by surface condition used for each model.

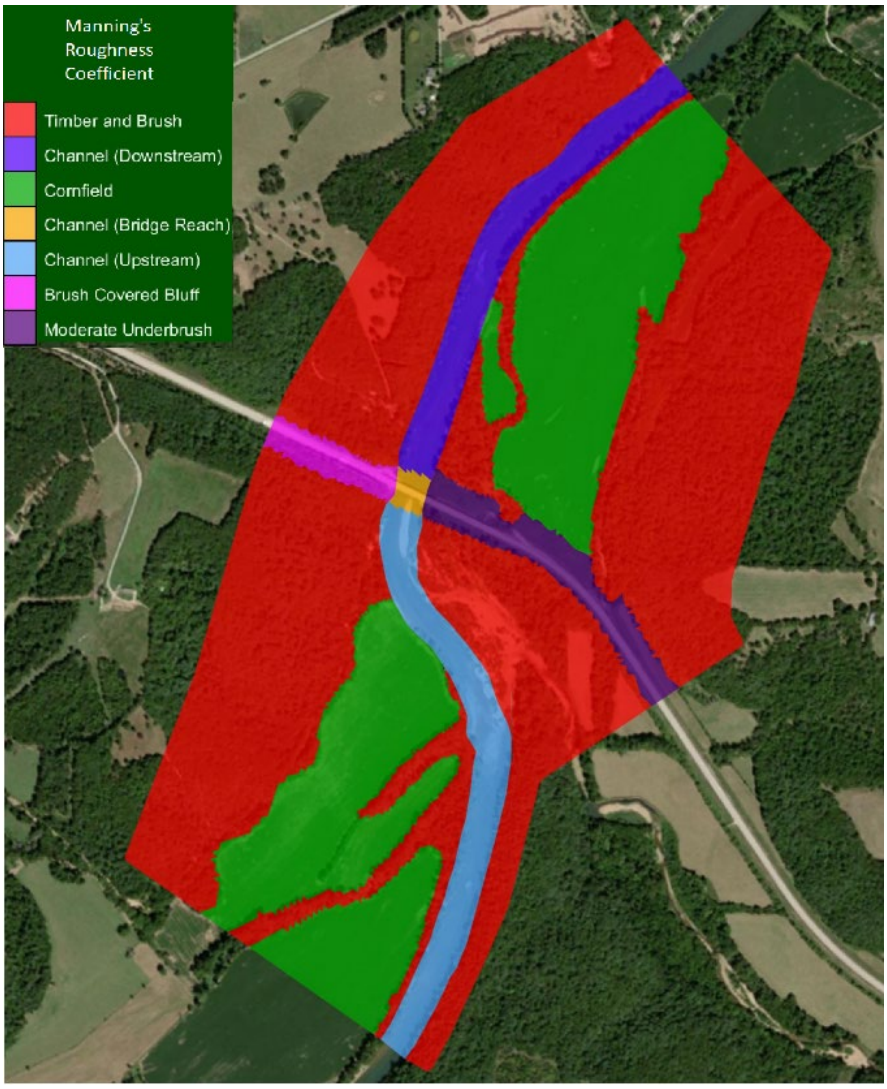

Figure 5-4. Manning's roughness coefficient coverage for the Gasconade River (A-3760) site.

Table 5-3. Summary of Manning's roughness coefficients for SRH-2D modeling.

Surface Condition	Manning's Roughness Coefficient (Flow Depth)
Creek (H-0024)	
Kept Pasture	0.040
Channel	0.042
Heavy Timber	0.060
Light Timber	0.050
Wolf Creek (L-0022)	
Beanfield	0.068 (0 ft.) - 0.055 (2 ft.)
Channel (Upstream)	0.038 (0 ft.) - 0.050 (3 ft.)
Channel (Bridge Reach)	0.050
Channel (Downstream)	0.035 (0 ft.) - 0.045 (2 ft.)
Moderate Brush	0.062 (0 ft.) - 0.048 (2 ft.)
Moderate Timber	0.085 (0 ft.) - 0.078 (2 ft.)
Brush with Timber	0.068 (0 ft.) - 0.052 (2 ft.)
Dry Fork Creek (L-0564)	
Cornfield	0.055
Moderate Brush	0.085
Channel	0.042
Gasconade River (A-3760)	
Cornfield	0.070 (4 ft.) - 0.040 (8 ft.)
Timber and Brush	0.100 (4 ft.) - 0.080 (8 ft.)
Channel (Upstream)	0.035
Channel (Bridge Reach)	0.033
Channel (Downstream)	0.031
Brush Covered Bluff	0.070
Moderate Underbrush	0.060
Missouri River (L-0550)	
Tree Covered Bluff	0.012 (0 ft.) - 0.090 (20 ft.)
Channel (Upstream)	0.035 (0 ft.) - 0.025 (30 ft.)
Channel (Bridge Reach)	0.036 (0 ft.) - 0.027 (30 ft.)
Channel (Downstream)	0.045 (0 ft.) - 0.036 (30 ft.)
Moderate Timber	0.120 (0 ft.) - 0.090 (20 ft.)
Developed Land	0.090 (0 ft.) - 0.070 (20 ft.)
Crops	0.043
Airport with Timber	0.075 (0 ft.) - 0.043 (10 ft.)
Raised Roadway	0.070 (0 ft.) - 0.048 (10 ft.)
Bridge Section	0.150 (0 ft.) - 0.090 (15 ft.)

Unstructured meshes were created using the Surface-water Modeling Software (SMS) by Aquaveo. River and overbank areas were digitized into polygons with quadrilateral elements in the channel and triangular elements in the overbank areas and areas immediately adjacent to the bridge structure. Figure 5-5 provides an example of the entire mesh used for the Gasconade River (A-3760) site and Figure 5-6 shows the mesh in the vicinity of the bridge structure. Figures showing the mesh locations for all five sites are provided in Appendix B. Mesh element length in the main channel varied by site with approximately 8-ft long elements for the smallest site (Creek H-0024) and 60-ft long elements for the largest site (Missouri River L-0550). All piers were modeled as holes in the mesh with the exception of the piers at Dry Fork Creek (L-0564) and the overbank piers in the Missouri River (L-05500) site. These piers were significantly smaller than the size of the converged mesh and could not be reasonably included in the simulation. Further, these relatively small piers would have a negligible effect on the hydraulic conditions.

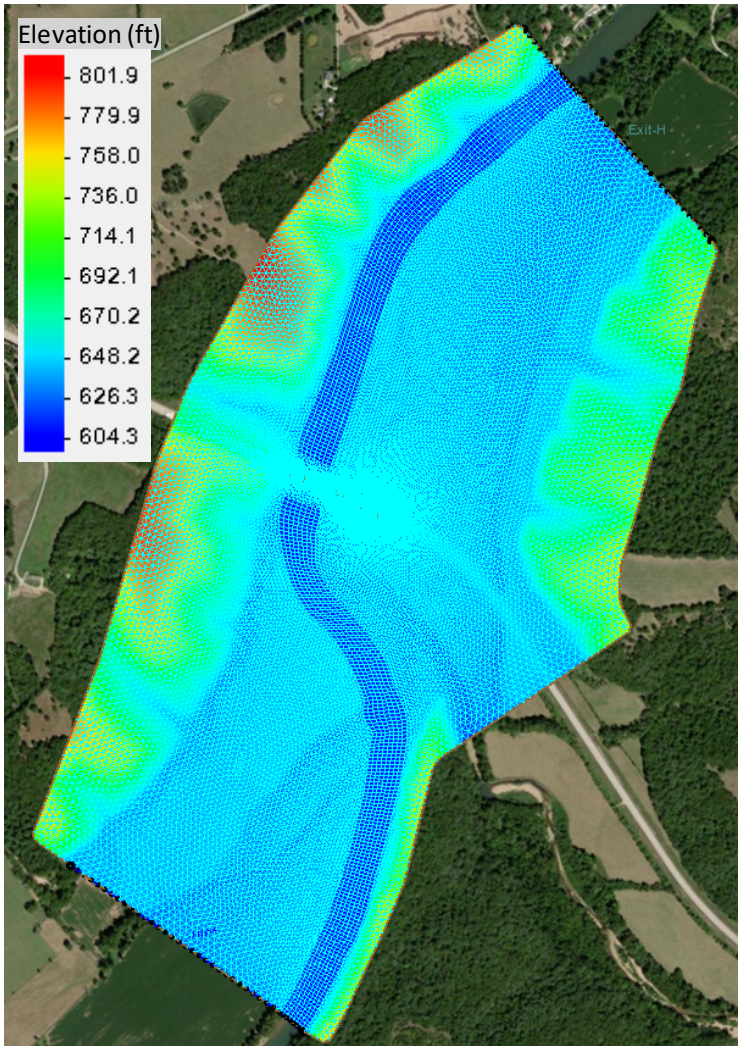

Figure 5-5. Gasconade River (A-3760) – SRH-2D mesh with bed elevations and boundary arcs.

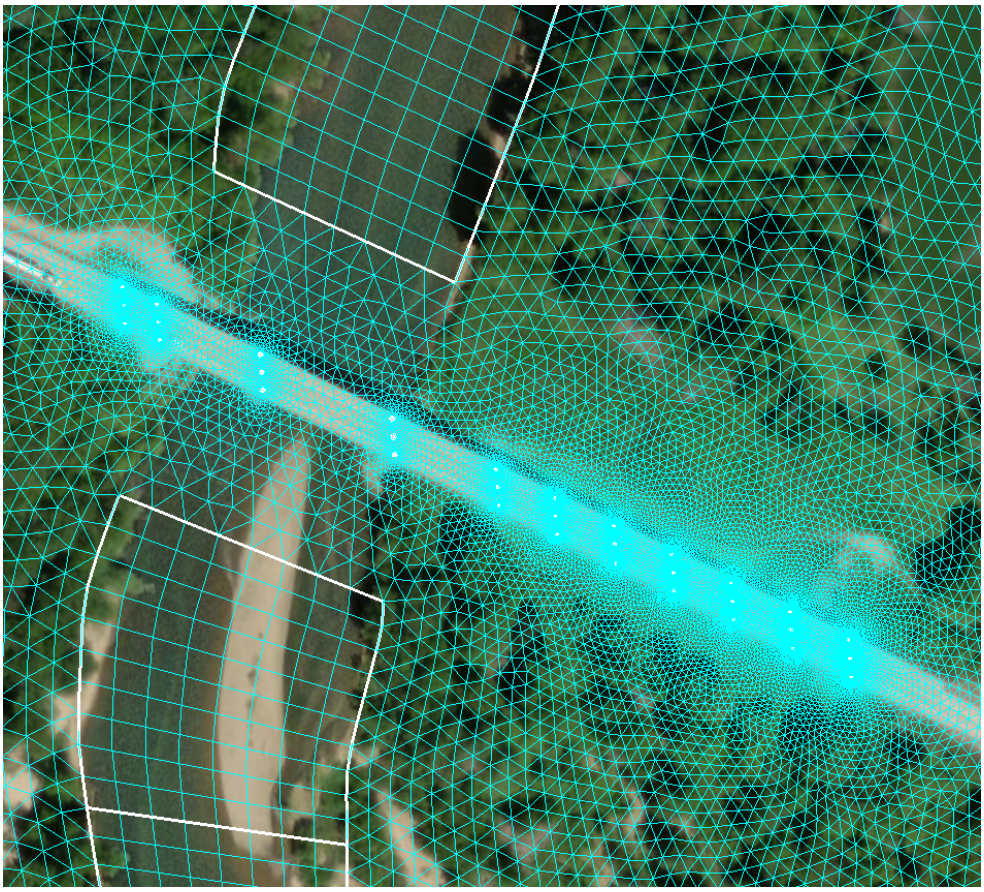

Figure 5-6. Gasconade River (A-3760) – SRH-2D mesh with piers at the bridge section.

5.2.2 SRH-2D Simulation Inputs

For each simulation, SRH-2D requires a time step, simulation duration, and information on boundary conditions, specifically the upstream inflow rate and the downstream water-surface elevation. Table 5-4 provides this simulation information for each site and includes details on the total number of mesh elements, approximate length of mesh elements in the channel, and channel bedslope. For all models, a normal depth downstream hydraulic control was used. SRH-2D computes normal depth (and associated water-surface elevation) for the boundary arc based on elevation geometry, flow rate, channel bedslope, and roughness information. The bedslopes used for normal depth input were computed using a trendline on the thalweg elevation profile of each channel.

Table 5-4. Summary of SRH-2D inputs and settings.

	Creek H-0024	Wolf Creek L-0022	Dry Fork Creek L-0564	Gasconade River A-3760	Missouri River L-0550
100-yr Flow Rate (cfs)	1,615	3,860	8,775	202,500	588,000
500-yr Flow Rate (cfs)	2,180	5,300	11,500	270,000	772,000
Number of Elements	25,663	83,077	31,241	57,678	162,960
Approximate Element Length in the Channel (ft)	8	14	20	30	60
Time Step (s)	1	1	1	0.05	0.5
Simulation Duration (hrs)	1	2	1.5	2	2
Bedslope (ft/s)	0.002623	0.00283	0.001228	0.000296	0.000212
Setting for Downstream Water-Surface Elevation Control	Normal Depth	Normal Depth	Normal Depth	Normal Depth	Normal Depth

SRH-2D simulations are inherently unsteady flow simulations. To obtain steady-state flow conditions, the models were set up with constant boundary conditions (upstream inflow rates and downstream water-surface elevations) and a sufficient simulation duration to reach steady-state conditions. Monitoring lines were digitized, as shown in Figure 5-7 for the A-3760 site, and used to monitor flow conditions such as water-surface elevation and discharge during the simulations. Figure 5-8 shows the monitoring line discharge data from 100-yr simulation for the A-3760 site which illustrates how the discharges approach constant values as steady-state conditions are achieved.

Figure 5-7. Monitor lines used to determine steady-state conditions for the Gasconade River (A-3760) SRH-2D simulations.

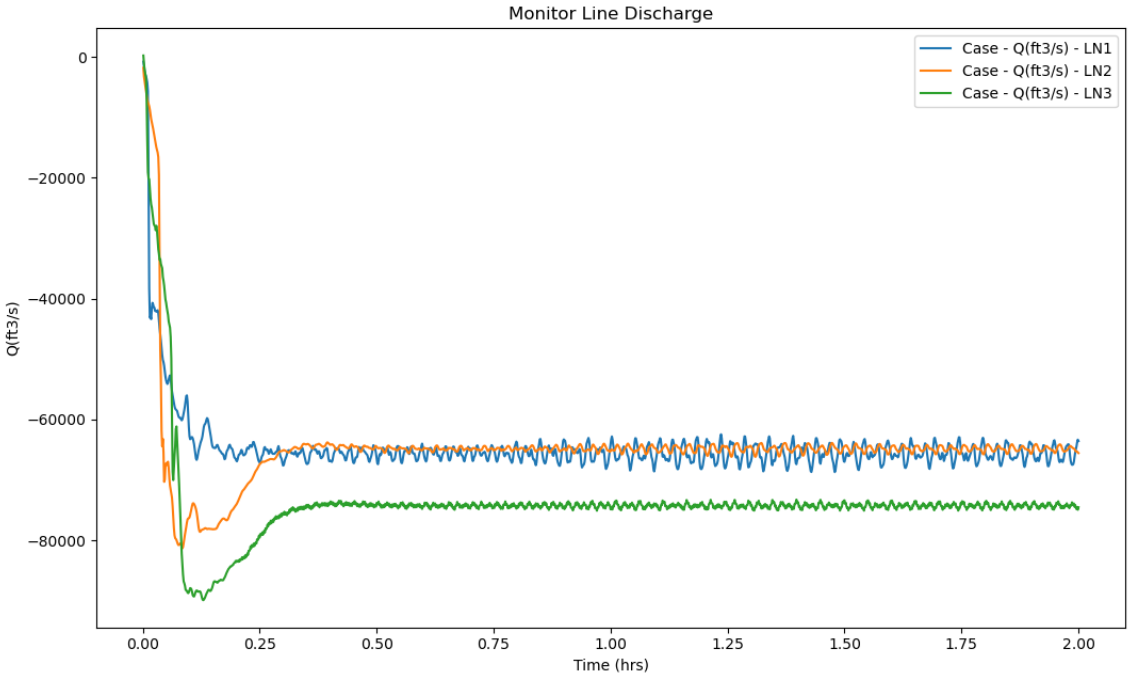

Figure 5-8. Discharge versus time for the A-3760 monitoring lines used to determine steady-state conditions.

A mesh convergence and time-step convergence analysis were conducted for each site to determine the appropriate mesh size and time step. Initially, a coarse, medium, and fine mesh were generated with approximately four, eight, and sixteen elements across the channel, respectively (see medium mesh in Figure 5-6). The suitable mesh size for each site was determined based on a comparison between simulation results for flow velocity and flow depth. The appropriate mesh size was selected when reducing the mesh further produced flow velocity and flow depth results with less than approximately 5% difference at three different monitoring arc locations. The time-step convergence was conducted in a similar approach which reduced the time step by a factor of two between simulations. The appropriate time step was selected when reducing the time-step further produced flow velocity and flow depth results with less than approximately 5% difference at three different monitoring arc locations.

Model input data are used with the discretized (finite-different) governing equations to produce a solution. The time required to run a simulation is dependent upon the number of elements and the type of computer used for the simulation. The smallest model, the Creek (H-0024) site with approximately 26,000 elements, required approximately five minutes to complete a simulation for one flow condition. Simulations of our largest model, the Missouri River (L-0550) site with approximately 163,000 elements, required approximately two hours to complete.

The SRH-2D program has been publicly and freely available since 2008; however, it lacks a graphical user interface (GUI). The proprietary Surface-water Modeling Software (SMS) program developed by Aquaveo was used to pre-process data for the SRH-2D executable, monitor simulations in progress, and post-process model results. The SMS GUI was used to generate the input mesh from Geographical Information System (GIS) data and visualize the model output data in GIS formats.

5.3 Scour Analysis

Three different mechanisms can cause bridge scour: long-term degradation, contraction scour, and local scour around piers and abutments. These different types of scour are combined to determine an

estimated cross section bed elevation after a storm event known as a scour prism. For this study, bridge scour estimates were conducted using the FHWA's Hydraulic Toolbox software program (FHWA, 2021) which uses the guidelines and methods provided by the FWHA's Hydraulic Engineering Circular (HEC) No. 18 (Arneson et al., 2012). These methods were described in Section 2 of this report and the following sections detail the input parameters for each of the analysis conditions. Hydraulic modeling results, soil/sediment data, and bridge geometries are used as inputs into the calculation methods. None of the bridge sites exhibited any indication of long-term aggradation or degradation; thus, those analysis components were not included in this study.

5.3.1 Hydraulic Toolbox Analysis

The FHWA's Hydraulic Toolbox software is a publicly and freely available program. Scour calculations using the Hydraulic Toolbox software require an array of information such as approach flow depth and velocity, flow rate through the bridge opening, bridge geometries, and bed material properties. Bridge geometry information was obtained by digitizing the bridge drawings and bed material properties were determined through the various analyses detailed in Section 4.2. Hydraulic data inputs were derived from the 1-D and 2-D numerical models. Specific details of the different scour analyses and required input parameters are described in Section 2.2. Table 5-5 provides a summary of the most relevant soil/sediment information that was used for the scour analysis.

Table 5-5. Soil/sediment information used for scour analyses.

Bridge Site	D_{50} (mm)		
	Left Overbank	**Main Channel**	**Right Overbank**
Creek H-0024	0.008	0.014	0.010
	Lean Clay	Lean Clay w/ Sand	Lean Clay w/ Sand
Wolf Creek L-0022	1.30	1.30	1.30
	Well Graded Sand w/ Gravel	Well Graded Sand w/ Gravel	Well Graded Sand w/ Gravel
Dry Fork Creek L-0564	1.04	4.20	2.70
	Poorly Graded Sand w/ Gravel	Poorly Graded Sand w/ Gravel	Poorly Graded Sand w/ Gravel
Gasconade River A-3760	17.0	11.25	0.260
	Well Graded Gravel w/ Sand	Well Graded Gravel	Silty Sand or Clayey Sand
Missouri River L-0550	0.010	0.620	n/a
	Lean Clay	Poorly Graded Sand	Bedrock

5.3.2 Total Scour Prism

Initially, contraction scour estimates in the left overbank (LOB), channel, and right overbank (ROB) sections are subtracted from the original cross-section bed elevations to determine a contraction scour bed elevation. As the abutment scour depths are based on an amplification factor applied to a simplified contraction scour estimate, the abutment scour depths are also subtracted from the original bed elevation (i.e., not subtracted from the contraction scour elevation). Computed pier scour depths are subtracted

from the contraction scour bed elevation at the respective pier stations. An angle of repose value of 40° was used to determine the lateral extent of pier and abutment scour holes. Figure 5-9 shows a total scour prism example for the Hydraulic Toolbox User's Manual (FHWA, 2021).

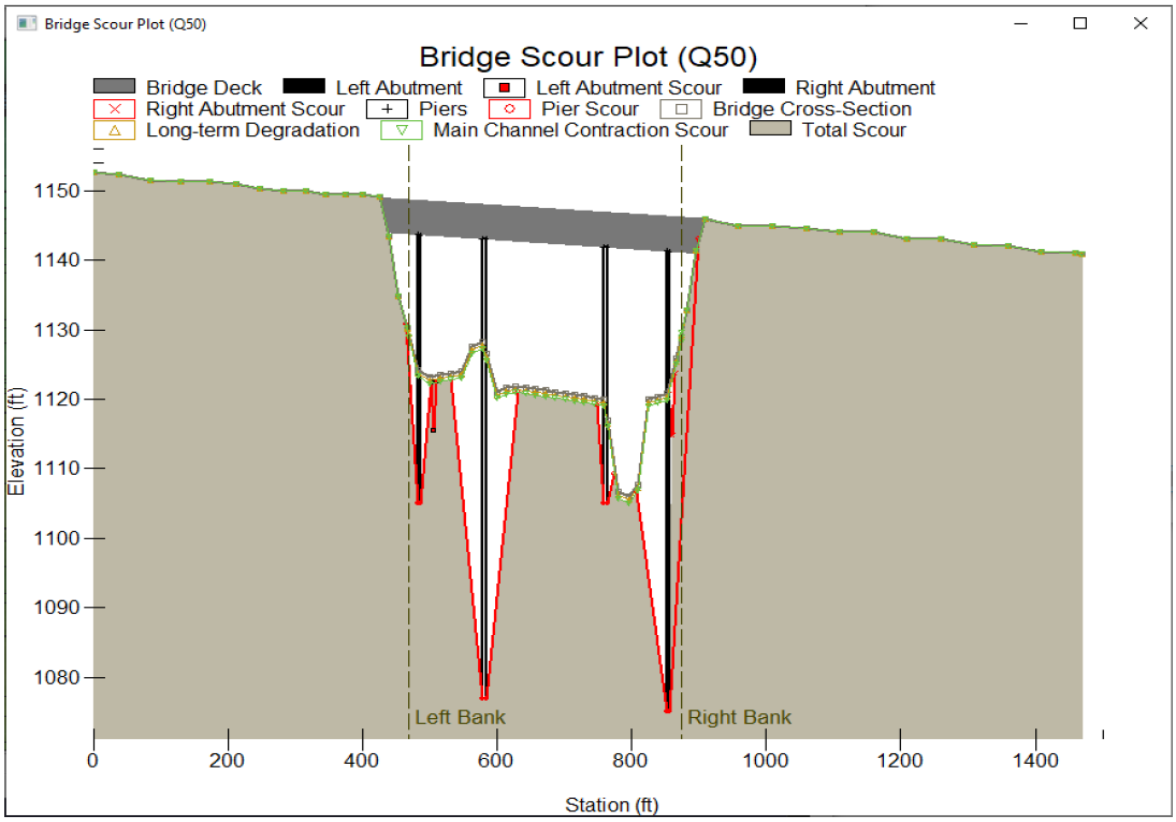

Figure 5-9. Total scour prism example (from FHWA, 2021).

6 ANALYSIS RESULTS

6.1 Soil/Sediment Analysis

Soil/sediment analysis was carried out on select samples for each bridge site. The methods used were the ones described in Section 4.2 of this report. The detailed soil laboratory results are all presented in Appendix C of this report. The following sections describe the geologic and soil conditions encountered at each bridge site as it relates to scour. Example soil sampling locations and laboratory results are only shown for the Gasconade A-3760 site in Figure 6-1 through Figure 6-3.

6.1.1 Creek (H-0024)

The Creek H-0024 bridge site is located in the Eastern Glaciated Plains near the City of Vandalia. The bridge is a small span bridge located east of Vandalia on Route P. The surficial geology consists of the typical glacial drift, which is predominantly clay deposits, occasionally covered by Loess. Bedrock is approximately 50 feet deep, and it is likely shale rock. The results of the soil analyses show that the soils are primarily fine-grained and contain more coarse-grained soils as part of the bedload material within the river channel. This bedload material was found in the areas where flow may become strong enough to move the sediment, but in most cases the bottom of the creek was cohesive. A total of seven (7) samples were collected, five (5) near the bridge piers and two (2) further upstream from the bridge. The general locations of the soil sampling are shown in Appendix C.

6.1.2 Wolf Creek (L-0022)

The Wolf Creek L-0022 bridge site is located in the SE Lowlands near the town of Bell City on Route MO 25 South. The geologic conditions are typical of those found in the Mississippi Embayment Alluvium (A). However, in nearby areas, it is intermixed with Residuum deposits, which are more prevalent in the northwest. The results of the soil analyses show that the soils are primarily fine-grained and contain more coarse-grained soils as part of the bedload material within the river channel. The general locations of the soil sampling are shown in Appendix C.

6.1.3 Dry Fork Creek (L-0564)

The L-0564 Bridge Site is located on the Missouri Ozarks border with a depth to bedrock of less than 25 feet. Highway K runs from Big Spring to Americus and follows the Dry Fork Valley, which floods seasonally. The surficial geology consists of Residuum deposits that are surrounded by higher elevation deposits of Loess. Within the floodplain, most of the surficial geology is residuum and within the channel, there are considerable bedload materials consisting of sands and gravels. Soil/sediment samples were obtained within the channel and the floodplain immediately under the bridge and upstream for the bedload materials. The general locations of the soil sampling are shown in Appendix C.

6.1.4 Gasconade River (A-3760)

The A-3760 bridge site is located in the Upper Ozarks within the alluvium of the Gasconade River. The bridge is on Route 63 about 5 miles south of Vienna, MO. The surficial geology consists of shallow bedrock within the river channel and alluvium in the floodplain, all surrounded by Residuum deposits. The bridge is supported on shallow bedrock in the northern abutment to alluvium on the southern abutment. Soil samples were collected for this bridge location at both the overbank floodplains and in the channel locations. The unique conditions of shallow bedrock within the river channel caused difficulty retrieving samples from a watercraft using the FISP sampler, so samples were obtained from exposed gravel bars during low water conditions. A total of twenty-one (21) samples were collected and transported to the laboratories for soil analysis. Sixteen (16) samples were in the overbank/floodplain areas and five (5) were

within the channel. The sampling locations are shown graphically in Figure 6-1. Figure 6-2 and Figure 6-3 show the grain size distributions and Atterberg limits, respectively, for the for the A-3760 site samples.

Figure 6-1. Soil sampling locations for the Gasconade River (A-3760) site.

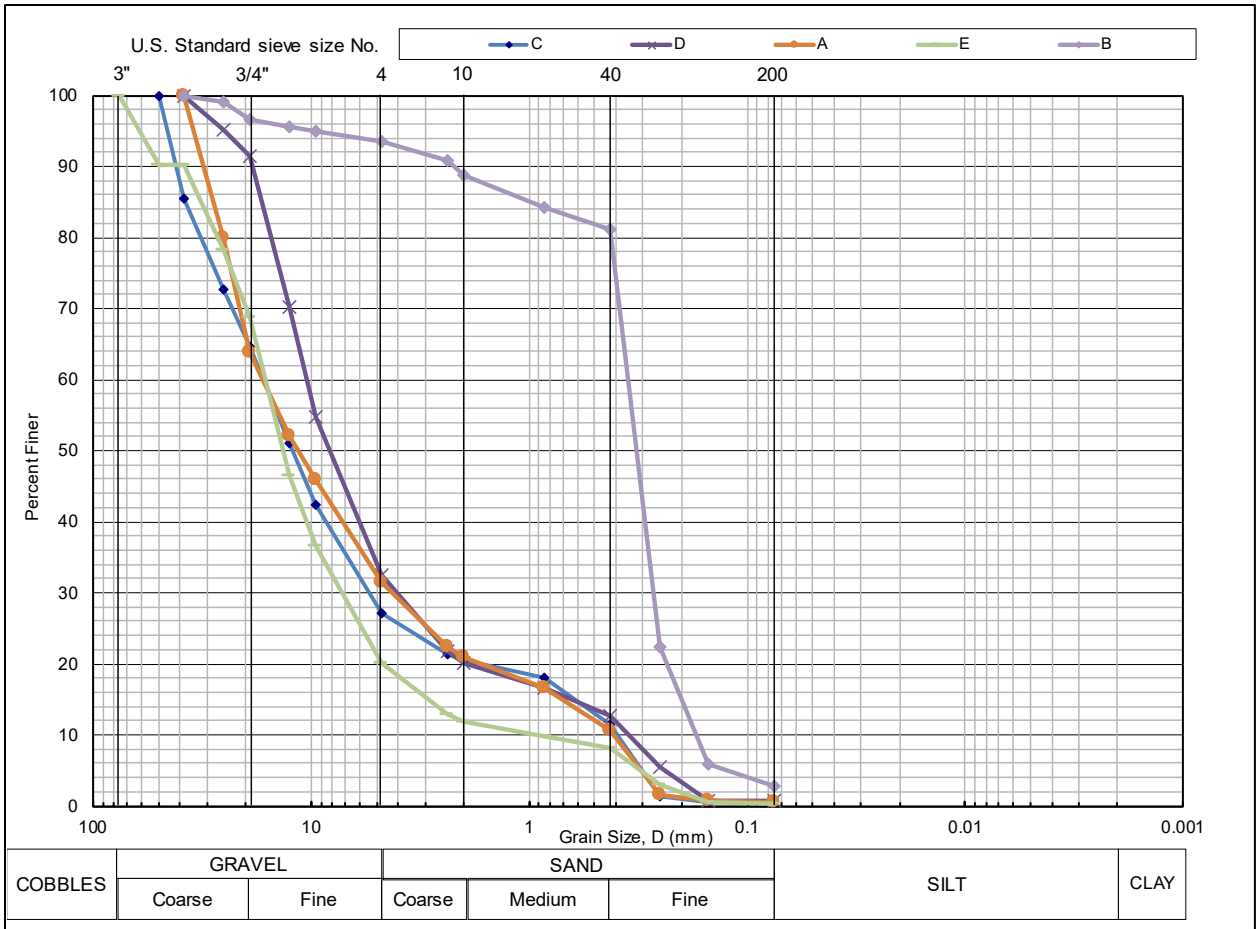

Specimen ID	D60	D50	D30	D10	Cc	Cu	LL	PI
C	17.00	12.00	4.40	0.40	2.85	42.50		
D	10.00	8.00	3.00	0.35	2.57	28.57		
A	17.00	12.00	3.00	0.40	1.32	42.50		
E	17.00	13.00	7.00	1.00	2.88	17.00		
B	0.32	0.31	0.27	0.17	1.34	1.88		

Specimen ID	% Gravel	% Sand	% Silt	% Clay	Classification	
C	73.0	26.6	0.5		GW	Well Graded Gravel
D	67.6	31.7	0.7		GW	Well Graded Gravel
A	68.5	30.9	0.6		GW	Well Graded Gravel
E	79.9	19.8	0.3		GW	Well Graded Gravel
B	6.6	90.7	2.7		SP	Poorly Graded Sand

SAINT LOUIS UNIVERSITY

GRAIN SIZE DISTRIBUTION RESULTS

Site:	A3760
Project:	MODOT Bridge Scour
Location:	Gasconade River

Figure 6-2. Gasconade River (A-3760) – Soil/sediment grain size distribution.

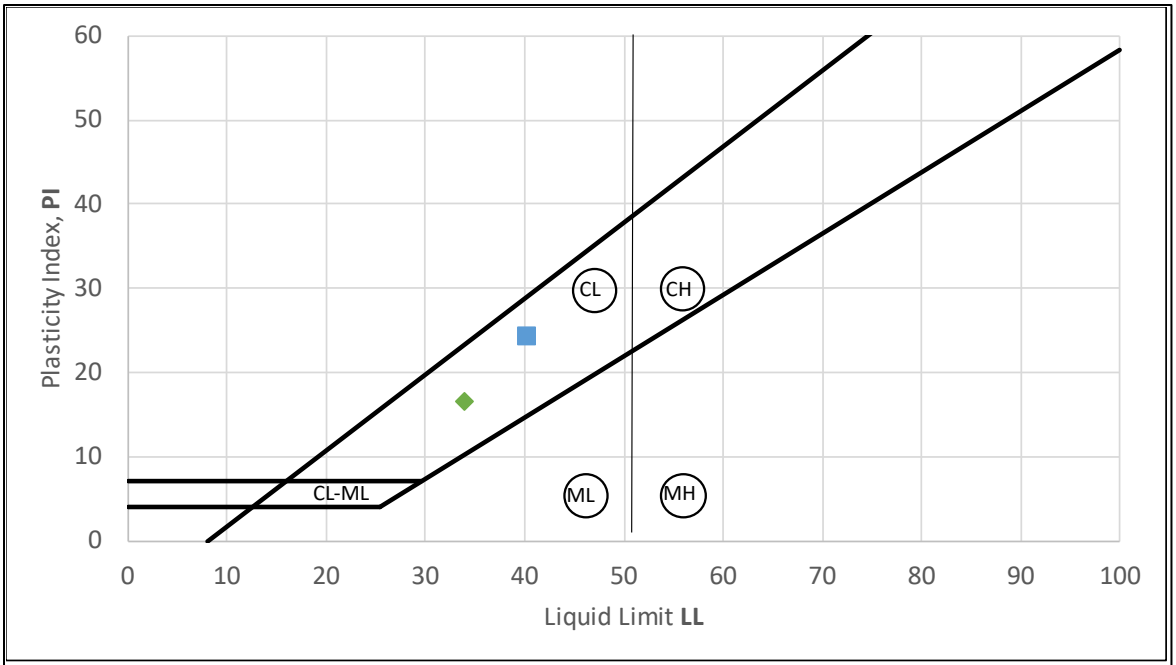

Legend	Borehole	Sample	Depth	LL	PL	PI	% Fines	Description
■	S0	1	6"-12"	40	16	24		CL
◆	S2	5	0"-6"	34	17	17		CL
▲	S3	6	6"-12"	NP	NP	NA		

	Borehole	Sample	Depth	w.c.	Dry	Retained	% Fines	Description
#200 Wash	S5	8	6"-12"	19%	123.91	57.09	54%	
	S6	9	6"-12"	26%	153.01	103.33	32%	
	S10	13	6"-12"	24%	113.07	40.22	64%	
	S13	16	6"-12"	20%	123.36	58.65	52%	

SAINT LOUIS UNIVERSITY

ATTERBERG LIMIT and #200 WASH RESULTS	
Site:	A3760
Project:	MODOT Bridge Scour
Location:	Gasconade River

Figure 6-3. Gasconade River (A-3760) – Soil/sediment Atterberg limits.

6.1.5 Missouri River (L-0550)

The Missouri River Bridge site (L-0550) is located on the Missouri Ozarks border with a depth to bedrock varying from 25 to 75 feet within the river channel. The Missouri River alluvium is about 1.5 to 1.75 miles wide in the Jefferson City area. At the bridge location, the floodplain is predominantly to the north. The soil conditions are typical of an alluvium deposit, consisting of a mixture of sands and interbedded fine-grained soils. Within the channel, the sediment was primarily bedload material consisting of sands and gravels and in the floodplain, the soil contained more medium fine sands with clays and silts. Soil samples were collected for this bridge location at both the overbank floodplains and within the channel locations. A total of twenty-one (21) samples were collected and transported to the laboratories for soil analysis. Sixteen (16) samples were in the overbank/floodplain areas and five (5) were within the channel. The sample collection methods were described in Section 4.2 and all sampling locations are shown in Appendix C.

6.1.6 Summary of Soil/Sediment Descriptions at Bridge Sites

Table 6-1 summarizes the soil/sediment conditions described in the above sections. Note that the soil conditions vary across the bridge sites and are the basis for the scour analyses input parameters described in Section 6.5.

Table 6-1. Soil/sediment conditions at bridge sites.

Bridge Site	Geologic Setting	Left Overbank			Main Channel			Right Overbank		
		Soil Symbol	D_{50}	PI	Soil Symbol	D_{50}	PI	Soil Symbol	D_{50}	PI
Creek H-0024	Eastern Glaciated Plains	CL w/ sand	--	18	CL	--	17	CL w/ sand	--	23
Wolf Creek L-0022	SE Lowlands Alluvium	ML, CL	--	12	--	1.3	--	ML, CL	--	10
Dry Fork Creek L-0564	Ozarks Residuum	SP	2.5	--	GP	8	--	SP, CL	--	12
Gasconade River A-3760	Upper Ozarks Residuum	Rock	--	--	GW	12	--	SM, CL	--	20
Missouri River L-0550	Missouri River Alluvium	ML, CL	20	--	SP	0.5	--	Rock	--	--

6.2 1-D Hydraulic Modeling Results

Velocity distribution plots were developed from the HEC-RAS results for all modeled scenarios (i.e., the 100-yr and 500-yr flow events for each site) and are located in Appendix D. Although HEC-RAS is a 1-D model with solutions only computed at the cross sections, the RAS Mapper feature in HEC-RAS can interpolate values between cross sections to generate an estimate of the flow velocities across the entire inundated area. Figure 6-4 provides an example velocity distribution plot from the 100-yr flow event at the Gasconade River (A-3760) site and Figure 6-5 shows a close-up of the velocity distribution near the vicinity of the bridge. The highest flow velocities (approximately 13 ft/s) were observed in the contracted channel section at the bridge with negligible velocities overtopping the roadway embankment on the right overbank area.

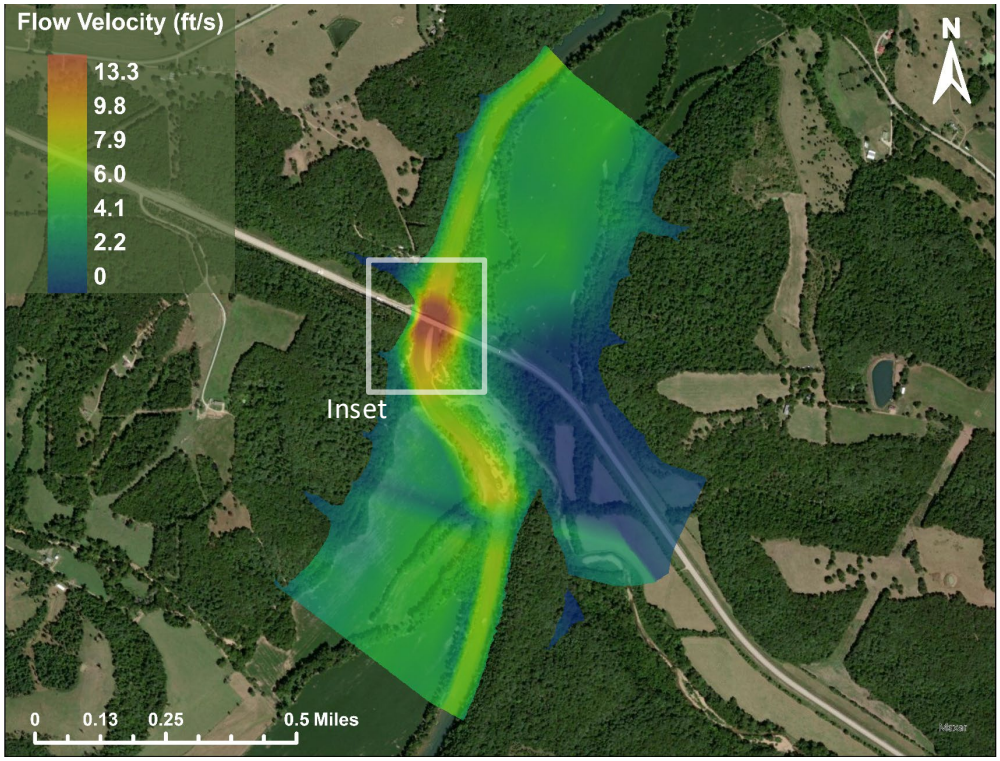

Figure 6-4. Gasconade River (A-3760) – HEC-RAS 100-yr flow velocity distribution.

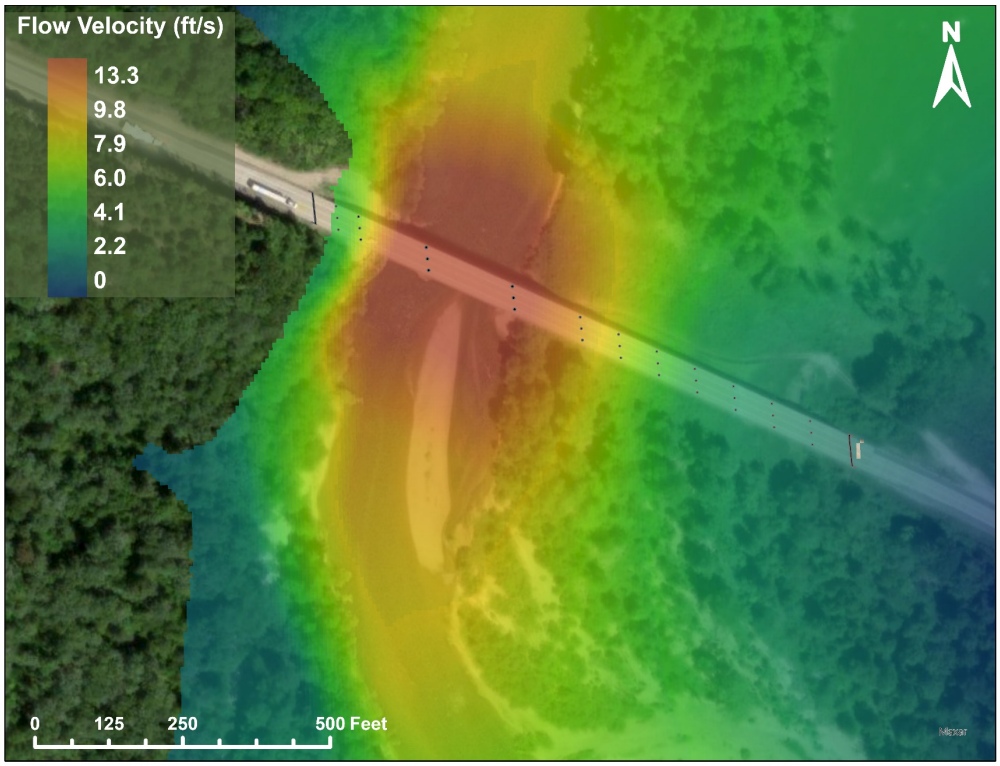

Figure 6-5. Gasconade River (A-3760) – HEC-RAS 100-yr flow velocity distribution - Inset.

Several hydraulic parameters are required as input for scour calculations. The key hydraulic parameters for computing contraction scour, pier scour, and abutment scour, are provided in Table 6-2, Table 6-3, and Table 6-4, respectively. Table 6-2 (contraction scour) includes upstream flow depth and velocity and flow through the bridge opening; Table 6-3 (pier scour) includes approach flow depth and velocity; and Table 6-4, (abutment scour) includes approach flow depth, flow depth at the abutment prior to scour, upstream unit discharge (q_1), and the unit discharge in the constricted opening (q_2).

Table 6-2. HEC-RAS (1-D) hydraulic conditions for contraction scour.

Bridge Site	Storm Event	Upstream Flow Depth (ft)			Average Velocity Upstream (ft/s)			Flow Through Bridge Opening (cfs)		
		LOB	Main Channel	ROB	LOB	Main Channel	ROB	LOB	Main Channel	ROB
Creek H-0024	100-yr	5.46	7.5	4.08	2.33	4.01	2.52	695	606	314
	500-yr	6.21	8.16	4.84	2.44	3.44	2.54	509	472	238
Wolf Creek L-0022	100-yr	0.55	7.56	1.45	0.96	4.01	1.89	0.63	1,992	58
	500-yr	0.97	8.26	2.15	1.54	4.84	3.17	3.8	2,533	137
Dry Fork Creek L-0564	100-yr	6.11	10.98	6.59	2.12	3.77	0.46	3,084	5,148	156
	500-yr	6.88	11.75	7.35	2.28	3.85	0.63	3,658	5,592	204
Gasconade River A-3760	100-yr	18.44	36.68	22.36	2.68	9.09	3.75	6,930	129,687	47,711
	500-yr	21.41	41.31	27.26	2.84	9.47	4.19	11,106	131,602	45,689
Missouri River L-0550	100-yr	16.22	44.48	4.87	3.62	9.36	1.27	98,926	485,856	242
	500-yr	20.83	49.09	7.38	5.51	9.05	1.50	187,829	532,672	663

Table 6-3. HEC-RAS (1-D) hydraulic conditions for pier scour.

Bridge Site	Storm Event	Approach Flow Depth (ft)	Approach Flow Velocity (ft/s)
Creek H-0024	100-yr	8.42	4.53
	500-yr	9.17	3.95
Wolf Creek L-0022	100-yr	14.89	7.77
	500-yr	15.59	9.06
Dry Fork Creek L-0564	100-yr	12.98	4.54
	500-yr	13.75	4.61
Gasconade River A-3760	100-yr	39.27	12.78
	500-yr	44.17	12.71
Missouri River L-0550	100-yr	54.97	11.17
	500-yr	59.58	10.77

Table 6-4. HEC-RAS (1-D) hydraulic conditions for abutment scour.

Bridge Site	Storm Event	Approach Depth (ft)	Depth at Abut. Toe (ft)	q_1 (ft^2/s)	q_2 (ft^2/s)	q_2/q_1 (-)
Creek H-0024	Left Abutment					
	100-yr	5.46	6.3	30.4	38.0	1.25
	500-yr	6.21	7.05	29.3	28.7	0.98
	Right Abutment					
	100-yr	4.08	3.62	30.4	38	1.25
	500-yr	4.84	4.37	29.3	28.7	0.98
Wolf Creek L-0022	Left Abutment					
	100-yr	10.47	9.95	61.5	24.4	0.40
	500-yr	11.13	10.47	83.5	31.8	0.38
	Right Abutment					
	100-yr	6.67	6.18	61.5	24.4	0.40
	500-yr	7.33	6.71	83.5	31.8	0.38
Dry Fork Creek L-0564	Left Abutment					
	100-yr	4.1	4.64	13.0	33.3	2.57
	500-yr	4.87	5.41	15.7	37.6	2.40
	Right Abutment					
	100-yr	6.59	7.53	43.5	33.3	0.77
	500-yr	7.35	8.3	47.3	37.6	0.79
Gasconade River A-3760	Left Abutment					
	100-yr	36.18	0.36	361	110	0.30
	500-yr	40.69	2.1	448	171	0.38
	Right Abutment					
	100-yr	22.36	22.19	118	178	1.51
	500-yr	27.26	27.09	130	175	1.35
Missouri River L-0550	Left Abutment					
	100-yr	16.22	12.96	65	199	3.1
	500-yr	20.01	17.5	151	245	1.6
	Right Abutment					
	100-yr	n/a	n/a	n/a	n/a	n/a
	500-yr	n/a	n/a	n/a	n/a	n/a

6.3 2-D Hydraulic Modeling Results

Velocity distribution plots were also developed from the SRH-2D results for all modeled scenarios (i.e., the 100-yr and 500-yr flow events for each site) and are located in Appendix E. Figure 6-6 provides an example velocity distribution plot from the 100-yr flow event at the Gasconade River (A-3760) site and Figure 6-7 shows a close-up of the velocity distribution near the vicinity of the bridge. The highest flow velocities (approximately 7 ft/s) were observed in the contracted channel section and near the right abutment. There are also notably high velocities (approximately 6 ft/s) over the road embankment on the right overbank area indicating a significant portion of the flow is being conveyed across the embankment. In addition to velocity magnitudes, SRH-2D computes the flow direction which determines the angle of attack required for pier scour calculations. Figure 6-8 shows the velocity vector plot for the 100-yr flow event at the Dry Fork Creek (L-0564) site. This plot provides a good illustration of the 2-D flow fields near the bridge.

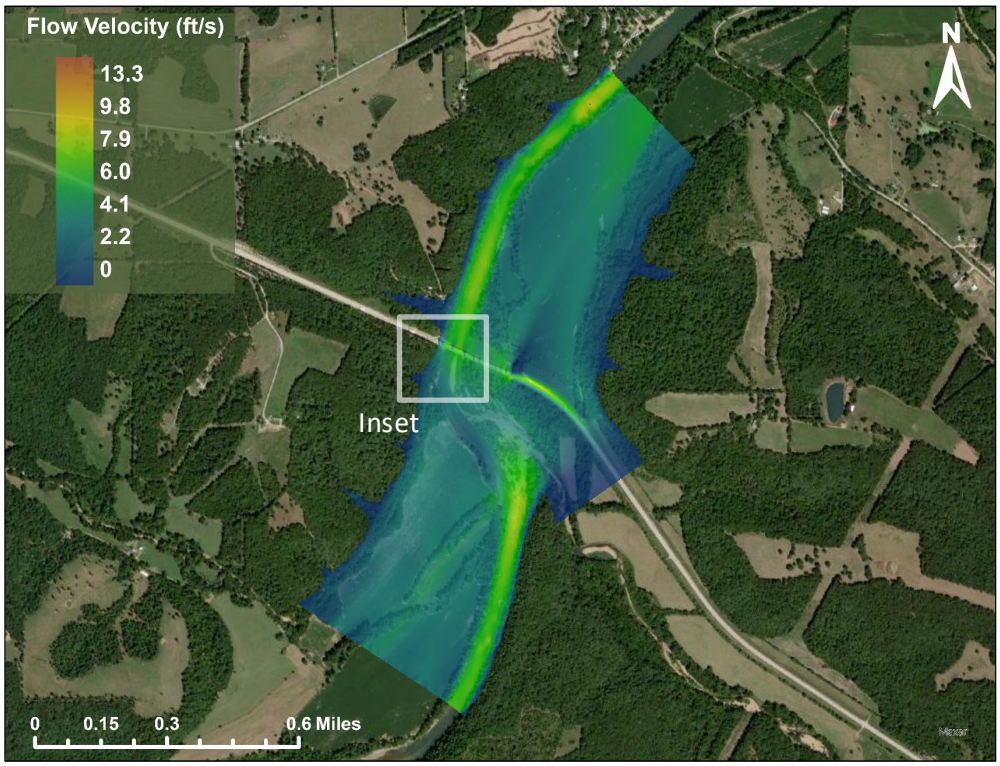

Figure 6-6. Gasconade River (A-3760) – SRH-2D 100-yr flow velocity distribution.

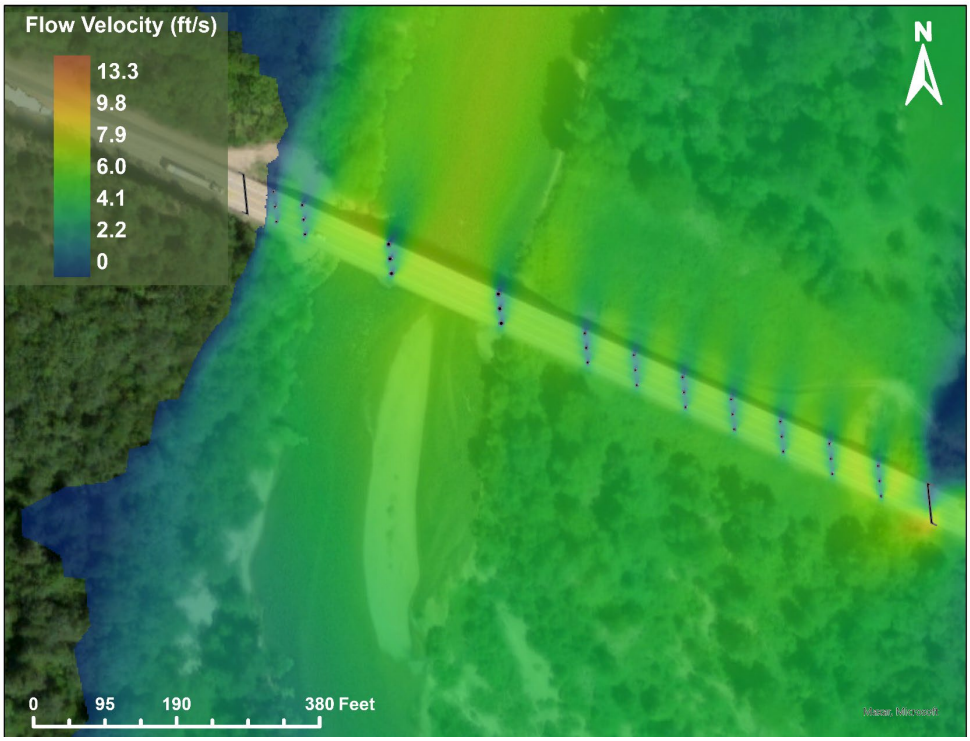

Figure 6-7. Gasconade River (A-3760) – SRH-2D 100-yr flow velocity - Inset.

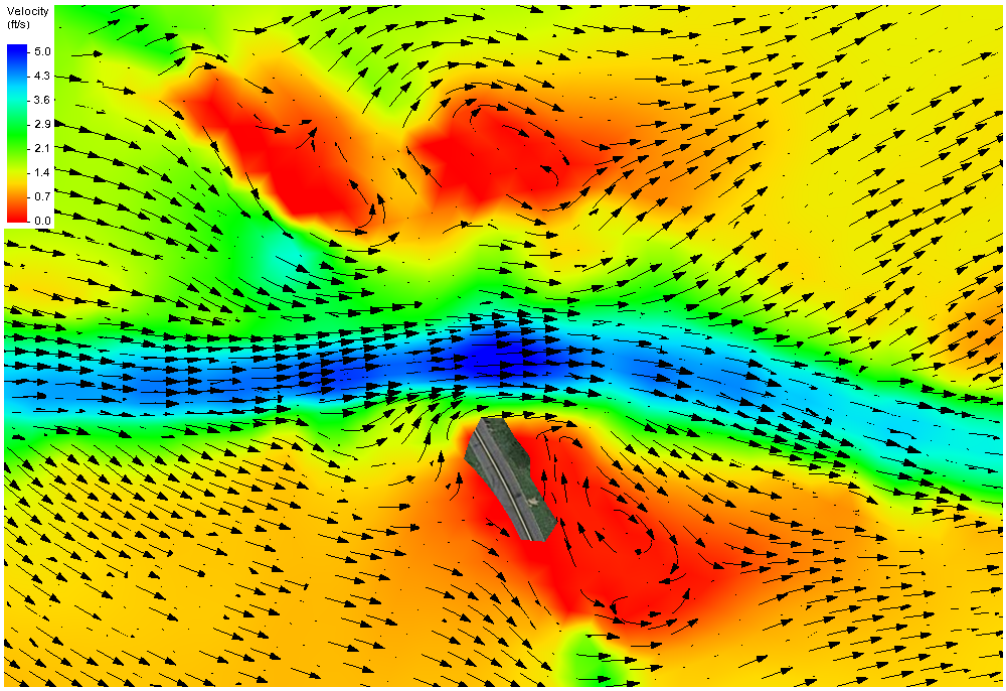

Figure 6-8. Flow velocity vector plot for the 100-yr event at the Dry Fork Creek (L-0564) site.

The key hydraulic parameters for computing contraction scour, pier scour, and abutment scour, are provided in Table 6-5, Table 6-6, and Table 6-7, respectively. Table 6-5 (contraction scour) includes upstream flow depth and velocity and flow through the bridge opening; Table 6-6 (pier scour) includes approach flow depth and velocity; and Table 6-7 (abutment scour) includes approach flow depth, flow depth at the abutment prior to scour, upstream unit discharge (q_1), and the unit discharge in the constricted opening (q_2).

Table 6-5. SRH-2D hydraulic conditions for contraction scour.

Bridge Site	Storm Event	Upstream Flow Depth (ft)			Average Velocity Upstream (ft/s)			Flow Through Bridge Opening (cfs)		
		LOB	Main Channel	ROB	LOB	Main Channel	ROB	LOB	Main Channel	ROB
Creek H-0024	100-yr	2.08	7.14	2.76	1.20	2.40	1.45	454	843	203
	500-yr	2.19	7.62	2.96	1.35	2.66	1.79	582	904	540
Wolf Creek L-0022	100-yr	1.45	10.83	2.64	1.28	2.45	0.79	206	1,760	163
	500-yr	2.10	11.89	3.73	1.15	2.04	0.84	343	2,259	248
Dry Fork Creek L-0564	100-yr	4.55	10.63	2.79	2.08	4.13	1.37	1,985	2,682	727
	500-yr	5.25	11.34	3.53	1.98	3.88	1.58	2,290	2,797	860
Gasconade River A-3760	100-yr	25.84	40.4	27.91	2.46	4.07	4.42	8,984	63,655	76,660
	500-yr	28.86	44.97	32.39	2.49	4.52	4.60	10,995	71,621	91,380
Missouri River L-0550	100-yr	15.85	47.29	20.88	2.15	6.13	1.46	56,315	338,930	1,483
	500-yr	20.01	51.53	11.49	2.39	6.99	1.69	81,174	448,863	2,441

Table 6-6. SRH-2D hydraulic conditions for pier scour.

Bridge Site	Storm Event	Approach Flow Depth (ft)	Approach Flow Velocity (ft/s)
Creek H-0024	100-yr	7.16	4.42
	500-yr	7.66	4.42
Wolf Creek L-0022	100-yr	14.89	6.58
	500-yr	15.59	6.57
Dry Fork Creek L-0564	100-yr	13.16	4.54
	500-yr	13.89	4.34
Gasconade River A-3760	100-yr	41.84	6.58
	500-yr	46.42	6.57
Missouri River L-0550	100-yr	56.88	8.22
	500-yr	61.16	7.92

Table 6-7. SRH-2D hydraulic conditions for abutment scour.

Bridge Site	Storm Event	Approach Depth (ft)	Depth at Abut. Toe (ft)	q_1 (ft^2/s)	q_2 (ft^2/s)	q_2/q_1 (-)
Creek H-0024	Left Abutment					
	100-yr	7.14	1.04	17.1	44.4	2.60
	500-yr	7.62	1.58	20.3	47.6	2.35
	Right Abutment					
	100-yr	7.14	3.02	17.1	44.4	2.60
	500-yr	7.62	3.57	20.3	47.6	2.35
Wolf Creek L-0022	Left Abutment					
	100-yr	10.83	10.48	26.5	111	4.20
	500-yr	11.89	10.59	24.3	171	7.03
	Right Abutment					
	100-yr	10.83	6.38	26.5	111	4.20
	500-yr	11.89	7.05	24.3	171	7.03
Dry Fork Creek L-0564	Left Abutment					
	100-yr	10.63	3.57	43.9	55.6	1.27
	500-yr	11.34	3.51	44.0	59.2	1.35
	Right Abutment					
	100-yr	10.63	2.47	43.9	55.6	1.27
	500-yr	11.34	3.19	44.0	59.2	1.35
Gasconade River A-3760	Left Abutment					
	100-yr	41.69	2.35	156	268	1.72
	500-yr	44.84	6.97	206	330	1.60
	Right Abutment					
	100-yr	27.91	20.66	123	126	1.02
	500-yr	32.39	25.24	149	151	1.01
Missouri River L-0550	Left Abutment					
	100-yr	15.85	13.24	34.1	29.5	0.87
	500-yr	20.01	17.44	47.7	42.6	0.89
	Right Abutment					
	100-yr (*)	n/a	n/a	n/a	n/a	n/a
	500-yr (*)	n/a	n/a	n/a	n/a	n/a

* not applicable: flood waters do not reach the right abutment

6.4 Comparison of Hydraulic Modeling Results

The 1-D and 2-D models were constructed, simulated, and compared based on their outputs to each other and the WSPRO study results. When comparing the models, HEC-RAS was referred to as the 1-D model. The hydraulic modeling results such as flow depths, velocities, unit discharges, and others were then used to compute theoretical scour depths. Three different types of scour were computed based on these results: contraction, pier, and abutment scour. Each scour type requires a specific array of inputs, often

unique from each other. Significant components of the scour equations were chosen to be represented in the results tables based on scour type. Separate tables were generated for the hydraulic conditions relevant to the scour computations at each bridge site.

For contraction scour, the key tabulated hydraulic parameters for each site are upstream flow depth, average velocity upstream, and flow through the bridge opening. Since contraction scour is computed for three areas in the contracted section – LOB, main channel, and ROB, the hydraulic results were determined specific to these areas, thus three results were given for each hydraulic variable. For pier scour, the key tabulated hydraulic parameters are the thalweg approach depth and velocity. The thalweg is the deepest part of the channel, which often also has the highest flow velocity. The flow depth and velocity at the thalweg just upstream of the bridge are used to compute pier scour and are reported in this section for all bridge sites. For abutment scour, the key tabulated hydraulic parameters are approach depth, depth at abutment toe, q_1 (unit discharge upstream in the main channel) and q_2 (unit discharge in the constricted area), and the ratio q_2/q_1,

With three types of scour and five bridge sites, 15 total tables convey the hydraulic modeling results from the study. The results listed are a small portion of the overall components contributing to the scour computations. Multiple variables listed were not entirely available from the WSPRO study report, with the missing information denoted by "n/a" in the empty cells. The hydraulic results for each bridge site are shown in the following order: H-0024, L-0022, L-0564, A-3760, and L-0550.

6.4.1 Creek (H-0024)

For the Creek (H-0024) site, the key hydraulic parameters for contraction scour are shown in Table 6-8. Flow depths upstream were similar between the two models, with an average of 6% difference between the 1-D and 2-D models. HEC-RAS predicted faster flow velocities upstream of the contraction for each scenario by 38-60%. SRH-2D determined a larger portion of the flow would pass through the bridge opening than in the 1-D HEC-RAS model. High flow velocities through the bridge opening shown in Appendix E for the 2-D model contrast with the lower flow rates in Appendix D for the 1-D model.

Table 6-8. Creek (H-0024) – Summary of computed hydraulic conditions for contraction scour.

Model Type	Storm Event	Upstream Flow Depth (ft)			Average Velocity Upstream (ft/s)			Flow Through Bridge Opening (cfs)		
		LOB	Main Channel	ROB	LOB	Main Channel	ROB	LOB	Main Channel	ROB
WSPRO	100-yr	n/a	5.80	n/a	n/a	3.55	n/a	n/a	330	n/a
	500-yr	n/a	6.80	n/a	n/a	2.88	n/a	n/a	314	n/a
HEC-RAS	100-yr	5.46	7.50	4.08	2.33	4.01	2.52	695	606	314
	500-yr	6.21	8.16	4.84	2.44	3.44	2.54	509	472	237
SRH-2D	100-yr	2.08	7.14	2.76	1.20	2.40	1.45	454	843	203
	500-yr	2.19	7.62	2.96	1.35	2.66	1.79	582	904	540

Table 6-9 provides the key hydraulic parameters related to pier scour for bridge site H-0024. The thalweg approach depth applied toward the local scour at the single pier was greater using the 1-D model. The approach velocities varied only by 4% on average, a difference that would negligibly affect the scour results.

Table 6-9. Creek (H-0024) – Summary of computed hydraulic conditions for pier scour.

Model Type	Storm Event	Approach Depth (ft)	Approach Velocity (ft/s)
WSPRO	100-yr	6.46	6.77
	500-yr	7.43	8.34
HEC-RAS	100-yr	8.42	4.53
	500-yr	9.17	3.95
SRH-2D	100-yr	7.16	4.42
	500-yr	7.66	4.42

Table 6-10 shows the key hydraulic parameters for abutment scour at bridge site H-0024. Both abutments for H-0024 are vertical abutments with wing walls. The approach depth for each abutment was greater by 23-50% for SRH-2D. Depths at the abutment toes, in contrast, were greater for the 1-D model. The ratio of q_2/q_1 was greater for the 2-D model hydraulics, which relates to a greater increase in unit discharge through the contraction.

Table 6-10. Creek (H-0024) – Summary of computed hydraulic conditions for abutment scour.

Model Type	Storm Event	Approach Depth (ft)	Depth at Abut. Toe (ft)	q_1 (ft^2/s)	q_2 (ft^2/s)	q_2/q_1 (-)
Left Abutment						
WSPRO	100-yr	n/a	3.71	n/a	n/a	n/a
	500-yr	n/a	4.68	n/a	n/a	n/a
HEC-RAS	100-yr	5.46	6.30	30.4	38.0	1.25
	500-yr	6.21	7.05	29.3	28.7	0.98
SRH-2D	100-yr	7.14	1.04	17.1	44.4	2.60
	500-yr	7.62	1.58	20.3	47.6	2.35
Right Abutment						
WSPRO	100-yr	n/a	4.07	n/a	n/a	n/a
	500-yr	n/a	5.04	n/a	n/a	n/a
HEC-RAS	100-yr	4.08	3.62	30.4	38.0	1.25
	500-yr	4.84	4.37	29.3	28.7	0.98
SRH-2D	100-yr	7.14	3.02	17.1	44.4	2.60
	500-yr	7.62	3.57	20.3	47.6	2.35

6.4.2 Wolf Creek (L-0022)

For the Wolf Creek (L-0022) site, the key hydraulic parameters for contraction scour are shown in Table 6-11. The 1-D model determined flow depths upstream of the contraction to be less than those of the 2-D model by 36% in the main channel. The 1-D model determined average flow velocities upstream to be 65% greater in the main channel than the 2-D model. The flow rates through the contracted section were similar considering total flow through the opening, which is predicted when no bridge overtopping is present.

Table 6-11. Wolf Creek (L-0022) – Summary of computed hydraulic conditions for contraction scour.

Model Type	Storm Event	Upstream Flow Depth (ft)			Average Velocity Upstream (ft/s)			Flow Through Bridge Opening (cfs)		
		LOB	Main Channel	ROB	LOB	Main Channel	ROB	LOB	Main Channel	ROB
WSPRO	100-yr	n/a	7.0	n/a	n/a	3.61	n/a	n/a	1,354	n/a
	500-yr	n/a	8.8	n/a	n/a	1.88	n/a	n/a	1,007	n/a
HEC-RAS	100-yr	0.55	7.56	1.45	0.96	4.01	1.89	0.63	1,992	58
	500-yr	0.97	8.26	2.15	1.54	4.84	3.17	4	2,533	137
SRH-2D	100-yr	1.45	10.83	2.64	1.28	2.45	0.79	206	1,760	163
	500-yr	2.10	11.89	3.73	1.15	2.04	0.84	343	2,259	248

Table 6-12 provides the key hydraulic parameters related to pier scour for bridge site L-0022. Approach depth for local scour was slightly more – 6.6%, for the 2-D model than the 1-D model. The approach velocity for the piers was greater by an average of 33% for the 1-D model.

Table 6-12. Wolf Creek (L-0022) – Summary of computed hydraulic conditions for pier scour.

Model Type	Storm Event	Approach Depth (ft)	Approach Velocity (ft/s)
WSPRO	100-yr	10.36	10.71
	500-yr	10.77	13.21
HEC-RAS	100-yr	14.89	7.77
	500-yr	15.59	9.06
SRH-2D	100-yr	17.28	4.80
	500-yr	15.28	7.31

Table 6-13 shows the key hydraulic parameters for abutment scour at bridge site L-0022. Both abutments for L-0022 are spill-through abutments. Both the approach depths and depths at the abutment toes were greater using the 2-D model. The ratio of q_2/q_1 was significantly greater for the 2-D model, with q_1 being greater for the 1-D model and q_2 greater for the 2-D model. This relates to a higher contraction of flow through the bridge opening for the 2-D model.

Table 6-13. Wolf Creek (L-0022) – Summary of computed hydraulic conditions for abutment scour.

Model Type	Storm Event	Approach Depth (ft)	Depth at Abut. Toe (ft)	q_1 (ft^2/s)	q_2 (ft^2/s)	q_2/q_1 (-)
Left Abutment						
WSPRO	100-yr	n/a	3.07	n/a	n/a	n/a
	500-yr	n/a	3.48	n/a	n/a	n/a
HEC-RAS	100-yr	10.47	9.95	61.5	24.4	0.40
	500-yr	11.13	10.47	83.5	31.8	0.38
SRH-2D	100-yr	10.83	10.48	26.5	111	4.20
	500-yr	11.89	10.59	24.3	171	7.03
Right Abutment						
WSPRO	100-yr	n/a	0.16	n/a	n/a	n/a
	500-yr	n/a	0.57	n/a	n/a	n/a
HEC-RAS	100-yr	6.67	6.18	61.5	24.4	0.4
	500-yr	7.33	6.71	83.5	31.8	0.4
SRH-2D	100-yr	10.83	6.38	26.5	111.0	4.2
	500-yr	11.89	7.05	24.3	171.0	7.0

6.4.3 Dry Fork Creek (L-0564)

For the Dry Fork Creek (L-0564) site, the key hydraulic parameters for contraction scour are shown in Table 6-14. The flow depth upstream in the main channel only varied by 3% between the 1-D and 2-D models. The flow velocity upstream of the contraction was similar, though the right overbank area had a notably higher velocity for the 2-D model. The 1-D model had much greater conveyance through the bridge opening than the 2-D model. Appendix D shows the 1-D modeling velocity distribution for the 500-yr flow, and Appendix E for the 2-D model. The 1-D model has greater velocities through the opening while the 2-D model has greater velocities over the overtopped roadway.

Table 6-14. Dry Fork Creek (L-0564) – Summary of computed hydraulic conditions for contraction scour.

Model Type	Storm Event	Upstream Flow Depth (ft)			Average Velocity Upstream (ft/s)			Flow Through Bridge Opening (cfs)		
		LOB	Main Channel	ROB	LOB	Main Channel	ROB	LOB	Main Channel	ROB
WSPRO	100-yr	6.60	9.3	4.4	n/a	5.13	n/a	5,258	3,404	790
	500-yr	7.60	10.3	4.8	n/a	5.61	n/a	5,776	3,533	912
HEC-RAS	100-yr	6.11	10.98	6.59	2.12	3.77	0.46	3,084	5,148	156
	500-yr	6.88	11.75	7.35	2.28	3.85	0.63	3,658	5,591	204
SRH-2D	100-yr	4.55	10.63	2.79	2.08	4.13	1.37	1,985	2,682	727
	500-yr	5.25	11.34	3.53	1.98	3.88	1.58	2,290	2,797	860

Table 6-15 provides the key hydraulic parameters related to pier scour for bridge site L-0564. Approach depths for pier scour are nearly identical at this site. Approach velocities for pier scour are also

nearly identical. Differences between the 1-D and 2-D models were expected to have negligible effects on scour computations.

Table 6-15. Dry Fork Creek (L-0564) – Summary of computed hydraulic conditions for pier scour.

Model Type	Storm Event	Approach Depth (ft)	Approach Velocity (ft/s)
WSPRO	100-yr	9.88	9.07
	500-yr	10.80	8.56
HEC-RAS	100-yr	12.98	4.54
	500-yr	13.75	4.61
SRH-2D	100-yr	13.16	4.54
	500-yr	13.89	4.34

Table 6-16 shows the key hydraulic parameters for abutment scour at bridge site L-0564. Both abutments for L-0564 are spill-through abutments. The approach depth for abutment scour is greater using the 2-D model results. The depth at the abutment toe is greater using the 1-D model results. The variances in the q_2/q_1 ratio between the right and left abutments for the 1-D results were expected to have a significant impact on scour estimations.

Table 6-16. Dry Fork Creek (L-0564) – Summary of computed hydraulic conditions for abutment scour.

Model Type	Storm Event	Approach Depth (ft)	Depth at Abut. Toe (ft)	q_1 (ft^2/s)	q_2 (ft^2/s)	q_2/q_1 (-)
Left Abutment						
WSPRO	100-yr	n/a	2.71	n/a	n/a	n/a
	500-yr	n/a	3.63	n/a	n/a	n/a
HEC-RAS	100-yr	4.1	4.64	13.0	33.3	2.57
	500-yr	4.87	5.41	15.7	37.6	2.40
SRH-2D	100-yr	10.63	3.57	43.9	55.6	1.27
	500-yr	11.34	3.51	44.0	59.2	1.35
Right Abutment						
WSPRO	100-yr	n/a	n/a	n/a	n/a	n/a
	500-yr	n/a	0.89	n/a	n/a	n/a
HEC-RAS	100-yr	6.59	7.53	43.5	33.3	0.77
	500-yr	7.35	8.3	47.3	37.6	0.79
SRH-2D	100-yr	10.63	2.47	43.9	55.6	1.27
	500-yr	11.34	3.19	44.0	59.2	1.35

6.4.4 Gasconade River (A-3760)

For the Gasconade River (A-3760) site, the key hydraulic parameters for contraction scour are shown in Table 6-17. Upstream flow depths were greater across the approach section for the 2-D model. The average velocity upstream was significantly greater in the main channel for the 1-D model. The flow through the bridge opening was also much greater in the main channel for the 1-D model, shown in Figure

6-4. The lack of flow in comparison to the 2-D model was rather conveyed over the road deck outside of the contracted section, as seen in Figure 6-6.

Table 6-17. Gasconade River (A-3760) – Summary of computed hydraulic conditions for contraction scour.

Model Type	Storm Event	Upstream Flow Depth (ft)			Average Velocity Upstream (ft/s)			Flow Through Bridge Opening (cfs)		
		LOB	Main Channel	ROB	LOB	Main Channel	ROB	LOB	Main Channel	ROB
WSPRO	100-yr	n/a	36.3	n/a	n/a	8.94	n/a	n/a	115,187	n/a
	500-yr	n/a	41.3	n/a	n/a	9.85	n/a	n/a	144,516	n/a
HEC-RAS	100-yr	18.44	36.68	22.36	2.68	9.09	3.75	6,930	129,687	47,711
	500-yr	21.41	41.31	27.26	2.84	9.47	4.19	11,106	131,602	45,688
SRH-2D	100-yr	25.84	40.40	27.91	2.46	4.07	4.42	8,985	63,655	76,660
	500-yr	28.86	44.97	32.39	2.49	4.52	4.60	10,995	71,621	91,380

Table 6-18 provides the key hydraulic parameters related to pier scour for bridge site A-3760. Approach flow depths for pier scour were slightly greater with the 2-D model. Approach flow velocities for pier scour were much greater for the 1-D model. The difference in approach velocity between the 1-D and 2-D models can be attributed to the momentum properties of flowing water, which are ignored by the 1-D model. The curve in the channel prior to the contraction directed the flow well to the right of the contraction and over the road deck. The contrast between flow velocities in the bridge opening and over the road deck is shown in Figure 6-4 and Figure 6-6.

Table 6-18. Gasconade River (A-3760) – Summary of computed hydraulic conditions for pier scour.

Model Type	Storm Event	Approach Depth (ft)	Approach Velocity (ft/s)
WSPRO	100-yr	41.15	11.24
	500-yr	46.07	8.85
HEC-RAS	100-yr	39.27	12.78
	500-yr	44.17	12.71
SRH-2D	100-yr	41.84	6.58
	500-yr	46.42	6.57

Table 6-19 shows the key hydraulic parameters for abutment scour at bridge site A-3760. Both abutments for A-3760 are spill-through abutments. The 2-D model determined a greater approach depth for both abutments. The depths at the abutment toes were similar for the right abutment, but greater using the 2-D results for the left abutment. The q_2 and q_1 values varied between the abutments, with the ratio q_2/q_1 being less with the 1-D model for the left abutment (type A near the channel bank) and greater for the right abutment (type B in the floodplain).

Table 6-19. Gasconade River (A-3760) – Summary of computed hydraulic conditions for abutment scour.

Model Type	Storm Event	Approach Depth (ft)	Depth at Abutment Toe (ft)	q_1 (ft^2/s)	q_2 (ft^2/s)	q_2/q_1 (-)
Left Abutment						
WSPRO	100-yr	n/a	18.26	n/a	n/a	n/a
	500-yr	n/a	23.18	n/a	n/a	n/a
HEC-RAS	100-yr	36.18	0.36	362	110	0.30
	500-yr	40.69	2.10	448	171	0.38
SRH-2D	100-yr	41.69	2.35	156	268	1.72
	500-yr	44.84	6.97	206	330	1.60
Right Abutment						
WSPRO	100-yr	n/a	n/a	n/a	n/a	n/a
	500-yr	n/a	n/a	n/a	n/a	n/a
HEC-RAS	100-yr	22.36	22.19	118	178	1.51
	500-yr	27.26	27.09	130	176	1.35
SRH-2D	100-yr	27.91	20.66	123	126	1.02
	500-yr	32.39	25.24	149	151	1.01

6.4.5 Missouri River (L-0550)

For the Missouri River (L-0550) site, the key hydraulic parameters for contraction scour are shown in Table 6-20. The upstream flow depths were greater in the main channel for the 2-D model, but the right overbank depth for the 100-yr 2-D scenario was an outlier. The velocities upstream of the contraction were notably greater for the 1-D model in the main channel, 33.5 % greater than the average. The flow through the bridge opening was also greater for the 1-D model by a margin, 25% in the channel and 70% in the left overbank floodplain.

Table 6-20. Missouri River (L-0550) – Summary of computed hydraulic conditions for contraction scour.

Model Type	Storm Event	Upstream Flow Depth (ft)			Average Velocity Upstream (ft)			Flow Through Bridge Opening (cfs)		
		LOB	Main Channel	ROB	LOB	Main Channel	ROB	LOB	Main Channel	ROB
WSPRO	100-yr	n/a	40.3	n/a	n/a	10.42	n/a	n/a	457,926	n/a
	500-yr	n/a	44.2	n/a	n/a	11.65	n/a	n/a	561,086	n/a
HEC-RAS	100-yr	16.22	44.48	4.87	3.62	9.36	1.27	98,926	485,856	242
	500-yr	20.83	49.09	11.49	5.51	9.05	1.50	187,828	532,671	663
SRH-2D	100-yr	15.85	47.29	20.88	2.15	6.13	1.46	56,315	338,930	1,483
	500-yr	20.01	51.53	7.38	2.39	6.99	1.69	81,174	448,863	2,441

Table 6-21 provides the key hydraulic parameters related to pier scour for bridge site L-0550. Thalweg approach depths for the 2-D model were slightly greater. The approach flow velocity for each pier was greater for the 1-D model by 30% on average. The length of the bridge made average values a better reference for comparison of hydraulic results, though not specifically relevant to individual pier scour.

Table 6-21. Missouri River (L-0550) – Summary of computed hydraulic conditions for pier scour.

Model Type	Storm Event	Approach Depth (ft)	Approach Velocity (ft/s)
WSPRO	100-yr	58.15	14.38
	500-yr	61.71	16.46
HEC-RAS	100-yr	54.97	11.17
	500-yr	59.58	10.77
SRH-2D	100-yr	56.88	8.22
	500-yr	61.16	7.92

Table 6-22 shows the key hydraulic parameters for abutment scour at bridge site L-0550. Both abutments for L-0550 are spill-through abutments. The right abutment exists high above the floodplain on top of a bluff, not exposed to flow in either model. Approach depths and depths at the toe of the abutment were nearly identical. The unit discharges q_1 and q_2 were much greater for the 1-D model, and the ratio q_2/q_1 was also greater for the 1-D model. The left abutment is a type B abutment since it sits in the floodplain well setback from the channel.

Table 6-22. Missouri River (L-0550) – Summary of computed hydraulic conditions for abutment scour.

Model Type	Storm Event	Approach Depth (ft)	Depth at Abut. Toe (ft)	q_1 (ft^2/s)	q_2 (ft^2/s)	q_2/q_1 (-)
Left Abutment						
WSPRO	100-yr	n/a	9.76	n/a	n/a	n/a
	500-yr	n/a	13.32	n/a	n/a	n/a
HEC-RAS	100-yr	16.22	12.96	64.6	199	3.08
	500-yr	20.01	17.5	151	245	1.62
SRH-2D	100-yr	15.85	13.24	34.1	29.5	0.87
	500-yr	20.01	17.44	47.7	42.6	0.89
Right Abutment						
WSPRO	100-yr	n/a	n/a	n/a	n/a	n/a
	500-yr	n/a	n/a	n/a	n/a	n/a
HEC-RAS	100-yr	n/a	n/a	n/a	n/a	n/a
	500-yr	n/a	n/a	n/a	n/a	n/a
SRH-2D	100-yr *	n/a	n/a	n/a	n/a	n/a
	500-yr *	n/a	n/a	n/a	n/a	n/a

* not applicable: flood waters do not reach the right abutment

6.5 Scour Analysis

The scour calculations combine the different hydraulic modeling results with the conditions of the sediment under the bridge. Contraction and local (pier and abutment) scour were calculated and eventually combined into a total scour. This total scour resembles the new ground line after the storm event and therefore potentially affects the foundation conditions of the bridge.

For each bridge site, tables were produced containing the scour depth results for contraction scour, pier scour, and abutment scour. Six total scenarios of bridge scour were observed in the analysis with three different models – HEC-RAS (1-D), SRH-2D (2-D), and WSPRO (1-D, results from previous studies). Scour estimations were determined for the 100-yr and 500-yr storm events at each site. The maximum values of scour depth are specified considering lower flow rates can cause greater scour in certain scenarios. For each site, piers were assigned consecutive ID numbers based on their position from left to right looking in the downstream direction. This is also consistent with the orientation for all scour plots within the report.

6.5.1 Creek (H-0024)

6.5.1.1 H-0024 Scour Analysis

The soil conditions were similar across the span of this small bridge consisting of cohesive clay (CL) with variable sand content and there was no apparent bedload near the bridge. This total scour resembles the new ground line after the storm event and therefore potentially affects the foundation conditions of the bridge. The values for contraction scour are shown in Table 6-23 and for local scour (pier and abutments) in Table 6-24 for each hydraulic modeling method used. These values are then plotted along the bridge elevation for better comparison in Appendix F for the 1-D model and Appendix G for the 2-D model.

Table 6-23. Creek (H-0024) – Summary of computed contraction scour depths.

Model Type	Storm Event	Channel Scour Depth (ft)	Left Overbank Scour Depth (ft)	Right Overbank Scour Depth (ft)
WSPRO	100-yr	3.5 (Live Bed)	n/a	n/a
	500-yr	7.3 (Live Bed)	n/a	n/a
HEC-RAS	100-yr	5.1 (Live Bed)	3.6 (Live Bed)	1.3 (Live Bed)
	500-yr	5.2 (Pressure Flow)	7.8 (Pressure Flow)	3.7 (Pressure Flow)
SRH-2D	100-yr	11.8 (Pressure flow)	2.7 (Live Bed*)	0.5 (Live Bed*)
	500-yr	11.6 (Pressure Flow)	1.9 (Live Bed*)	0.7 (Live Bed*)

*Pressure flow conditions but live bed computed scour was greater than the pressure flow computed scour. Thus, the live bed scour depth was used.

The maximum contraction scour depths associated with the 1-D model hydraulics are 5.1 ft for the main channel, 7.8 ft for the left overbank, and 3.7 ft for the right overbank. For the 2-D model, the maximum contraction scour in the main channel was 11.8 ft, 2.7 ft in the left overbank, and 0.7 ft in the right overbank. The difference in contraction scour depths in the main channel between the 2-D and 1-D

models can be attributed to the greater portion of flow being conveyed through the main channel of the bridge opening, shown in Table 6-8.

The H-0024 bridge site was the smallest of the five, with only one round-nosed wall pier between the left and right abutments, which is seen in the scour plot comparisons shown in Figure 6-9. When using the 1-D model to estimate scour, the maximum local scour depth for the pier was 5.0 ft, with max local scour depths of 5.3 ft and 5.1 ft for the left and right abutments, respectively, as seen in Table 6-24. The 2-D model estimated much greater scour depths of 24.0 ft for the pier, 17.1 ft for the left abutment, and 15.1 ft for the right abutment.

Table 6-24. Creek (H-0024) – Summary of computed local scour (pier and abutments) depths.

Abutment Location or Pier ID Number	Bent ID Number	WSPRO 100-yr Scour Depth (ft)	WSPRO 500-yr Scour Depth (ft)	HEC-RAS 100-yr Scour Depth (ft)	HEC-RAS 500-yr Scour Depth (ft)	SRH-2D 100-yr Scour Depth (ft)	SRH-2D 500-yr Scour Depth (ft)
Left Abutment	1	6.7	9.7	5.3*	0.3*	17.1*	16.5*
1	2	5.4	7.4[CP]	5.0[CP]	4.7[CP]	23.1[CP]	24.0[CP]
Right Abutment	3	8.0	11.9	5.1*	1.3*	15.1*	14.5*

*D_{50} below the lower limit for the NCHRP method.
[CP] uses the complex pier calculation method.

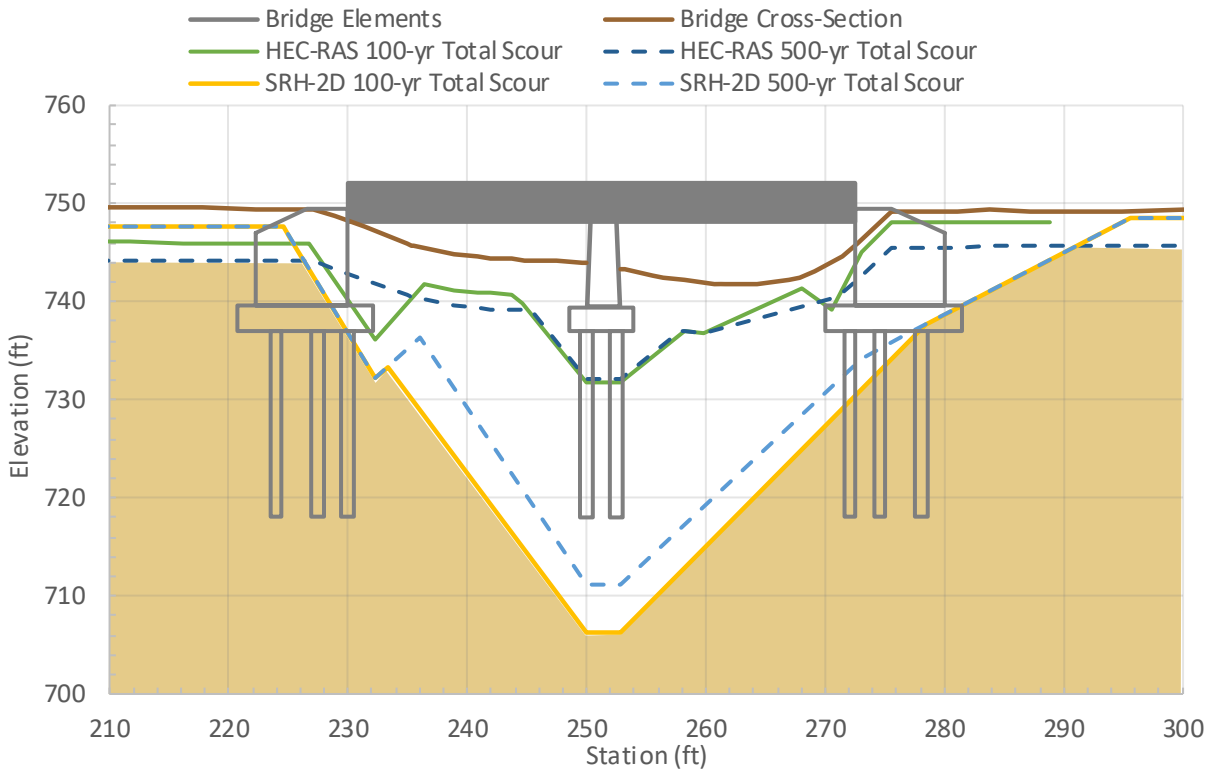

Figure 6-9. Creek (H-0024) – Total scour plot comparisons.

The depths of abutment scour being so significant for the 2-D model are related to the high q_2 values shown in Table 6-4 relative to the 1-D model. The amplification of abutment scour by contraction scour also contributed to the large scour depths. The difference in pier scour can be attributed to the flow angle of attack upstream of the pier. A value of 0 degrees was assumed for the 1-D hydraulic results while the 2-D model determines this number, which was between 19 and 21 degrees. The correction factor for angle of attack increases with pier skew to flow, as well as pier length, and this pier was long at 25.75 ft. When removing this angle of attack from the 2-D model inputs, the local scour is reduced from 20+ ft to around 1-2 ft. The increased flow depth associated with the greater discharge of the 500-yr flood caused road deck overtopping for the 1-D model, which decreased the flow concentration through the bridge opening. The approach flow velocity used to calculate the pier scour shown in Table 6-3 was then less for the 500-yr flood than the 100-yr flood, resulting in a slightly smaller computed pier scour depth as shown in Table 6-24.

6.5.1.2 H-0024 Assessment of Bridge Foundations Due to Scour

The 500-yr flood event conditions indicate that total scour will be about 25 feet depth for the middle pier and near the abutments it may be 12 ft depth. This 1925 bridge (98-yr old) is a small concrete slab bridge with two 20-ft spans supported by a single wall pier. The bridge is supported on 20-ft driven timber piles, and they were treated with creosote before installation. Each bridge bent has 13 piles under each pier and six additional piles for the abutment wingwalls. These piles are likely friction piles since a firm stratum is much deeper than 20-ft. Without the construction records, it is difficult to assess the actual length of the timber piles. The level of total scour predicted for the middle pier would undermine the foundations during the 500-yr storm event. Without this middle support, the bridge most likely will collapse. Because the pier is long and narrow (wall-like geometry), these predictions are strongly affected by the flow angle of attack and bridge skew which is the driving factor for the large local scour depths calculated. SRH-2D hydraulic modeling results indicate this bridge will experience pressure-flow conditions during both the 100-yr and 500-yr events. HEC-18 recommends countermeasures be installed at sites with pressure flow conditions. It should also be noted that the timber piles were treated with creosote, but since the water level changes along the floodplain, it is anticipated that the timber piles deteriorated with time.

6.5.2 Wolf Creek (L-0022)

6.5.2.1 L-0022 Scour Analysis

The soil conditions at L-0022 were similar along the multiple bridge bents consisting of cohesive materials silts (ML) and clays (CL) and there was limited bedload material near the bridge. The abutments have countermeasures of concrete shotcrete and additional riprap near the toe of the slope. The values for contraction scour are shown in Table 6-25 and for local scour (piers and abutments) in Table 6-26 for each hydraulic modeling method used. These values are then plotted along the bridge elevation for better comparison in Appendix F for the 1-D model and Appendix G for the 2-D model.

Table 6-25. Wolf Creek (L-0022) – Summary of computed contraction scour depths.

Model Type	Storm Event	Channel Scour Depth (ft)	Left Overbank Scour Depth (ft)	Right Overbank Scour Depth (ft)
WSPRO	100-yr	7.1 (Live Bed)	n/a	n/a
	500-yr	20.0 (Live Bed)	n/a	n/a
HEC-RAS	100-yr	0.0 (Live Bed)	0.0 (Clear Water)	0.1 (Clear Water)
	500-yr	0.0 (Live Bed)	0.0 (Clear Water)	0.0 (Live Bed)
SRH-2D	100-yr	8.5 (Clear Water)	2.1 (Clear Water)	3.2 (Clear Water)
	500-yr	16.9 (Clear Water)	3.4 (Clear Water)	2.8 (Clear Water)

The computed contraction scour depths for the 1-D model were zero. Maximum contraction scour depths computed using the 2-D model hydraulics were 16.9 ft for the main channel, 3.4 ft for the left overbank, and 3.2 for the right overbank. The hydraulic conditions shown in Table 6-11 favor the 1-D model for stronger, faster flow which would induce contraction scour, but another factor not listed caused the significant difference in computed contraction scour depths between the models. The bottom width in the contracted section and depth prior to scour computed by the 2-D model were drastically different from the values determined manually from the 1-D model. Though both models had bank stations in the contracted section 40+ feet apart, the 2-D model reduced the bottom width for the main channel to just 15.8 ft for the 100-yr storm event, and even less for the 500-yr event. The method for determining this adjusted bottom width was not clear and should be explored for future use of SRH-2D to estimate contraction scour.

Bridge L-0022 over Wolf Creek had a short span supported by two piers with sloping abutments. The local scour depths at the piers were computed for the two models. The 1-D model computed a maximum pier scour of 4.3 ft. The 2-D model computed a maximum local scour depth of 4.7 ft for a pier. The pier scour depths were similar between the models, including the depths estimated by the previous scour analysis done using WSPRO. As for abutment scour computations, the 1-D model estimated no abutment scour while the 2-D model estimated significant abutment scour, with a maximum depth of 43.9 ft at the left abutment and 47.4 ft at the right abutment, as seen in Table 6-26.

Table 6-26. Wolf Creek (L-0022) – Summary of computed local scour (piers and abutments) depths.

Abutment Location or Pier ID Number	Bent ID Number	WSPRO 100-yr Scour Depth (ft)	WSPRO 500-yr Scour Depth (ft)	HEC-RAS 100-yr Scour Depth (ft)	HEC-RAS 500-yr Scour Depth (ft)	SRH-2D 100-yr Scour Depth (ft)	SRH-2D 500-yr Scour Depth (ft)
Left Abut.	4	6.5	7.8	0.0	0.0	27.3	43.9
1	3	4.4	4.8	4.0	4.3	4.0	4.7
2	2	4.4	4.8	4.0	4.3	4.0	3.9
Right Abut.	1	0.7	2.1	0.0	0.0	31.4	47.4

Abutments: average flow velocity upstream and upstream flow depth
Piers: flow depth upstream of pier and flow velocity upstream of pier

With abutment scour being an amplification of contraction scour, the different values associated with the 1-D and 2-D models are congruent with the contraction scour depths for the site. The pier scour depths are different despite the faster and shallower approach flow associated with the 1-D model. The angle of attack of flow associated with the 2-D model makes up for the less intense flow conditions to reach similar pier scour levels as the 1-D model. The bridge elements and total scour plots for each storm event and each model are shown in Figure 6-10, where the effects of the deep contraction scour computed by the 2-D model contrast sharply with the shallow contraction scour for the 1-D model.

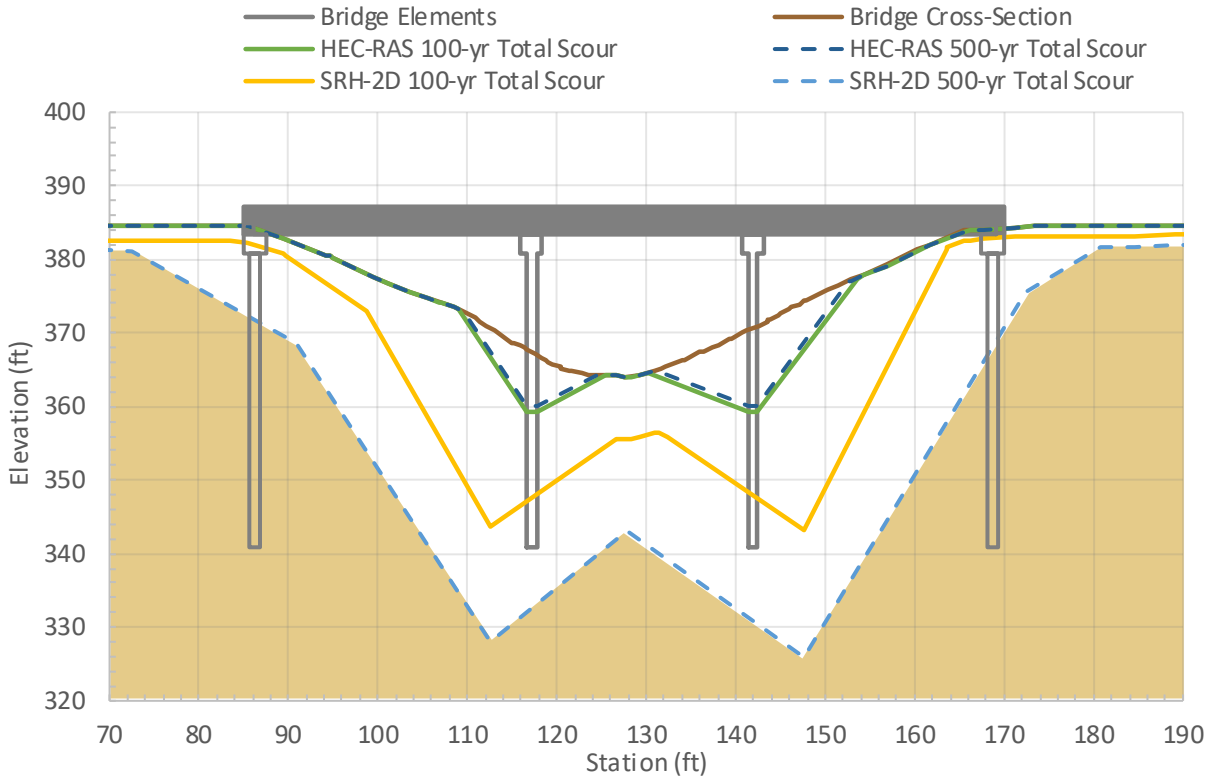

Figure 6-10. Wolf Creek (L-0022) – Total scour plot comparisons.

6.5.2.2 L-0022 Assessment of Bridge Foundations Due to Scour

The 500-yr flood event conditions indicate that total scour will be about 40 ft at the middle bents and less near the abutments. This 1945 bridge (78-yr old) is a small concrete slab bridge with three 25-ft spans supported by two rows of piers. The bridge bents are supported on precast concrete-driven piles, and they are continuous from the bridge bent to the pile tip or toe. Each intermediate bent has six piles, and the abutment bents have seven piles. This bridge does not have any wingwalls given the sloped geometry and it is experiencing instabilities on the southeast abutment (Bent 4). The length of the piles is unknown, only some notes in the plans indicate that the test pile should be 40-ft long and all pile tips should be driven to a minimum elevation, resulting in shorter piles. Therefore, it is assumed that the pile lengths are approximately 40 ft long from the bottom of the bents. These piles are likely friction piles since a firm stratum is much deeper than 40-ft. Without the construction records, it is difficult to assess the actual length of the concrete piles. With the severe total scour prediction and the undermined intermediate bents, the entire bridge would collapse and wash out. However, it is important to realize that this type of bridge, due to its age and scour risk conditions, needs mitigation or even replacement.

6.5.3 Dry Fork Creek (L-0564)

6.5.3.1 L-0564 Scour Analysis

For the L-0564 bridge the soil conditions were quite uniform (silty sand) except within the channel the material was a bit more coarse compared to the floodplain. Minimal countermeasures or rock protection were observed at the base of the piers, and minimal rock protection was observed on the abutments. The countermeasures were not included in this scour analysis. The values for contraction scour are shown in Table 6-27 and for local scour (piers and abutments) in Table 6-28 for each hydraulic modeling method used. These values are then plotted along the bridge elevation for better comparison in Appendix F for the 1-D model and Appendix G for the 2-D model.

Table 6-27. Dry Fork Creek (L-0564) – Summary of computed contraction scour depths.

Model Type	Storm Event	Channel Scour Depth (ft)	Left Overbank Scour Depth (ft)	Right Overbank Scour Depth (ft)
WSPRO	100-yr	2.8 (Clear Water)	14.7 (Clear Water)	7.5 (Clear Water)
	500-yr	2.2 (Clear Water)	15.5 (Clear Water)	7.2 (Clear Water)
HEC-RAS	100-yr	4.0 (Clear Water)	2.8 (Clear Water)	0.0 (Clear Water)
	500-yr	4.2 (Clear Water)	3.4 (Clear Water)	0.0 (Clear Water)
SRH-2D	100-yr	0.0 (Live Bed)	0.0 (Clear Water)	0.0 (Clear Water)
	500-yr	0.0 (Clear Water)	0.0 (Clear Water)	0.0 (Clear Water)

The maximum contraction scour depths computed by the 1-D model were 4.2 ft for the main channel, 3.4 ft for the left overbank, and no contraction scour in the right overbank. The 2-D model, in contrast to the 1-D model, computed zero contraction scour within the contracted bridge section of the site. The average velocities and flow depths upstream were similar between the two models as seen in Table 6-14, but the differing input variable for contraction scour computation is also shown in the table.

The flow through the bridge opening is estimated to be significantly higher for the 1-D model, thus computing greater contraction scour as well. The cause of lower flow for the 2-D model was the sinuous river geometry prior to the contraction directed a greater portion of the flow over the road deck rather than through the bridge opening, whereas the 1-D model assumes conveyance will always prefer the deepest section of the channel. The flow velocity distribution maps associated with the different model types display this phenomenon.

The local scour depths for piers and abutments are shown in Table 6-28. The maximum pier scour computed using 1-D HEC-RAS model hydraulics was 3.2 ft. The maximum pier scour for the 2-D model was 7.0 ft. The maximum abutment scour for the left abutment using the 1-D model was 13.2 ft and 0.0 ft for the right abutment. The 2-D model estimated maximum abutment scour depths of 28.0 ft for the left abutment and 21.0 ft for the right abutment.

Table 6-28. Dry Fork Creek (L-0564) – Summary of computed local scour (piers and abutments) depths.

Abutment Location or Pier ID Number	Bent ID Number	WSPRO 100-yr Scour Depth (ft)	WSPRO 500-yr Scour Depth (ft)	HEC-RAS 100-yr Scour Depth (ft)	HEC-RAS 500-yr Scour Depth (ft)	SRH-2D 100-yr Scour Depth (ft)	SRH-2D 500-yr Scour Depth (ft)
Left Abut.	1	6.7	8.6	11.2	13.2	23.6	28.0
1	2	3.6	3.6	3.1	3.2	6.8	7.0
2	3	3.8	3.7	3.1	3.2	3.9	3.6
3	4	4.0	4.0	3.1	3.2	3.1	3.4
4	5	4.0	4.0	3.1	3.2	3.8	3.8
Right Abut.	6	0.0	3.2	0.0	0.0	19.3	21.0

The thalweg flow depths and velocities used to compute pier scour were similar and the differences between the 1-D model and 2-D model have negligible effects on the pier scour depths. The defining variable contributing to greater pier scour depths when using the 2-D model was the angle of attack applied in the computations for each pier. The angled flow increased the area of the piers interacting with the flow, leading to deeper pier scour depths than the 1-D model computed with angle of attack inputs of zero. Abutment scour depths computed with the 2-D model hydraulics exceed those of the 1-D model, with multiple factors possibly contributing to the differences visible in the total scour plot, Figure 6-11. The value of q_1 for the 1-D model is much lower at the left abutment than at the right abutment, which impacts the q_2/q_1 ratio important to abutment scour computations. The higher abutment scour estimations for the 2-D model were unexpected, given the zero contraction scour present. The abutment scour values were irregular for this site, which is possible considering the complicated and raw computations particularly present when computing abutment scour.

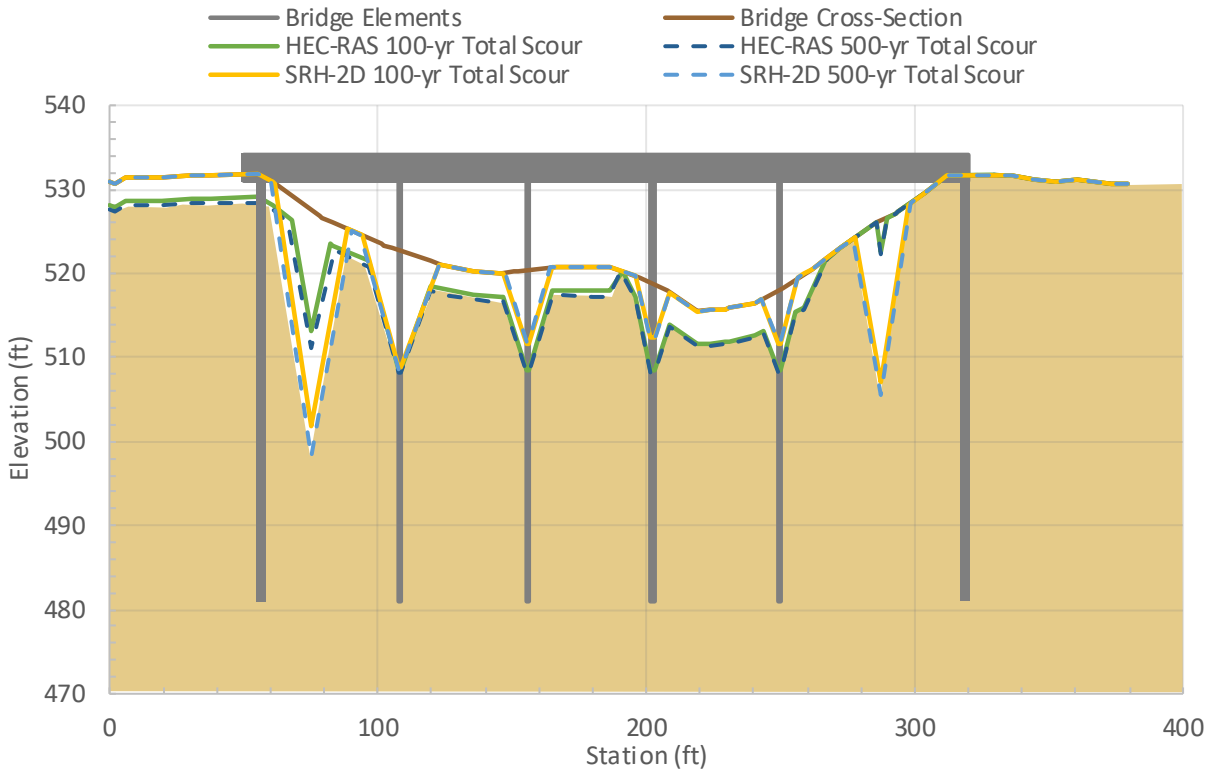

Figure 6-11. L-0564 – Total scour plot comparisons.

6.5.3.2 L-0564 Assessment of Bridge Foundations Due to Scour

The 500-yr flood event conditions indicate that total scour will not exceed a depth of 20 ft and near the abutments, it may be as much as 30 ft depth. This old bridge (70-yr) is a unique design with bents consisting of a combination of timber and steel, the deck has deteriorated significantly and there are signs of several repair attempts. The bridge is supported on deep foundations that consist of 50-ft driven timber piles (order length). The foundations are likely friction piles, but some of the piles may have reached capacity at less penetration. Without the construction records, it is difficult to assess the actual length of the timber piles. Each bent has a minimum of five (5) piles and the abutments have additional smaller piles (20-ft long) for the wing walls. Significant pile capacity may be lost if this level of total scour is experienced during the 500-yr storm event. Most of the lateral capacity is developed in the upper third to the pile embedment, therefore some will be lost, and given the age and current condition of this old bridge, the overall stability may be compromised. It should also be noted that the timber piles were treated with creosote, but since the water level changes along the floodplain, it is anticipated that the timber piles have deteriorated.

6.5.4 Gasconade River (A-3760)

6.5.4.1 A-3760 Scour Analysis

For the A-3760 bridge, the soil conditions were different at the channel (gravel) when compared to the floodplain (silty sands and clays). At the base of each bridge pier (ground level), there are countermeasures (large-size rock protection) installed to prevent some of the pier scour, but this is not included in this scour analysis. The values for contraction scour are shown in Table 6-29 and for local scour (piers and abutments) in Table 6-30 for each hydraulic modeling method used. These values are

then plotted along the bridge elevation for better comparison in Appendix F for the 1-D model and Appendix G for the 2-D model.

Table 6-29. Gasconade River (A-3760) – Summary of computed contraction scour depths.

Model Type	Storm Event	Channel Scour Depth (ft)	Left Overbank Scour Depth (ft)	Right Overbank Scour Depth (ft)
WSPRO	100-yr	0.7 (Live Bed)	0.0 (Clear Water)	9.8 (Clear Water)
	500-yr	0.0 (Live Bed)	0.0 (Clear Water)	9.5 (Clear Water)
HEC-RAS	100-yr	0.0 (Live Bed)	0.0 (Clear Water)	7.7 (Pressure Flow)
	500-yr	7.8 (Pressure Flow)	0.0 (Clear Water)	6.9 (Pressure Flow)
SRH-2D	100-yr	0.0 (Clear Water)	0.0 (Clear Water)	14.4 (Pressure Flow)
	500-yr	13.1 (Pressure Flow)	0.0 (Clear Water)	19.0 (Pressure Flow)

The maximum depth of contraction scour in the channel determined using the 1-D model hydraulics was 7.8 ft. The maximum depth of contraction scour in the channel for the 2-D model was 13.1 ft. Neither model predicted contraction scour for the left overbank. The maximum contraction scour estimated in the right overbank was 7.7 ft for the 1-D model and 19.0 ft for the 2-D model.

Hydraulic Toolbox guidelines state that where coarse sediments are present, the recommended practice is to calculate live-bed and clear-water contraction scour and use the smaller calculated contraction scour depth for design. If pressure flow conditions are present, the greater scour depth (or lower elevation) of pressure flow, live-bed or clear-water contraction scour for design should be used.

The larger sediment sizes present in the Gasconade River prevented contraction scouring in the left overbank, while contraction scour in the main channel only occurred when the water surface rose above the bottom of the bridge deck and caused pressure flow. The pressure flow conditions for the 500-yr storm event in both models raised the flow velocities enough to surpass the critical velocity for bed material displacement. The average depth in the contracted section for the 2-D model was almost 4 ft greater than the 1-D model – a possible cause of greater channel contraction scour depth. The computed contraction scour depths for the right overbank varied significantly between the model types, with the 2-D model estimating a max contraction scour depth more than twice that of the 1-D model. In the right overbank region of the contraction, the discharges and flow depths shown in Table 6-17 for the 2-D model exceed those of the 1-D model enough to cause significant differences in contraction scour depths.

Bridge A-3760 over the Gasconade River was the second longest bridge studied with 11 piers and two abutments. Maximum pier scour was estimated at Pier 3 for both the 1-D and 2-D models with depths of 14.8 ft and 18.2 ft, respectively. The estimated pier and abutment scour at each bent are shown in Table 6-30. As for the maximum abutment scour, the right abutment was the only one likely to scour. The 1-D model estimated an abutment scour depth of 49.2 ft while the 2-D model estimated 15.9 ft.

Table 6-30. Gasconade River (A-3760) – Summary of computed local scour (piers and abutments) depths.

Abutment Location or Pier ID Number	Bent ID Number	WSPRO 100-yr Scour Depth (ft)	WSPRO 500-yr Scour Depth (ft)	HEC-RAS 100-yr Scour Depth (ft)	HEC-RAS 500-yr Scour Depth (ft)	SRH-2D 100-yr Scour Depth (ft)	SRH-2D 500-yr Scour Depth (ft)
Left Abut.	1	37.3[F]	45.9 [F]	17.6	21.5	56.9	67.6
1	2	4.5	4.9	10.5	10.6	9.5	9.6
2	3	5.7	6.1	9.7	10.1	14.4	15.0
3	4	13.9	12.7	14.6	14.8	17.9	18.2
4	5	13.9	12.7	14.6	14.8	14.9	13.5
5	6	7.8[CP]	6.7[CP]	11.6	11.7	10.5	10.6
6	7	8.5[CP]	7.4[CP]	10.5	10.6	9.5	9.6
7	8	8.9[CP]	7.9[CP]	10.5	10.6	9.5	9.6
8	9	8.8[CP]	7.8[CP]	10.5	10.6	9.5	9.6
9	10	8.2[CP]	7.2[CP]	10.5	10.6	9.5	9.6
10	11	8.1[CP]	7.0 [CP]	10.5	10.6	9.5	9.6
11	12	9.0[CP]	8.0[CP]	10.5	10.6	9.5	9.6
Right Abut.	13	0.0	0.0	47.4	49.2	15.9	11.4

[F] uses Froelich's (1989) calculation method
[CP] uses complex pier calculation method.

The local scour depths at the piers were overall slightly greater (approximately 10%) for the 1-D model than the 2-D model. This is caused, in part, by the estimated thalweg approach velocities in the 1-D model being approximately two times greater than those in the 2-D model as shown in Table 6-18. The difference between the 1-D and 2-D model velocities is due to larger velocities, and associated discharge, being conveyed over the roadway embankment in the left floodplain of the 2-D model. These significantly larger flow velocities for the 1-D model are being counterbalanced by the higher attack angles from the 2-D modeling which results in only slightly larger (~10%) estimated pier scour depths on average.

The abutment scour depths estimated are rather extreme and vary widely and non-uniformly between the two models. The left abutment was type A and the right abutment was type B. The geological characteristics of the left bank would prevent abutment scour during the occurrence of an extreme flood event since it is a vertical rock bluff of non-erodible material visible on the left side of Figure 6-12. The right abutment would be much more susceptible to scour, as it sits in the floodplain and is at the location of the most significant flow contraction. The 1-D model predicts greater abutment scour as Table 6-19 shows the higher q_2/q_1 ratio values, which lead to a larger scour amplification factor.

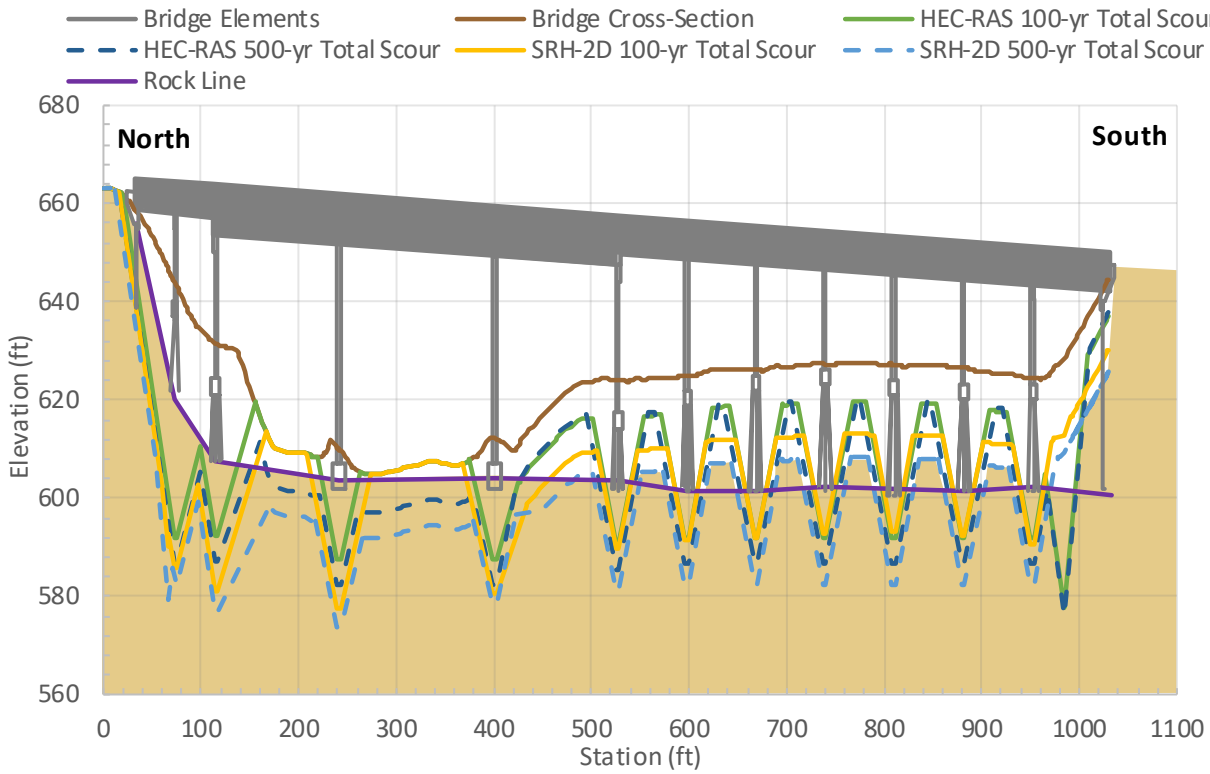

Figure 6-12. Gasconade River (A-3760) – Total scour plot comparisons.

6.5.4.2 A-3760 Assessment of Bridge Foundations Due to Scour

The 500-yr flood event conditions indicate that significant total scour will certainly reach the bedrock material. This means that the calculations for total scour will be limited to the top of bedrock elevation (~El. 604). Fortunately, this bridge is supported by foundations reaching the bedrock material. Within the channel, the bridge's main span is supported on shallow footings directly on rock, and outside the channel the bridge bents are supported on deep foundations, steel piles driven to rock. The driven piles were installed at a batter angle to account for lateral loads in the longitudinal direction of the bridge. The total scour conditions could leave the deep pile foundations without lateral support. However, the battered piles will be able to temporarily carry the lateral load during these unique critical local scour conditions. SRH-2D hydraulic modeling results indicate this bridge will experience pressure-flow conditions during the 500-yr event. HEC-18 recommends countermeasures be installed at sites with pressure flow conditions. The risk for bridge collapse is low given the design and as-built conditions of the bridge. However, the abutment scour on the alluvium side of the bridge (south) is a critical condition for the embankment stability. It would be imperative that mitigation and countermeasures be installed soon after such 500-yr storm event.

6.5.5 Missouri River (L-0550)

6.5.5.1 L-0550 Scour Analysis

The soil conditions are relatively constant within the alluvium but change in the channel and encounter rock in the south abutment. For the L-0550 bridge, the level of total scour calculated does reach the bedrock in some of the piers (2, 3, 4, and 5). As in previous bridge conditions where the bedrock is within reach, the total scour should be truncated once the rock is reached. Therefore, the total scour line should

not be deeper than the "Rock Line" shown in purple in the following figures. It should be noted that at the base of bridge Pier 4 in the main channel there are countermeasures (large-size rock protection) installed after 2015, according to the plans submitted. Besides Pier 4, it was not apparent that any other piers received any countermeasure. Again, the countermeasures are not included in this total scour analysis for this study. See the summary of computed contraction scour depths in Table 6-31 and the local scour (piers and abutments) depths in Table 6-32. These values are then plotted along the bridge elevation for better comparison in Appendix F for the 1-D model and Appendix G for the 2-D model.

Table 6-31. Missouri River (L-0550) - Summary of computed contraction scour depths.

Model Type	Storm Event	Channel Scour Depth (ft)	Left Overbank Scour Depth (ft)	Right Overbank Scour Depth (ft)
WSPRO	100-yr	5.4 (Live Bed)	3.2 (Clear Water)	0.0 (Clear Water)
	500-yr	6.8 (Live Bed)	11.0 (Clear Water)	0.0 (Clear Water)
HEC-RAS	100-yr	2.2 (Live Bed)	0.0 (Live Bed)	0.0 (Clear Water)
	500-yr	4.0 (Live Bed)	0.0 (Live Bed)	0.0 (Clear Water)
SRH-2D	100-yr	6.2 (Live Bed)	0.0 (Live Bed)	0.0 (Clear Water)
	500-yr	9.9 (Live Bed)	0.0 (Live Bed)	1.5 (Clear Water)

The maximum contraction scour computed in the main channel using the 1-D HEC-RAS model hydraulics was 4.0 ft, with no contraction scour in the left and right overbank areas. The maximum contraction scour computed using the 2-D model was 9.9 ft, with no contraction scour in the left overbank and 1.5 ft in the right overbank. The right overbank consists of a rail line at the base of a rocky bluff, thus contraction scour here due to contraction is unlikely. The hydraulic conditions applied for contraction scour computations were similar, even stronger for the 1-D model based on Table 6-20, since the 1-D model predicted greater flow velocity, less flow depth, and greater flow through the opening in the main channel. The two ratios important for live-bed contraction scour prediction in the main channel are: 1) the ratio of the width upstream transporting sediment to the width in the contracted section, and 2) the ratio of the discharge in the contracted section to the discharge upstream transporting sediment. These ratios were both slightly greater for the 2-D model, which leads to a greater computed contraction scour depth in the main channel.

The computed scour depths for the individual piers and both abutments are shown in Table 6-32. The maximum pier scour depth using the 1-D model was 39.7 ft and 74.3 ft for the 2-D model. The maximum abutment scour for the 1-D model at the left abutment was 49.9 ft and zero at the right abutment. For the 2-D model, the maximum abutment scour at the left abutment was 0.8 ft and zero for the right abutment.

Table 6-32. Missouri River (L-0550) – Summary of computed local scour (piers and abutments) depths.

Abutment Location or Pier ID Number	Bent ID Number	WSPRO 100-yr Scour Depth (ft)	WSPRO 500-yr Scour Depth (ft)	HEC-RAS 100-yr Scour Depth (ft)	HEC-RAS 500-yr Scour Depth (ft)	SRH-2D 100-yr Scour Depth (ft)	SRH-2D 500-yr Scour Depth (ft)
Left Abut.	19	18.9 [H]	27.1 [H]	49.9	48.0	0.8	0.7
1	18	6.0	13.5[CP]	13.7	13.6	15.9	13.5
2	17	6.5	9.0[CP]	14.8	14.7	13.4	13.1
3	16	7.0	8.9[CP]	15.8	15.8	14.8	14.0
4	15	6.0	8.5[CP]	13.7	13.6	13.2	12.0
5	14	6.5	8.6[CP]	14.8	14.7	13.9	13.6
6	13	7.0	8.9[CP]	15.8	15.8	13.9	14.7
7	12	6.5	9.4[CP]	14.8	14.7	13.6	14.3
8	11	6.5	14.7[CP]	14.8	14.7	13.8	13.1
9	10	7.0	13.4[CP]	15.8	15.8	14.7	14.1
10	9	7.0	16.0[CP]	15.8	15.8	16.5	15.6
11	8	7.8	20.2[CP]	17.8	17.7	18.3	17.3
12	7	6.9	10.2[CP]	15.8	15.8	17.7	16.7
13	6	11.3	17.4[CP]	30.9	30.8	32.8	31.3
14	5	12.5	20.6[CP]	39.7	39.5	74.3	70.2
15	4	43.9[CP]	46.5[CP]	35.9	35.7	33.3	33.2
16	3	24.8 [CP]	26.2[CP]	27.6	27.5	38.1	37.9
17	2	0.0	0.0	13.7	13.6	18.3	15.3
Right Abut.	1	0.0	13.9 [F]	0.0	0.0	0.0	0.0

[H] uses the HIRE (1990) calculation method.
[F] uses Froelich's (1989) calculation method.
[CP] uses complex pier calculation method.

Excluding Pier 14, the local scour depths were similar across the entire span for both models. Though the flow velocity used in the pier scour computations was greater for the 1-D model, the angle of attack present in the 2-D model had a much more significant effect on the pier scour depth. The difference in scour depth at Pier 14 adjacent to the main channel, illustrated in Figure 6-13, can almost entirely be attributed to the difference in angle of attack. The abutment scour at the left abutment was virtually zero for the 2-D model and almost 50 ft for the 1-D model. The ratio of q_2/q_1 was 1.62 for the 1-D model and 0.89 for the 2-D model during the 500-yr storm event. The other variables used in the abutment scour computation, upstream flow depth, and depth prior to scour, were virtually the same. The unit discharge values for the 1-D model were manually calculated to be greater than those of the 2-D model by a factor of three to five.

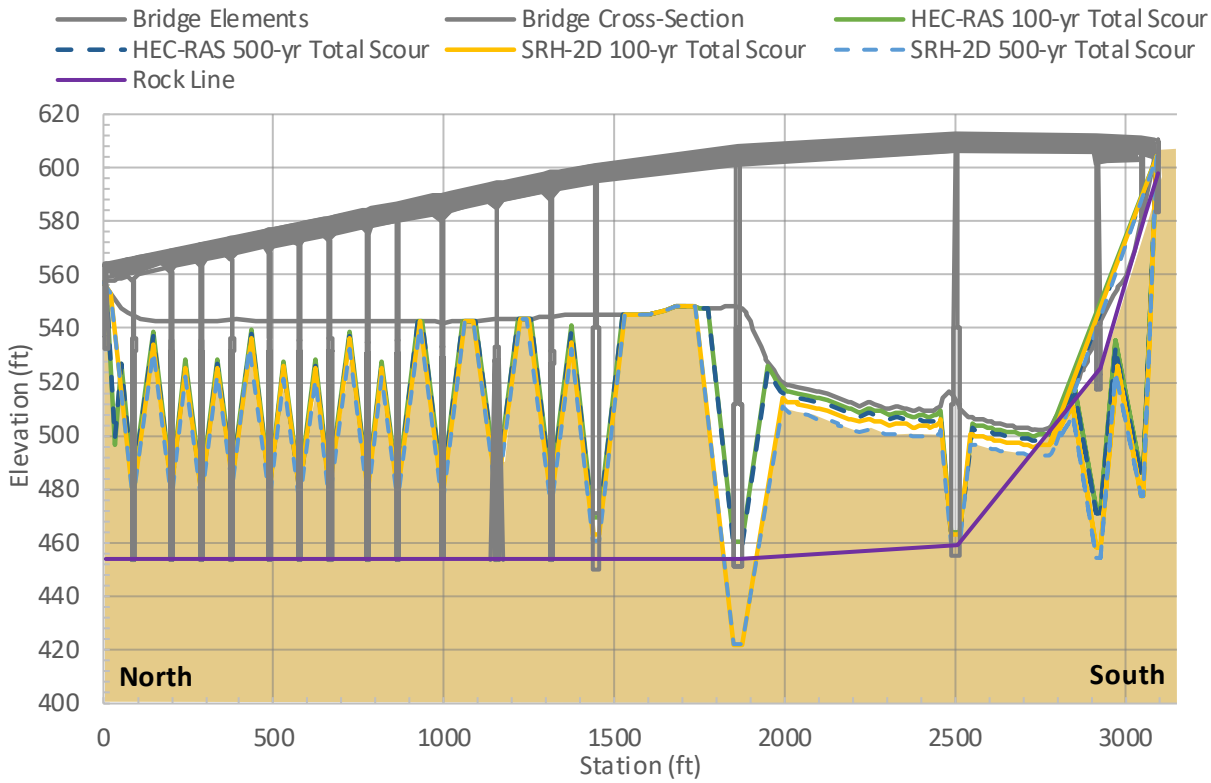

Figure 6-13. Missouri River (L-0550) – Total scour plot comparisons.

6.5.5.2 L-0550: Assessment of Bridge Foundations Due to Scour

The 500-yr flood event conditions indicate that the total scour will reach the bedrock material in several piers (Piers 1, 2, 3, 4, and 5). This means that the calculations for total scour will be limited to the top of bedrock elevation (~El. 454). Fortunately, this bridge is supported by foundations reaching the bedrock material. Within the channel, the bridge main span is supported on piers on drilled shafts directly on rock, and outside the channel the bridge bents are supported on deep foundations, steel piles driven to rock. The driven piles were installed at a batter angle to account for lateral loads in the longitudinal direction of the bridge. The total scour conditions could leave the deep pile foundations without lateral support. However, the battered piles will be able to carry the lateral load during these unique critical scour conditions. The risk for bridge collapse is low given the design and as-built conditions of the bridge. It would be imperative that mitigation and countermeasures be installed soon after such 500-yr storm event.

7 DISCUSSION OF RESULTS

7.1 Overall Comparison Between Methodologies

The objective of this bridge scour study was to compare bridge scour estimations computed using the hydraulics from a simplified 1-D model (WSPRO), a comprehensive 1-D model (HEC-RAS), and a 2-D model (SRH-2D). By computing scour for two different models for two storm events across five bridge sites, twenty data sets were acquired for scour scenarios. When including the previous studies conducted at the same bridge sites, thirty total scenarios were available for comparison and pattern identification. From these data sets, bar graphs were produced to directly compare model outputs. In total, nine bar graphs visualize hydraulic model outputs (thalweg approach depth, thalweg approach velocity, and flow in the main channel through the bridge opening) and scour model outputs (average pier scour depth, main channel contraction scour depth, right and left abutment scour, and right and left overbank contraction scour) for each scenario.

Two-dimensional models are preferred over 1-D models for scour analysis in complex flow, such as rivers with high sinuosity, flow obstructions, bridge openings, and culverts (Arneson et al., 2012). The difference between the 1-D and 2-D results would be considered an error from the preferred method. The study followed the hydraulic modeling procedures of the FHWA, including the use of HEC-RAS for 1-D modeling and SRH-2D for 2-D modeling. Figure 7-1 through Figure 7-9 serve to visualize the differences in hydraulic conditions and scour computed by the models in this study. Trend observations were made of relative imprecision in the result comparisons, either higher or lower. Causations of the trends were determined by investigating specific hydraulic inputs to the scour calculation methods and their relevance to specific modeling approaches.

The hydraulic modeling results consisted of flow data computed using the different models with their different computation methods. Boundary conditions, set as model inputs, were consistent with the HEC-RAS models calibrated based on the downstream water surface elevation of the SRH-2D model. The WSPRO study used input flow rates acquired over two decades ago, while three of the five sites modeled with HEC-RAS and SRH-2D used flow rates from modern computation methods (i.e., Streamstats). The tables containing hydraulic results were for comparing flow data. The scour results would be influenced by the results seen in the tables. The thalweg approach depths and velocities computed by the models are shown in Figure 7-1 and Figure 7-2. These values, used in the pier scour equation, were factors used to compare important flow characteristics of the model.

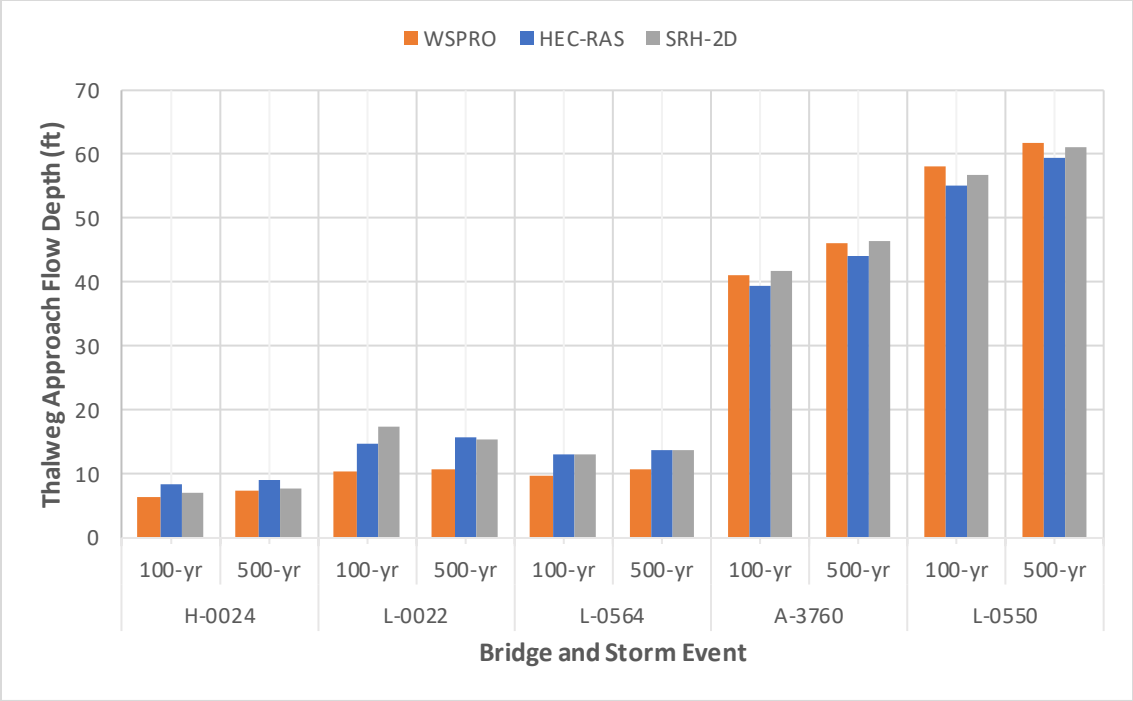

Figure 7-1. Thalweg approach flow depths used to compute pier scour.

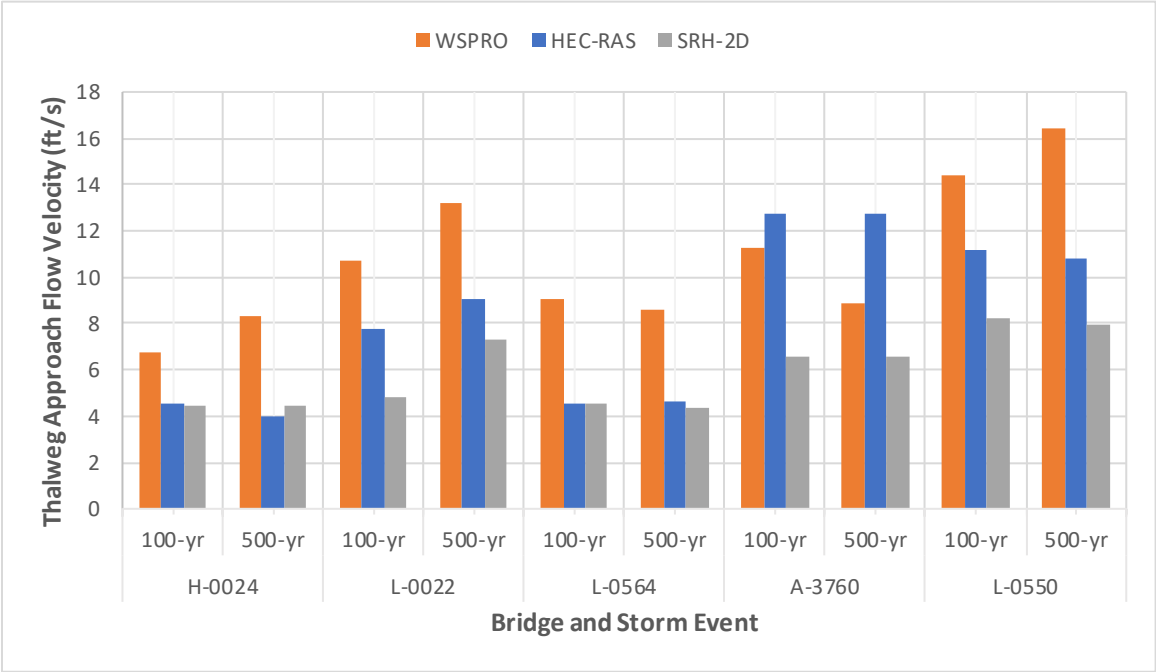

Figure 7-2. Thalweg approach flow velocities used to compute pier scour.

Seven out of the ten scenarios differed between the models by less than 7%, and seven out of ten models computed smaller flow depths for HEC-RAS. Differences in flow depth would cause insignificant scour differences, as the average difference in computed thalweg approach depths was 0.62%.

A significant difference, 46.9%, was observed between thalweg flow velocities in the WSPRO 1990s study and the HEC-RAS model revealing possible inaccuracies in the previously conducted bridge scour studies. The lack of input data resolution (4 cross-sections) at each site by the WSPRO study contrasted with the HEC-RAS models (approximately 20 cross-sections) was the apparent source of error. The methodology of acquiring cross-section topography has evolved to much greater precision in the time between the WSPRO and current studies, as discussed in Section 4.4. The natural change in geomorphology in the river basin over the last two decades did not likely influence the thalweg flow velocity.

The HEC-RAS models computed, on average, a flow velocity 34.3% greater than the SRH-2D model. Only one of the ten scenarios had an estimated approach velocity by the 2-D model greater than the HEC-RAS model. Overall, the 1-D models computed higher flow velocities than the 2-D model, attributable to the differences in flow computations where 1-D models distribute flow based on flow depth and Manning's roughness, not the realistic 2-D dynamics present in complex flow situations. Instances of highly two-dimensional flow affecting channel flow velocities were apparent when 1-D and 2-D flow velocity distributions (located in Appendices D and E) were compared for each bridge site. The momentum equation, utilized by the 2-D model, allowed flow to move in all horizontal directions and follow paths based on momentum. One-dimensional flow strictly followed the contours of the cross-sections and was oriented in the downstream direction, which does not accurately represent realistic flow conditions. The Gasconade River (A-3760) site provides clear visuals and numerical results supporting this concept. The velocity distributions display flow moving from south to north, with Figure 6-4 showing 1-D flow concentrated in the main channel while Figure 6-6 shows greater flow conveyance over the roadway in the floodplain, a characteristic of the 2-D hydraulic model maintaining flow momentum from the channel upstream prior to the meander across the floodplain.

The flow rate through the bridge opening in the main channel was the flow rate computed to pass through the main channel at steady-state conditions for each flood scenario. This flow characteristic computed by the models was important for contraction scour and abutment scour equations. The results shown in Figure 7-3 provide insight into the amount of flow rate estimated to threaten bridge stability in the main channel, where the flow rate is generally the largest.

The HEC-RAS 1-D model estimated a flow rate through the bridge opening in the main channel 39% higher than the 2-D model, on average. The only outlying scenarios were the 1-D model flow rates which were not higher for the H-0024 site, again the smallest of the five. The logarithmic scale on the vertical axis of the graph, used to effectively discharge the large range of flow rates for the study, appears deceiving as differences in flow rates were rather significant. For example, bridge site L-0564 had flows for the 1-D model that were approximately 90% greater than the 2-D model. Higher flow rates observed in the main channel are correlated to the high flow velocities computed by the 1-D model as shown in Figure 7-2 and Appendices D and E, with example bridge site A-3760 being an example detailed in Sections 6.2 and 6.3.

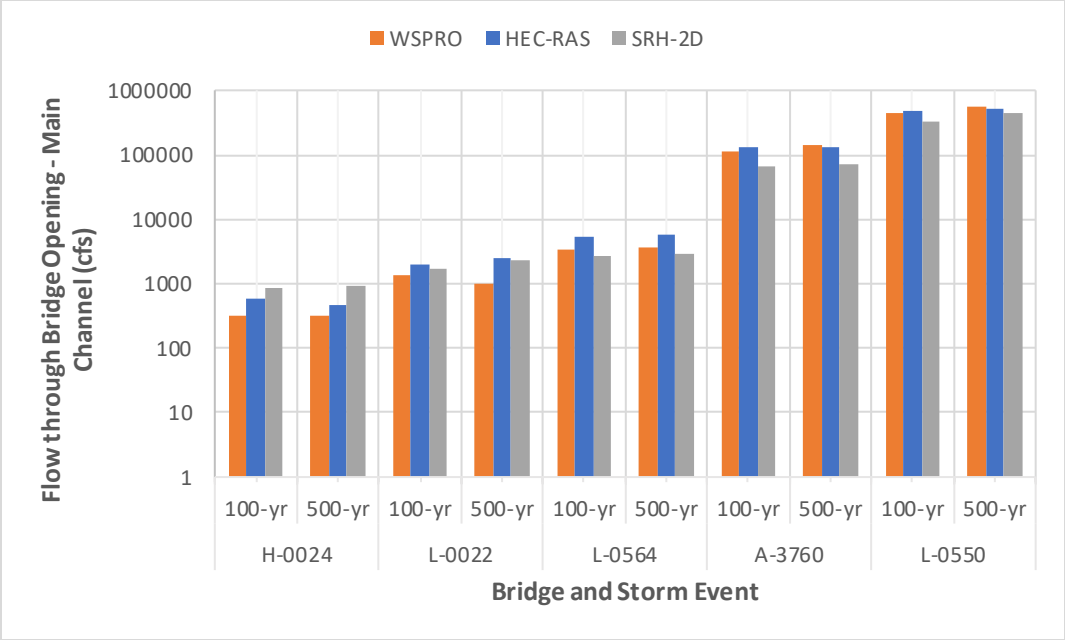

Figure 7-3. Flow rate through the bridge opening in the main channel that is used to compute contraction scour.

Comparisons between the main channel flow rates of the WSPRO study and the HEC-RAS models showed the discharge in the main channel was 24.4% less on average for the WSPRO study. Factors influencing these results and causing this trend were smaller flow rates in the WSPRO study for three of the five sites, inconsistent channel widths between models used to compute discharge, and low-resolution geometric data.

Hydraulic conditions from each model were input to Hydraulic Toolbox's scour analysis tool which computed contraction, pier, and abutment scour to give a final total scour plot. The hydraulic conditions directly influenced the scour computation methods, as they are circumstantially dependent on the flow data inputs. Different scour equations apply in different scenarios based on parameters like flow depth for pressure flow (e.g., when the water surface elevation is greater than the bottom cord of the bridge), complex pier scour (e.g., when a pier pile cap is exposed by the thalweg contraction scour depth), and live-bed or clear-water contraction scour, which depends on flow velocities and sediment transport conditions. The pier scour depth results shown in Figure 7-4 were averaged across all piers to capture the trends across each site, though individual pier scour depths are shown in Section 6.5.

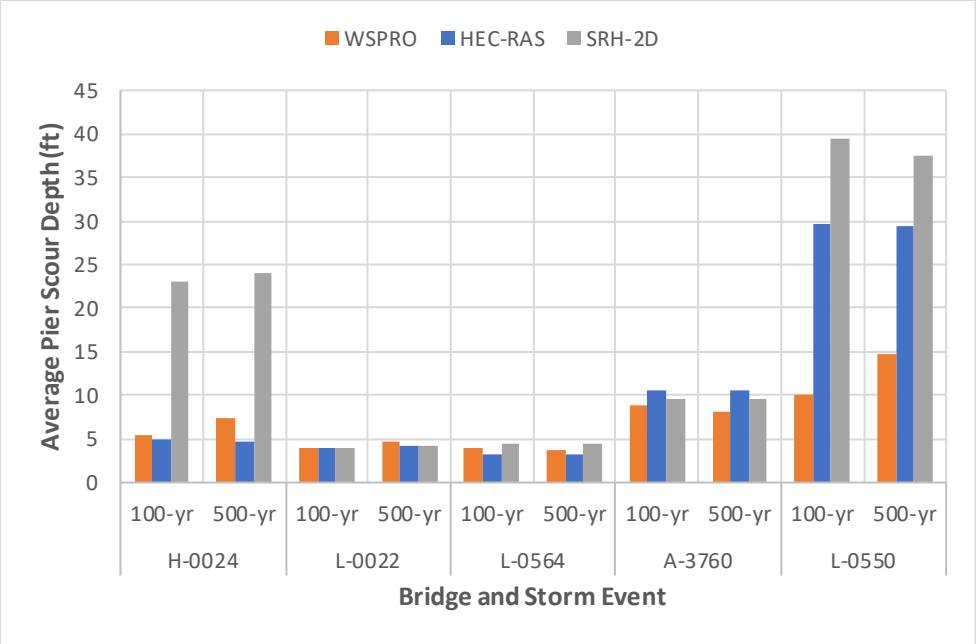

Figure 7-4. Average pier scour depths.

The WSPRO model computed average pier scour depths 3.4% less than HEC-RAS with a mean absolute percent error of 27.7%, as shown in Figure 7-4. The methods for determining the pier scour inputs varied. The previous study used the local flow depths at each pier and maximum velocities in their respective region (left overbank, channel, right overbank) (Huizinga and Rydlund, 2002; Rydlund and Huizinga, 2001; Rydlund and Huizinga, 2002a; Rydlund and Huizinga, 2002b; Huizinga and Rydlund, 2003), while the HEC-RAS and SRH-2D models used thalweg flow depth and velocity for all bridge piers (Arneson et al., 2012). The variations of thalweg depth and velocity only apply to pier scour in the main channel when comparing the 1-D models. Overall, the average pier scour depths were different by a relatively small margin except for the pier scour depths computed for H-0024 from SRH-2D hydraulic inputs.

On average, the HEC-RAS model produced scour depths 24.2% less than SRH-2D with a mean absolute percent error of 28.5%. The key defining factor separating the model types on pier scour depth was the angle of attack. The 2-D model computes and automatically populates the angle of attack input in Hydraulic Toolbox. The pier lengths and approach flow angle of attack were used to compute the correction factor K_2 for the angle of attack, which increases with increasing attack angle. The attack angles used for the 1-D models were zero in congruence with the WSPRO study. Procedures to determine the angle of attack from a 1-D model were not detailed in HEC-18 or the Hydraulic Toolbox Manual. The only site which returned a deeper average pier scour for the HEC-RAS model was A-3760 which had a thalweg flow velocity in the 1-D model nearly two times that of the 2-D model. Overall, the angle of attack differences had a greater influence on pier scour depths than flow velocity differences.

The main channel contraction scour depths computed by each model did not vary in an identifiable pattern for one reason. Contraction scour depths have the potential to vary widely based on minor differences in flow depth and flow velocity. The flow velocity relative to the critical velocity for the input sediment size determined whether clear-water or live-bed scour was occurring. The water surface elevation relative to the bridge deck determined the presence of pressure flow through the bridge opening. Small differences in velocity and depth could cause the use of equations that compute scour differently. The graph in Figure 7-5 shows the main channel contraction scour depths at each site. The

irregularity of scour computations made the causes of different results difficult to isolate, though observations were made for that purpose.

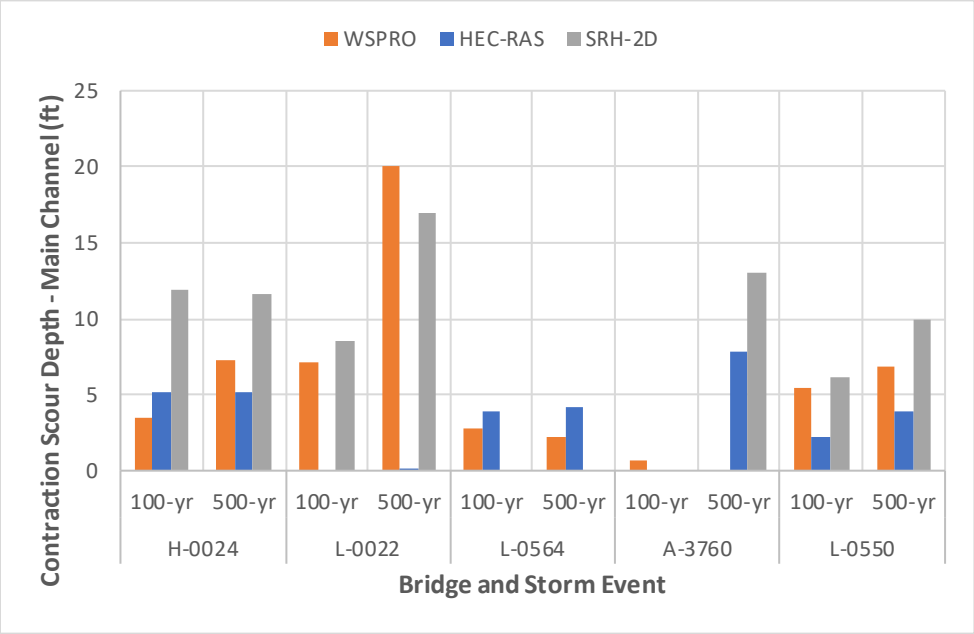

Figure 7-5. Main channel contraction scour depths.

General trends in main channel contraction scour depth were not apparent between the WSPRO study and the HEC-RAS models. The variability of multiple model input methods produced results unrelatable to each other.

For seven out of the ten scour scenarios, the contraction scour depths in the main channel were less for the HEC-RAS model than the 2-D model by an average of 68%. The other three scenarios had no scour for the 2-D model and less than 5 ft of scour for the 1-D model. Each site had detailed causes of the difference in main channel contraction scour in Section 6.5. The bottom width of the main channel was used as an input for each contraction scour equation; this parameter is inversely related to computed scour depth. The bottom width of the main channel in the contracted section, less the pier widths, was computed to be less for SRH-2D than the values manually computed from HEC-RAS for four of the five bridge sites. The bottom widths for the HEC-RAS model were computed by subtracting the in-channel pier widths from the difference in bank stations. The SRH-2D model computed the same variable automatically (Lai, 2010). Discharge in the main channel was directly correlated to contraction scour for both equations. The flow depth prior to scour was inversely related to contraction scour for both equations. Both discharge and depth prior to scour would generate greater contraction scour for HEC-RAS, though the difference in contracted section width had a greater impact on overall results and caused higher computed contraction scour in the main channel for SRH-2D. The L-0564 site was an outlier for main channel contraction scour with greater scour depth for HEC-RAS since the main channel discharge for HEC-RAS exceeded the value for SRH-2D by approximately 96% and flow depth prior to scour was less for HEC-RAS than SRH-2D.

The abutment scour depths were computed using an amplification factor applied to a simplified contraction scour estimate. The graphs did not reveal any pattern between model type and scour depths

for the values shown in Figure 7-6 and Figure 7-7 (left overbank and left abutment scour depths) or Figure 7-8 and Figure 7-9 (right over bank and right abutment scour depths).

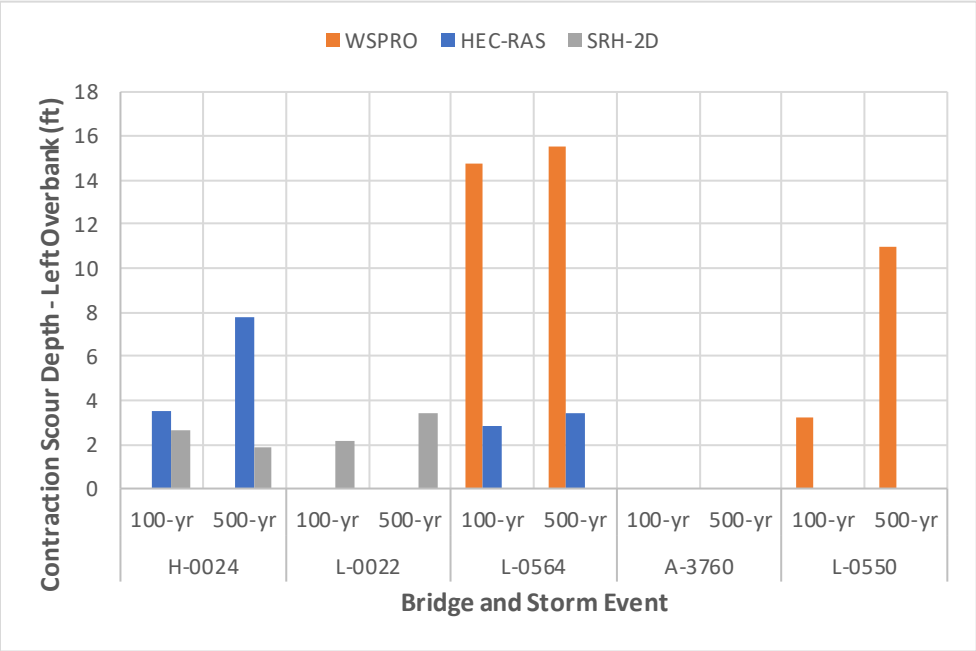

Figure 7-6. Left overbank contraction scour depths.

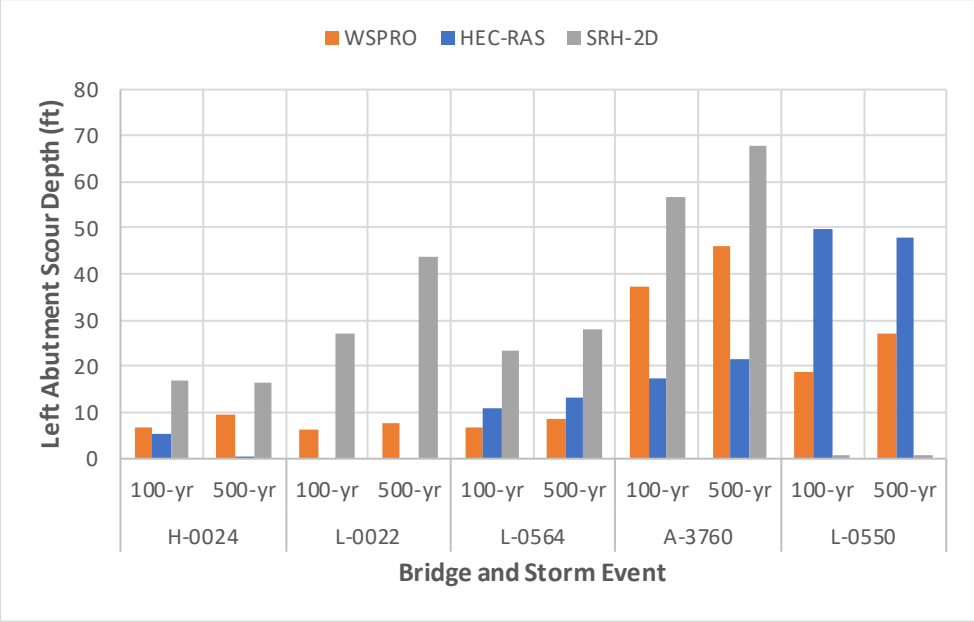

Figure 7-7. Left abutment scour depths.

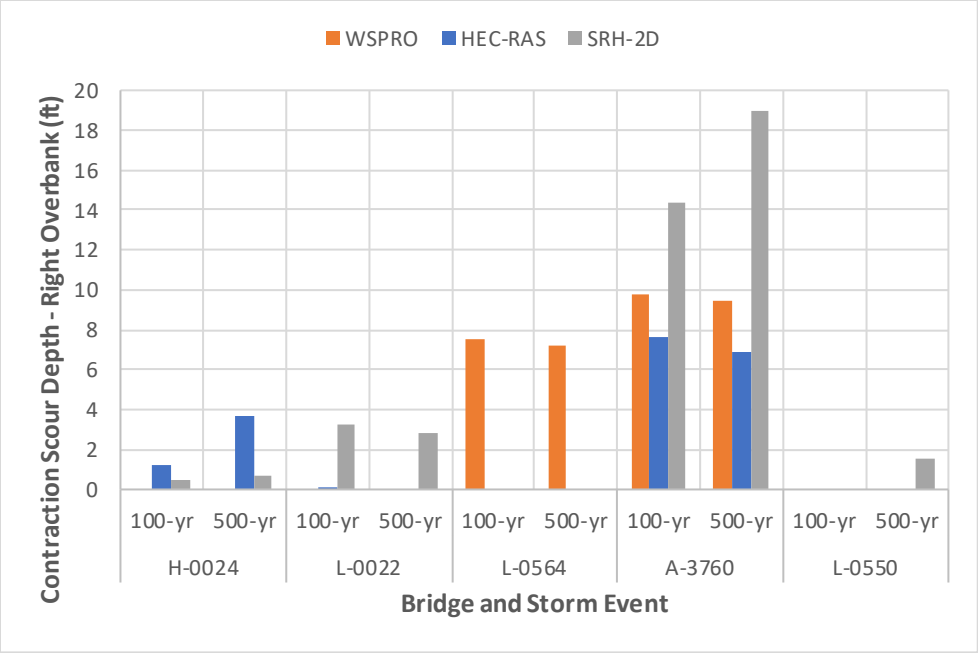

Figure 7-8. Right overbank contraction scour depths.

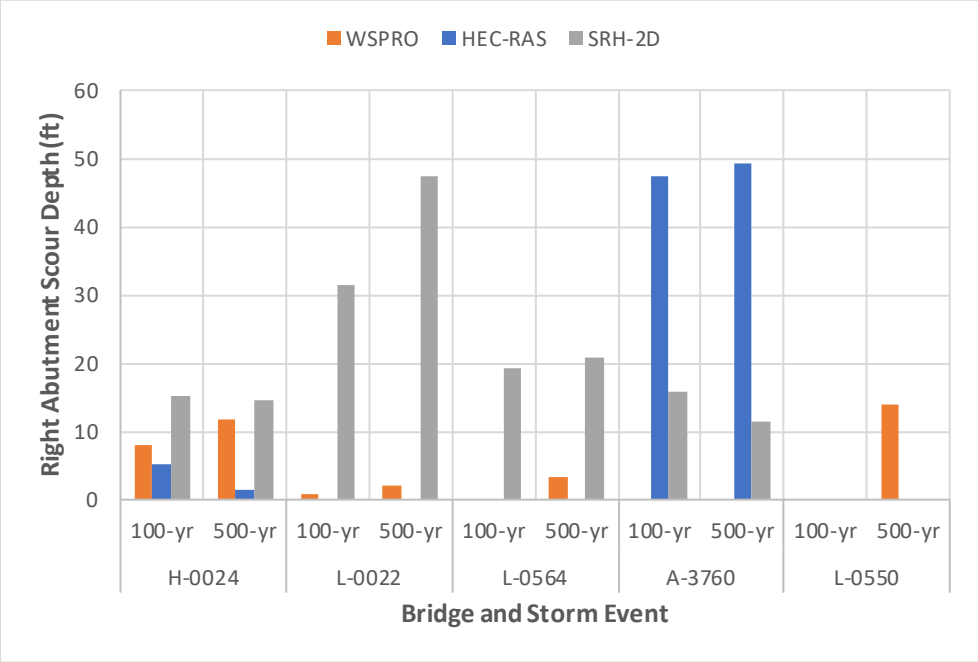

Figure 7-9. Right abutment scour depths.

Numerous instances of zero abutment scour were present in the analysis and occurred either due to the abutment not being inundated or the computed simplified contraction scour estimate, y_c, (used just for abutment scour calculations) was smaller than the flow depth at the abutment prior to scour, y_0. There appeared to be no correlation between abutment and contraction scour in the overbanks. The discontinuity of the data required analysis to be on a site-by-site basis, shown in Section 6.5, without any general patterns presenting themselves across the overbank scour values. Computing abutment scour by

applying an amplifier to the simplified contraction scour contributes more uncertainty regarding relationships between flow hydraulics and abutment scour that differentiate the model types.

Considering the data from both right and left abutments, SRH-2D computed abutment scour greater than HEC-RAS for 14 of 18 scour scenarios, or 78% of the time. This includes all cases for the three smaller bridge sites (H-0024, L-0022, L-0564). The abutment type, dependent on the set-back ratio (SBR) (Arneson et. al., 2012), determined how discharges were calculated for the ratio q_2/q_1. With 14 of the 18 abutment scour scenarios being with type A abutments, abutment scour was less for HEC-RAS than SRH-2D. The hydraulic conditions for each of the type A scenarios returned a q_2/q_1 ratio less for HEC-RAS than SRH-2D 86% of the time. For the four scenarios where abutment scour was greater for HEC-RAS than SRH-2D, the abutments were each type B and the unit discharge ratios were greater for HEC-RAS than SRH-2D. It was concluded that HEC-RAS returns less scour for type A abutments and greater scour for type B abutments than SRH-2D. The q_2/q_1 ratio was correlated to abutment scour depth, with smaller values for HEC-RAS computing smaller abutment scour depth for SRH-2D, and vice versa.

HEC-18 recommended the use of 2-D modeling to determine velocity and unit discharge for abutment scour calculations (Arneson et. al., 2012). It outlined the method for computing velocity and unit discharge using 1-D modeling as well. While the unit discharges used from the 2-D model were computed by the model, manual calculations were computed using flow data from HEC-RAS. The variation in computation methods and flow characteristics returned an identifiable pattern in the results. The specific methods for computing the unit discharges by SRH-2D in relation to abutment type were unclear and could not qualitatively be compared to the 1-D modeling methods.

7.2 Total Scour Prism for Each Bridge

For this study, total scour is comprised of the contraction scour and local scour at the piers and abutments. The first scour component is a consequence of contraction as the flood waters enter the constricted area under the bridge and is expressed as a uniform scour or lowering of the original grade. Abutment scour, the second scour component, is computed by applying an amplification factor to a simplified contraction scour estimate and occurs at the toe of the abutment not directly at the abutment bent. Computed abutment scour depths are applied to the original abutment toe elevation and not the contraction scour elevation. The third scour component is the local scour produced by the structural elements supporting the intermediate bents or piers. This produces additional scour beyond the contraction scour, and it is calculated at each pier. The resulting pier scour elevation is computed as the original bed elevation minus the sum of the contraction scour and pier scour depths. These three scour components are combined to produce the predicted total scour ground level under the bridge. When the piers or bents are close to each other, the computed local scour holes may extend to also erode material at the adjacent pier/bent.

The scour analyses are conducted with the assumption that the bed material has uniform properties in the lateral and vertical directions (properties based on analysis of surficial soil/sediment samples). Thus, the scour prism is a simplified representation of the site conditions and does not accurately reflect that the stratigraphy usually varies vertically and laterally. During a storm event, the surficial material, which is typically the weakest, will erode first, which is a conservative approach. Material generally gets denser with depth and hydrodynamic forces decrease as material is eroded. It is also important to note that the scour prisms do not account for countermeasures. The three largest sites (Dry Fork Creek L-0564, Gasconade River A-3760, and Missouri River L-0550) have countermeasures installed. Countermeasures at the Dry Fork Creek (L-0564) were installed by maintenance and with no apparent engineering design process documented.

For the Gasconade River (A-3760) and the Missouri River (L-0550) sites, the bridges are supported on rock because the bedrock is within reach of the foundations (shallow or deep foundations). Since the

scour is only calculated for one type of soil and cannot account for layered soil or rock, the analysis requires truncating the predicted scour to the top of bedrock, which tends not to scour during a storm event.

7.3 Potential Impact on Bridge Structures

Bridge scouring has been a well-known risk to bridge structures spanning over water with heavy flow during storm events. Missouri bridges are particularly vulnerable to this scour hazard given the numerous rivers with varying flow levels and the wide variety of geomorphic conditions. The changing climate conditions have resulted in more drastic changes in water flow during storm events and have resulted in designing for much longer return periods, like a 500-yr or 1000-yr storm events.

The SRH-2D modeling can better capture the unique conditions of flow under a bridge considering the overall terrain conditions in the floodplain. This more advanced modeling tool typically predicts worse flow and scour conditions that impact the bridge's stability. For all five sites analyzed in detail for this study, the 2-D model and associated scour calculations predict significantly worse conditions of scour. In some cases, the predicted conditions do call for a collapse or washout of the bridge structure, particularly for small old bridges with poor foundation support conditions.

8 CONCLUSIONS AND RECOMMENDATIONS

8.1 Advancements in Terrain and Hydrologic Data Collection and Accessibility

Since the WSPRO studies were conducted approximately twenty years ago, several advancements have been made in the collection and/or accessibility of terrain and hydrologic data. The WSPRO studies used four cross sections to model each site. Publicly and freely available lidar data have become more prevalent providing high-resolution terrain data to characterize topography and the use of real-time kinetic GPS instruments facilitating georeferenced bathymetric surveys are more common. These advancements enable the development of comprehensive terrain surfaces (topography and bathymetry) which can provide adequate resolution for both 1-D and 2-D models. Further, the USGS Streamstats portal provides a convenient method to estimate flow rates for a variety of return periods. The analysis inherent to Streamstats includes watershed delineation and application of regional regression equations.

8.2 Soil/Sediment Sampling and Analyses at Bridge Sites

Several soil sampling methods are available to engineers and a variety of them were attempted during the project. To examine the soil stratigraphy variability along the bridge alignment, one needs to consider vertical and horizontal sampling.

In the vertical subsurface direction, there are shallow (or near-surface) methods and deep methods requiring mechanical drill or penetration. For this project, shallow or near-surface methods were used since the deep subsurface investigations were done by MoDOT for the original bridge design. Also, as the depth increases the soil tends to be more competent and one may also reach bedrock. The depth of sampling shall not exceed three to five feet, and in most cases, three feet would suffice.

In the horizontal direction, the focus was to conduct sampling at the upstream of each bridge bent including the abutments. At times, when the conditions changed drastically, an intermediate sampling was conducted between bents or along the abutment.

It is recommended that samples be collected upstream of each bridge pier or abutment. The preferred and recommended shallow methods used in this study were all hand explorations and they consisted of the following:

- On dry land: Hand auger to a depth of about three to five feet and shovel, as necessary.
- Over water: FISP Samplers (BM 30, 54, 60) as shown in Figure 4-3, and Bonar sampler. The maximum depth is about four inches from the mudline.

Depending on the anticipated sediment or bedload material, the size of the sampler is important in overwater conditions. For example, the FISP samplers were just too small to sample the gravel at the bottom of the A-3760 Bridge over the Gasconade. So, when the FISP sampler failed, the sampling location was moved to the closest shallow water using a shovel.

8.3 Comparison of Hydraulic Modeling and Scour Results

The following conclusions were made by comparing 1-D and 2-D modeling and associated computed scour depths:

- The use of 1-D hydraulic models such as HEC-RAS for scour studies is not recommended, as many sources of error combine to produce estimated scour depths inconsistent with SRH-2D estimates.
- 1-D hydraulic modeling near bridge sites is tedious and subjective, and provides many opportunities for error, most notably defining cross-sections and interpreting hydraulic results required as input parameters for scour calculations.

- Pier scour computations were dominated by the flow angle of attack, which is an input parameter for pier scour that is automatically populated in the Hydraulic Toolbox software from SRH-2D results. HEC-RAS lacks the ability to compute flow angle of attack and computed pier scour depths on average 24.2% less than SRH-2D.
- HEC-RAS overestimated thalweg flow velocity and discharge in the main channel by 34% and 39%, respectively, on average across the five bridge sites. This was primarily due to the difference in flow conveyance at overtopped roadways. HEC-RAS failed to account for the 2-D flow momentum and concentrated nearly all flow in the main channels.
- Manual computations of channel widths in the bridge section for HEC-RAS models varied from those automatically computed by the 2-D model. The greater widths for the 1-D models are related to less contraction scour in the main channel.
- The manual computations of unit discharges associated with abutment scour depth for the HEC-RAS models consistently underestimated scour for type A abutments and overestimated scour for type B abutments.
- Even for straight uniform channels with no flow overtopping a road embankment, 1-D and 2-D models would not be expected to compute similar hydraulic conditions due to the differences in how input parameters are determined. The angle of attack for piers near abutments would still be significant for a 2-D model with a straight channel.
- For all bridge sites evaluated, estimates for at least one of the main scour categories (i.e., channel contraction scour, average pier scour, or average abutment scour) were more than 50% different between the HEC-RAS 1-D and SRH-2D results. Thus, all sites were significantly affected by the hydraulic modeling method.
- Based on the above findings, reanalyzing high-risk and/or visibly vulnerable bridges throughout the State's highway network is recommended.

8.4 Scour around Piers and Foundations

It is evident from previous documented experience and the results in this study, that scour conditions around piers and foundations are intensified at these structural components supporting the bridges. This loss of ground compromises the axial and lateral capacity of the deep foundations, particularly for friction piles. Two of the bridges (A-3760 and L-0550) were supported as end bearing piles into bedrock, which was at a relatively shallow depth. Both driven and drilled shafts were used for these major bridges, which are the prevalent foundations used by MoDOT. None of the bridges examined during this study were supported on shallow foundations. However, numerous water crossings on roadways consist of box culverts supported with shallow foundations. Only one bridge had some piers supported on shallow foundations directly on sound rock, which is not anticipated to scour.

The construction records of the foundations were not available for this study but are typically required documentation during construction. Therefore, it is important to retain these records with the as-built plans/archives, so that this critical information is available when scour assessments are conducted during the design-life of the bridge.

8.5 Recommendations for Future Research

- The intensity of storms has increased in recent years due to climate change. Several agencies are considering increasing the design storm to 1000-yr return periods. This would not only impact bridge scour, but the design of other structural components. It is recommended to evaluate the consequences of future climate intense changes (1000-yr storms).
- A time-consuming and laborious portion of the analysis is the preparation of data. Particularly defining the ground surface terrain model (above and below water bodies) using different data

sources. Some of these data sources are: airborne Lidar, traditional survey, and bathymetric (ADCP, single-beam, and multi-beam). It is recommended that automated stitching procedures are investigated to merge the different terrain data sources with resolutions.

- Currently, the available scour models consider one soil type during the scour calculations. The subsurface conditions are typically layered in riverine basins. Therefore, it would be pertinent to investigate methods to incorporate this layered stratigraphy into the predictive scour models.
- Most large bridges crossing rivers with significant flow have some type of countermeasure in the way of riprap or large rock protection to dissipate some of the energy and prevent scouring. There is no current approach to consider these countermeasures in the available scour models. Therefore, it is recommended to develop an approach to consider these countermeasures in the scour analysis.
- Pronounced scouring around piers and abutments exposes the foundation elements and may lose ground support. The result is loss of axial and lateral foundation capacity during storm events. Even though these conditions may be temporary, in some cases they may be critical to the stability of the bridge structure. It is recommended to investigate the loss of capacity and the reduction in the factor of safety or resistance factors in these short-term conditions.
- Some of the findings in this study using 2-D models resulted in significant flow extending beyond the bridge structure in the floodplain embankments. This study did not address the overtopping or overflow scour over embankments, which can produce erosion of this earthen structure. It is recommended to investigate the consequences of erosion of roadway embankments that may experience overtopping flow conditions.
- Box culverts and large conduits under roadway embankments are important infrastructure for DOTs, but are sometimes not classified as bridges. Some of these structures may be significant and unique, in that they have flow patterns (pressurized) during storm events different than common bridges. Additionally, they are typically supported by shallow foundation soils, making them prone to being washed out or undermined. It is recommended to investigate the scour mechanisms that these unique culvert structures would experience during storm events and how hydraulic model inputs from 2-D versus 1-D models would affect scour calculations.

REFERENCES

American Society for Testing and Materials (ASTM), 2023). "Volume 04.08: Soil and Rock (I): D420–D5876/D5876m", ASTM, West Conshohocken, PA.

Amini, Ata & P, Taheri & Motamedi, Shervin & Hashim, Roslan. (2016). Physical Modelling of Local Scouring at Complex Bridge Piers.

Arneson, L. A., Zevenbergen, L. W., Lagasse, P. F., and Copper, P. E. (2012). "Evaluating Scour at Bridges Fifth Edition." Federal Highway Administration, Hydraulic Engineering Circular No. 18., Report No. FHWA-HIF-12-003 HEC-18.

Brunner, G. W. (2016). "HEC-RAS, River Analysis System Hydraulic Reference Manual." US Army Corps of Engineers Hydrologic Engineering Center, Report Number CPD-69, Davis, CA.

Chow, V.T. (1959). "Open-Channel Flow," Second Edition, Springer Science and Business Media, New York, NY.

Deal, E., Parr, A., Young, C. (2017). A Comparison Study of One- and Two-Dimensional Hydraulic Models for River Environments. The University of Kansas, Lawrence, Kansas

Federal Highway Administration (FHWA) - Arneson, L.A., Shearman, J.O. (1998). User's Manual for WSPRO. FHWA-SA-98-080

Federal Highway Administration (FHWA) - Robinson, D., Zundel, A., Kramer, C., Nelson, R., deRosset, W., Hunt, J., Hogan, S., Lai, Y. (2019). Two-Dimensional Hydraulic Modeling for Highways in the River Environment. FHWA-HIF-19-061.

Federal Highway Administration (FHWA) (2021). "FHWA Hydraulic Toolbox User's Manual V. 5.1." Washington, D.C.

FISP Sampler Catalog, Federal Interagency Sedimentation Project (FISP) (2023), United States Geological Service, https://water.usgs.gov/fisp/catalog_index.html (Online: 5/31/2023).

Garcia-Santiago, K. (2021). 1D and 2D Hydraulic Modeling to Estimate Bridge Scour: A Case Study. Polytechnic University of Puerto Rico – Repository. Guidelines for the Design Project Article (prcrepository.org)

Huizinga, R.J., 2019, Bathymetric data at highway bridges crossing the lower Gasconade River after the May 2017 flood in central Missouri (ver. 2.0, May 2019): U.S. Geological Survey data release, https://doi.org/10.5066/F7542MHG.

Huizinga, R. J., 2020, Bathymetric and velocimetric surveys at highway bridges crossing the Missouri River between Kansas City and St. Louis, Missouri, May 22–31, 2017: U.S. Geological Survey Scientific Investigations Report 2020–5018, 104 p., https://doi.org/10.3133/sir20205018

Huizinga, R. J., and Rydlund, P. H. (2002). "Level II Bridge Scour Analysis for Structure H 24 on State Route 'P', Crossing Creek in Audrain County, Missouri." Rolla, MO: U.S. Department of the Interior; U.S. Geological Survey.

Huizinga, R. J., and Rydlund, P. H. (2003). "Level II Bridge Scour Analysis for Structures A 4497 and L 550R2 on U.S. Route 54, Crossing Missouri River in Cole County, Missouri." Rolla, MO: U.S. Department of the Interior; U.S. Geological Survey.

Kleiss, B. E. (2000). *Water Quality in the Mississippi Embayment, Mississippi, Louisiana, Arkansas, Missouri, Tennessee, and Kentucky, 1995-98.* Reston: U.S. Geological Survey.

Lai, Y. (2008). SRH-2D version 2: Theory and User's Manual. Bureau of Reclamation Technical Service Center, Sedimentation and River Hydraulics Group. Manual-SRH2D-v2.0-Nov2008.pdf (aquaveo.com)

Lai, Y.G., (2010). Two-Dimensional Depth-Averaged Flow Modeling with an Unstructured Hybrid Mesh. J. Hydraulic Eng. 136: 12–23.

Minor, P. (1974). *Soil Survey of DeKalb County, Missouri.* Washington D.C.: United States Department of Agriculture - Soil Conservation Service.

Missouri Department of Natural Resources (MoDNR) (2007). Missouri Environmental Geology Atlas 2007. Rolla, MO.

Missouri Department of Natural Resources (MoDNR) (2020, June 29). *Missouri Surficial Geology.* Missouri Department of Natural Resources GIS. Retrieved July 6, 2023, from https://gis-modnr.opendata.arcgis.com/datasets/f05859214648478eb39a3ebeaaea3c50_0/explore?location=39.055969%2C-91.424561%2C7.84

Missouri Department of Transportation (MoDOT) (2023). *MoDOT Real-Time Network*. Missouri Department of Transportation. Retrieved July 7, 2023, from https://gpsweb3.modot.mo.gov/

Missouri State Highway Commission (1962). *Geology and Soils Manual 1962.* Jefferson City: Missouri State Highway Commission.

National Cooperative Highway Research Program (NCHRP) (2010b). "Estimation of Scour Depth at Bridge Abutments," NCHRP Project 24-20, Draft Final Report, Transportation Research Board, National Academy of Science, Washington, D.C. (Ettema, R., T. Nakato, and M. Muste).

Richardson, E. V. and Davis, S. R. (2001). "Evaluating Scour at Bridges Fourth Edition." Federal Highway Administration, Hydraulic Engineering Circular No. 18., Report No. FHWA NHI 01-001 HEC-18.

Rydlund, P. H., and Huizinga, R. J. (2001). Level II Bridge Scour Analysis For Structures L 21 and L 22 on State Route 25, Crossing Wolf Creek and Branch in Stoddard County, Missouri. Rolla, MO: U.S. Department of the Interior; U.S. Geological Survey.

Rydlund, P. H., and Huizinga, R. J. (2002a). Level II Bridge Scour Analysis for Structure A 3760 on U.S. Route 63, Crossing Gasconade River in Maries County, Missouri. Rolla, MO: U.S. Department of the Interior; U.S. Geological Survey.

Rydlund, P. H., and Huizinga, R. J. (2002b). Level II Bridge Scour Analysis for Structure L 564 on State Route 'K', Crossing Dry Fork Creek in Montgomery County, Missouri. Rolla, MO: U.S. Department of the Interior; U.S. Geological Survey.

Southard, R. E., and Veilleux, A. G. (2014). Methods for Estimating Annual Exceedance-Probability Discharges and Largest Recorded Floods for Unregulated Streams in Rural Missouri. Reston, VA: U.S. Geological Survey. Retrieved from https://pubs.usgs.gov/sir/2014/5165/.

U.S. Army Corps of Engineers (USACE) (1991). "HEC-2 Water Surface Profiles, User's Manual," CEIWR-HEC.

Yu, X., & Yu, X.B. (2008). 1D and 2D Hydraulic Simulations for Bridge Scour Prediction: A Comparative Study. Fourth International Conference on Scour and Erosion 2008. Microsoft Word - 1D and 2D Hydraulic Simulations for Bridge Scour Prediction_ A Comparative Study.doc (baw.de).